

FINAL REPORT

Integrated spatial models of non-native plant invasion, fire risk,
and wildlife habitat to support conservation of military and
adjacent lands in the arid Southwest

SERDP Project RC-1722

DECEMBER 2015

Brett G. Dickson, PhD
Thomas D. Sisk, PhD
Steven E. Sesnie, PhD
Bethany A. Bradley, PhD
**Northern Arizona University Landscape
Conservation Initiative School of Earth Sciences and
Environmental Sustainability**

Distribution Statement A

This document has been cleared for public release



This report was prepared under contract to the Department of Defense Strategic Environmental Research and Development Program (SERDP). The publication of this report does not indicate endorsement by the Department of Defense, nor should the contents be construed as reflecting the official policy or position of the Department of Defense. Reference herein to any specific commercial product, process, or service by trade name, trademark, manufacturer, or otherwise, does not necessarily constitute or imply its endorsement, recommendation, or favoring by the Department of Defense.

REPORT DOCUMENTATION PAGE

Form Approved
OMB No. 0704-0188

Public reporting burden for this collection of information is estimated to average 1 hour per response, including the time for reviewing instructions, searching existing data sources, gathering and maintaining the data needed, and completing and reviewing this collection of information. Send comments regarding this burden estimate or any other aspect of this collection of information, including suggestions for reducing this burden to Department of Defense, Washington Headquarters Services, Directorate for Information Operations and Reports (0704-0188), 1215 Jefferson Davis Highway, Suite 1204, Arlington, VA 22202-4302. Respondents should be aware that notwithstanding any other provision of law, no person shall be subject to any penalty for failing to comply with a collection of information if it does not display a currently valid OMB control number. **PLEASE DO NOT RETURN YOUR FORM TO THE ABOVE ADDRESS.**

| | | | | | |
|---|--------------------------|--------------------------------|---|---|---|
| 1. REPORT DATE (DD-MM-YYYY) 16/11/2015 | | 2. REPORT TYPE Final | | 3. DATES COVERED (From - To) 26/4/2010 – 25/10/2015 | |
| 4. TITLE AND SUBTITLE Integrated Spatial Models of Non-Native Plant Invasion, Fire Risk, and Wildlife Habitat to Support Conservation of Military and Adjacent Lands in the Arid Southwest. | | | | 5a. CONTRACT NUMBER W912HQ-10-C-0035 | |
| | | | | 5b. GRANT NUMBER | |
| | | | | 5c. PROGRAM ELEMENT NUMBER | |
| 6. AUTHOR(S) PIs: Brett G. Dickson, PhD, Thomas D. Sisk, PhD, Steven E. Sesnie, PhD, and Bethany A. Bradley, PhD | | | | 5d. PROJECT NUMBER RC-1722 | |
| | | | | 5e. TASK NUMBER | |
| | | | | 5f. WORK UNIT NUMBER | |
| 7. PERFORMING ORGANIZATION NAME(S) AND ADDRESS(ES) Northern Arizona University Landscape Conservation Initiative Box 5694 Flagstaff, AZ 86011-5694 University of Massachusetts, Amherst Department of Environmental Conservation 318 Holdsworth Hall University of Massachusetts Amherst, MA 01003 | | | | 8. PERFORMING ORGANIZATION REPORT NUMBER NA | |
| 9. SPONSORING / MONITORING AGENCY NAME(S) AND ADDRESS(ES) Department of Defense (DOD) Strategic Environmental Research and Development Program (SERDP) 4800 Mark Center Drive, Suite 17D08, Alexandria, VA 22350-3605 | | | | 10. SPONSOR/MONITOR'S ACRONYM(S) DOD, SERDP | |
| | | | | 11. SPONSOR/MONITOR'S REPORT NUMBER(S) | |
| 12. DISTRIBUTION / AVAILABILITY STATEMENT Approved for public release; distribution is unlimited | | | | | |
| 13. SUPPLEMENTARY NOTES | | | | | |
| 14. ABSTRACT This research sought to integrate empirically based models of non-native plant invasion, fire, and wildlife habitat in a spatially explicit decision-support package that informs sustainable resource management and recovery of native habitats and species in the face of ongoing climate change. We modeled distribution, biomass, invasion risk, and fire risk associated with five non-native invasive plant species on two military installations, two refuges, and one National Monument in the Sonoran Desert of Arizona. Research involved extensive field sampling efforts to train and test regional- and landscape-scale models of non-native invasive plant distribution and biomass. Species-specific models incorporated novel remote sensing techniques that identified targets based on both phenological and spectral differences using satellite platforms of differing spatial, temporal, and spectral resolutions. During this project, detections of Sahara mustard and <i>Schismus</i> spp. were relatively common across the study area, whereas African buffelgrass, arugula, and red brome were relatively uncommon. Results confirmed that the advanced remote sensing and modeling techniques enabled identification of NIS habitat. Our assessment of landscape and regional scale ecological risk in a spatial management framework puts DoD in a powerful position to integrate environmental objectives with training needs and explore feasible management responses to global change. | | | | | |
| 15. SUBJECT TERMS Biomass, connectivity, fire risk, invasion risk, non-native plant invasion, remote sensing, species distribution modeling | | | | | |
| 16. SECURITY CLASSIFICATION OF: | | | 17. LIMITATION OF ABSTRACT UU | 18. NUMBER OF PAGES 114 | 19a. NAME OF RESPONSIBLE PERSON Brett G. Dickson, PhD |
| a. REPORT UU | b. ABSTRACT UU | c. THIS PAGE UU | | | 19b. TELEPHONE NUMBER (include area code) (928)523-3592 |

Table of Contents

| | |
|--|------|
| List of Tables | iv |
| List of Figures | v |
| List of Acronyms | viii |
| Acknowledgments | 1 |
| Abstract | 2 |
| Core Project Objectives | 4 |
| Objective 1: | 4 |
| Objective 2: | 5 |
| Objective 3: | 5 |
| Objective 4: | 6 |
| Objective 5 | 6 |
| Objective 6: | 6 |
| Background | 7 |
| The ecology and phenology of target non-native invasive species | 8 |
| Remote sensing of plant phenology and invasive species detection..... | 9 |
| Land use and plant invasion | 9 |
| Climate change and ecological forecasting..... | 9 |
| The effects of increased fuel loads and treatments on fire risk | 10 |
| Predicting resource use and connectivity for Sonoran pronghorn and other sensitive species | 12 |
| Embedding landscape models in a decision-support package to translate science to practice..... | 12 |
| Research Approach..... | 13 |
| Objective 1: Develop empirical remote sensing-based models of the distribution and biomass of non-native invasive plants in the Sonoran Desert and surrounding ecoregions. | 13 |
| Objective 2: Model invasion risk from non-native plants under current and projected climate conditions..... | 39 |
| Objective 3: Model the impacts of recent and on-going land use disturbances on non-native plant invasion. | 42 |
| Objective 4: Model the effects of increased fuel loads caused by non-native plant invasion on regional fire risk..... | 43 |
| Objective 6: Integrate the above models in a spatial decision-support package that informs sustainable resource management and recovery of native habitats and species on DOD and adjacent lands. | 50 |
| Results and Discussion..... | 52 |
| Objective 1: Develop empirical remote sensing-based models of the distribution and biomass of non-native invasive plants in the Sonoran Desert and surrounding ecoregions. | 52 |

Objective 2: Model invasion risk from non-native plants under current and projected climate conditions..... 74

Objective 3: Model the impacts of recent and on-going land use disturbances on non-native plant invasion. 77

Objective 4: Model the effects of increased fuel loads caused by non-native plant invasion on regional fire risk..... 78

Objective 6: Integrate the above models in a spatial decision-support package that informs sustainable resource management and recovery of native habitats and species on DOD and adjacent lands. 83

Conclusions and Implications for Future Research/Implementation..... 87

Literature Cited..... 93

Appendix A..... 105

Peer-reviewed Publications from RC-1722 105

List of Tables

| | |
|---|----|
| Table 1: Attributes of target non-native invasive plant species. | 8 |
| Table 2: Description of the variables included in habitat suitability models 1-5..... | 18 |
| Table 3: Number and percentage of detections of five focal species by plot and subplot sampled in the Sonoran Desert during our 2011-2012 field season. | 29 |
| Table 4: Features used to predict the occurrence and cover of the invasive targets. The total number of features in each category are indicated parenthetically in the group column. | 30 |
| Table 5: Outreach and information exchange schedule for the Spatial Decision-Support System..... | 51 |
| Table 6: Summary of <i>Eragrostis</i> canopy cover model performance, based on MTMF. | 60 |
| Table 7: Cohen's kappa for regional and SWE models of <i>Schismus</i> and <i>Brassica</i> derived from 2011 field data. | 68 |
| Table 8: Contingency table for Landsat-based map of <i>Brassica</i> | 77 |
| Table 9: Informational needs identified by stakeholders. | 85 |
| Table 10: List of data products delivered to collaborators, given three general 'needs' classes identified during a formal NAS process..... | 87 |

List of Figures

| | |
|---|----|
| Figure 1: Relationships among the six, original primary technical objectives. Objective five was not pursued with SERDP funding | 4 |
| Figure 2: Current monthly and annual precipitation in southwestern Arizona, and median precipitation projection of 10 AOGCMs for 2100 using the SRESa1b emission scenario | 10 |
| Figure 3: Map of the study extent and historical fire occurrence locations, including focal jurisdictions..... | 11 |
| Figure 4: Example of a foundational data layer used to design a field sampling scheme for the Sonoran Desert..... | 13 |
| Figure 5: Boundaries of our study area in the Sonoran Desert of Arizona during the 2011 (solid line) and 2012 (dotted line) field seasons..... | 14 |
| Figure 6: Previously mapped locations of five target species which were used to guide field efforts in 2011 and 2012..... | 15 |
| Figure 7: Points and jurisdictions sampled in 2011 (left) and 2012 (right)..... | 16 |
| Figure 8: Spatially nested field sampling design used to detect and measure non-native invasive plants..... | 17 |
| Figure 9. Focal area (red boundary) for detection of <i>Eragrostis</i> detection using WorldView-2 on BANWR (black boundary). | 26 |
| Figure 10: Vegetation plot sampling methods from Hubbard et al. (2012)..... | 27 |
| Figure 11: To integrate field-collected spectra with a data sensor, spectra must be convolved (or cleaned and fit) to that sensor’s bands..... | 28 |
| Figure 12: Regional and SWE models of <i>Schismus</i> (A, C) and <i>Brassica</i> (B, D) likelihood as well as the difference between SWE and Regional predictions (E, F). | 32 |
| Figure 13: Location of Data Acquisition Request (DAR) positions (A) and yearly winter MODIS NDVI time series from 2000 to 2011 for DAR positions (B). | 34 |
| Figure 14: Difference in MODIS NDVI values from 2012 vs. 2011, using image dates from peak spring (March) production period. | 35 |
| Figure 15: Location and extent of Hyperion scene acquired on March 6, 2012, in relation to study area and plots visited in 2012..... | 35 |
| Figure 16: Example of original Hyperion band 9 (A) and de-striped Hyperion band 9 (B)..... | 36 |
| Figure 17. Spatial locations of data collection for <i>Bromus rubens</i> and <i>Brassica tournefortii</i> | 41 |

Figure 18: Values of NDVI within the burn perimeter of two large fires that burned in the study area: the King Valley Fire (A) burned in October 2005 and the Goldwater Fire (B) burned in June44

Figure 19. (A) In circuit theory models, a resistor’s value is given by the probability of movement between its incident nodes. (B) Study extent was represented as a circuit network by representing landscape grid cells as nodes connected to adjacent nodes by resistors. (C) An ‘omnidirectional’ approach was used to account for overall fire connectivity..... 47

Figure 20: The percentage of subplots containing different amounts of biomass sampled in 2011 and 2012. The number of subplots from which biomass was collected in the two years varied significantly, with 1171 subplots sampled in 2011 and 591 sampled in 2012. 53

Figure 21: Monthly departure from average Landsat NDVI and EVI values for steep, shaded terrain across the study area. The dotted line (black) represents the percent difference between TM NDVI and EVI values..... 57

Figure 22: Jitter plot showing the distribution of absence and presence records (0 and 1 along the x-axis, respectively) for *Schismus* on the predicted occurrence probabilities. 62

Figure 23: a) Receiver Operating Characteristic curve and b) cost function for the *Schismus* occurrence model. An arbitrary threshold of 0.5 was used here for illustration purposes only. 63

Figure 24: a) Receiver Operating Characteristic curve and b) cost function for the *Brassica* occurrence model. An arbitrary threshold of 0.5 was used here for illustration purposes only. 63

Figure 25: Predicted occurrence probability for *Schismus* in 2005 and 2012 (left and right columns, respectively). 64

Figure 26: Predicted occurrence probability for *Brassica* in 2005 and 2012 (left and right columns, respectively). 65

Figure 27: Difference between the predicted occurrence probabilities in 2005 and 2012 for *Schismus*. .66

Figure 28: Difference between the predicted occurrence probabilities in 2005 and 2012 for *Brassica*. ...67

Figure 29: Map of SMACC EM 26, which had the highest correlation with *Brassica* cover on intersection subplots. 70

Figure 30: A) Footprint of Worldview 2 images (blue) acquired during the 2012 field season. B) Footprints of SPOT Imagery during the 2012 field season..... 71

Figure 31: Spectral bands of WV2, Landsat TM, SPOT, and Hyperion satellite sensors. The yellow, red edge, and NIR2 bands are unique to WorldView-2 among present-day multispectral sensors..... 72

Figure 32: WorldView-2 imagery of abandoned farm fields dominated by *Eruca* located near Sentinel, Arizona. Images are WV2 band combinations 5, 7, and 3 (left) and 4, 8, and 6 (right)..... 73

Figure 33: Species distribution models for *Bromus* and *Brassica*..... 75

Figure 34: The relative percentage of pixels with *Brassica* present and absent relates to disturbance and geography. A) Proximity to railroads is a strong predictor of *Brassica* presence, and B) *Brassica* is highly likely to be found on sandy geologic surfaces. 78

Figure 35: Map-based prediction of large fire probability in the lower Sonoran Desert of southwestern Arizona, based on 2005 conditions (i.e., high large fire probability). 79

Figure 36: FlamMap simulation outputs for predicted potential (A) fire behavior, (B) hazard, and (C) rate of spread with constant winds blowing from the southwest at 40 kph and under current landscape and fuels conditions..... 81

Figure 37: Map of fire likelihood across the lower Sonoran Desert of southwestern Arizona, based on a circuit theoretic model of connectivity. 82

Figure 38: Images from the ‘Managers Workshop’ November 15, 2013, designed to foster tech transfer and cross-jurisdictional discussions. 86

List of Acronyms

| | |
|------------|--|
| AGFD | Arizona Game and Fish Department |
| AIC | Akaike's information criterion |
| ASD | Analytical Spectral Devices, Inc. |
| AUC | Area under the (receiver operating characteristic, or ROC) curve |
| AVHRR | Advanced Very High Resolution Radiometer |
| BLM | Bureau of Land Management |
| BMGR | Barry M. Goldwater Air Force Range (east and west jurisdictions are indicated by '-E' and '-W' suffixes, respectively) |
| Bromus | <i>Bromus rubens</i> |
| Brassica | <i>Brassica tournefortii</i> |
| BTU | British Thermal Unit |
| DEM | Digital elevation model |
| DOD | Department of Defense |
| EM | Endmember |
| Eragrostis | <i>Eragrostis lehmanniana</i> |
| Eruca | <i>Eruca vesicaria</i> var. <i>sativa</i> |
| ETM+ | Enhanced Thematic Mapper Plus |
| ENSO | El Niño–Southern Oscillation |
| ENVI | Environment for Visualizing Images (image analysis software) |
| EROS | Earth Resources Observation and Science |
| FLAASH | Fast Line-of-sight Atmospheric Analysis of Spectral Hypercubes |
| GIS | Geographic information system |
| GLIMMIX | SAS procedure to fit generalized linear mixed models by likelihood-based techniques |
| HypIRI | Hyperspectral Infrared Imager |
| IPR | In-progress Review |
| KNWR | Kofa National Wildlife Refuge |
| LCRD | Lower Colorado River Desert |
| MNF | Minimum Noise Fraction |
| MODIS | Moderate Resolution Imaging Spectroradiometer |
| MF | Matched filtering |
| MTMF | Mixture-tuned matched filtering |
| NAS | Needs Assessment Survey |
| NASA | National Aeronautics and Space Administration |
| NDVI | Normalized Difference Vegetation Index |
| NED | National Elevation Dataset |
| NIR | Near infrared |
| NOAA | National Oceanic and Atmospheric Administration |
| NPS | National Park Service |
| Pennisetum | <i>Pennisetum ciliare</i> |
| PI | Principal investigator |
| PRISM | Parameter-elevation Regressions on Independent Slopes Model Climate Group, Oregon State University |
| RAWS | Remote Automatic Weather Station |
| RMSE | Root-mean-square error |
| ROC | Receiver operating characteristic |
| SAS | Statistical analysis software by SAS Institute, Inc. |
| Schismus | <i>Schismus spp.</i> |

| | |
|-------|--|
| SDSS | Spatial decision-support system |
| SERDP | Strategic Environmental Research and Development Program |
| SDRP | Sonoran Desert Research Program |
| SMACC | Sequential maximum angle convex cone |
| SPOT | Sistema Para la Observación de la Tierra |
| SWE | Spatially Weighted Ensemble |
| SWEMP | Southwest exotic plant mapping program |
| TM | Thematic Mapper |
| USFWS | U.S. Fish and Wildlife Service |
| VI | Vegetation Index |

Acknowledgments

We would like to thank Richard Whittle from the Barry M. Goldwater Air Force Range and Laura Merrill from the U.S. Army Yuma Proving Ground for the generous contributions of their time and commitment to the success of our project. Special thanks are also due to Karen Howe from Tohono O'odham Nation for support during training and field work, to Sue Rutman at Organ Pipe Cactus National Monument, and to Steve Rosenstock (project cooperater) and John Romero with the Arizona Game and Fish Department for providing invaluable technical guidance and for safety training in the Sonoran Desert and U.S.-Mexico border region, respectively. Multiple staff with the Bureau of Land Management and U.S. Fish and Wildlife Service, namely and Susanna Henry, John Hervert, John Morgart, and Lindsey Smythe were helpful in the scoping and data collection phases of our project. John Arnett and Chris Black from the Barry M. Goldwater Air Force Range also were kind collaborators throughout the course of our research. Field data were collected by a small 'army' of biological technicians during the spring of 2011 and 2012. Their endurance, enthusiasm, and professionalism were invaluable. Numerous members of the Lab of Landscape Ecology and Conservation Biology contributed to the success of our project, namely Miranda Gray, Cerissa Hoglander, Valerie Horncastle, Karl Jarvis, Aaryn Olsson, Jill Rundall, Teki Sankey, Sasha Stortz, and Ophelia Wang. Clare Aslan graciously assisted with the assembly of this final report. The administrative efforts of Kimberly Cotter, Winnie Ennenga, and Cindy Judge allowed us to stay focused on doing strong science. Similarly, we thank Lori Pelech and Caroline Curtis at the University of Massachusetts, Amherst. Truly, this project 'took a village!'

Abstract

Objectives: The principal objective of the proposed research was to integrate empirically based models of non-native plant invasion, fire, and native species habitat in a spatially explicit decision-support package that informs sustainable resource management and recovery in the face of ongoing climate change. The project team modeled distribution, biomass, invasion risk, and fire risk associated with the following non-native invasive species (NIS): African buffelgrass (*Pennisetum ciliare*), red brome (*Bromus rubens*), Sahara mustard (*Brassica tournefortii*), Mediterranean grass (*Schismus* spp.), and arugula (*Eruca vesicaria sativa*) on the U.S. Army Yuma Proving Ground, Barry M. Goldwater Air Force Range, Kofa and Cabeza Prieta National Wildlife Refuges, and Organ Pipe Cactus National Monument.

Technical Approach: Research involved extensive field sampling efforts to train and test regional- and landscape-scale models of non-native invasive plant distribution and biomass. Species-specific models incorporated novel remote sensing techniques that identified NIS based on both phenological and spectral differences using satellite platforms of differing spatial, temporal, and spectral resolutions. Species distribution maps at landscape and regional scales were used to assess biogeographical relationships of invasive plants to land use and climate and to model changing invasion risk with global change. Biomass maps were used to model fuel loads and to predict areas of high fire risk, hazard, and behavior. Invasion and fire risk predictions, taking into account potential management and mitigation responses, were integrated with models of resource use and habitat connectivity for wildlife species. The research culminated with the embedding of the above results into a spatial decision-support package to guide management on Department of Defense (DoD) and surrounding lands.

Results: During this project, detections of *B. tournefortii* and *Schismus* spp. were relatively common across the study area, whereas *P. ciliare*, *E. vesicaria sativa*, and *B. rubens* were relatively uncommon. *B. tournefortii* demonstrated relatively specific habitat conditions under which it becomes dominant, whereas *Schismus* spp. exhibited more generalist habitat requirements and were present in most sampled ecosystems. By contrast, *P. ciliare* and *B. rubens* exhibited greater invasion potential in upland ecosystems. *E. vesicaria sativa* appeared likely to spread beyond its current distribution. Modeling results confirmed that the advanced remote sensing and modeling techniques developed by the project enabled identification of NIS habitat. In particular, models derived from MODIS and Landsat TM were appropriate for describing the likelihood of finding *B. tournefortii*, due to the unique phenology of the species and a strong contrast with native vegetation green-up. *Schismus* spp. were less distinct, both spectrally and temporally. The use of a spatially weighted ensemble approach to mapping improved our *B. tournefortii* models, likely because spatial heterogeneity in precipitation drove phenological variability across the study area for this species. For both species, models were challenged by low abundances of the target species as a result of unusually low precipitation in both 2011 and 2012. In all, the project (1) generated more than 400 post-processed time series (2000 to 2014) MODIS, Landsat, WorldView-2 (WV2), and SPOT5 images and associated derived phenometrics/indices; (2) generated probabilistic models of habitat suitability across the study area for all target species; (3) developed regional models of presence, cover, and biomass for all target species (based on MODIS, Landsat, WV2, SPOT5); (4) refined existing spatial databases of *Schismus* spp., *B. tournefortii*, *B. rubens*, *P. ciliare*, and *E. vesicaria sativa* occurrence for the study area and region (CA, AZ, NV, UT, NM); (5) updated regional models of current and future risk of invasion by *B. rubens* and *B. tournefortii*; and (6) derived regional models of significant fire risk under different fuel load/climate scenarios, as well as a novel regional model of fire connectivity. The project's sampling design was deliberately iterative and targeted. Results from this design, along with the habitat suitability and occurrence models, enables mapping of key species of ongoing management concern over a large geographic area encompassing multiple DoD installations and other jurisdictions. Results also highlighted areas where ongoing or new fuels monitoring activities might be focused.

Benefits: This research effort developed new techniques, models, and maps related to fundamental ecological changes driven by NIS, fire, and global change in the Southwest. The research products are practical and relevant to management on DoD lands and across the surrounding Sonoran Desert ecoregion. Importantly, the approaches advanced by the project were designed to leverage multiple new and freely-available information sources, so that the methods would be easily transferrable and repeatable. The project's assessment of landscape- and regional-scale ecological risk in a spatial management framework enables DoD to integrate environmental objectives with training needs, and to provide leadership on feasible management responses to global change.

Core Project Objectives

To directly address Statement of Need SISON-10-01, the proposed research developed novel methods and tools that integrated models of plant invasion, fire, wildlife habitat, and climate change, and guided scenario-based ecological analyses at extensive spatial scales. By working at both landscape and regional scales, we assessed the spatial relationships between non-native plant invasion and other fundamental ecological processes, enabling us to provide practical management recommendations for sustainable military testing and training activities. Working on the U.S. Army Yuma Proving Ground (YPG) and the Barry M. Goldwater Air Force Range (BMGR), on the adjacent Kofa (KNWR) and Cabeza Prieta (CPNWR) National Wildlife Refuges, and on Organ Pipe Cactus National Monument (OPCNM), our research increased the ability of the Department of Defense (DOD) and regional stakeholders to identify and implement spatially explicit, cross-jurisdictional planning and management strategies needed to reduce the impact of non-native invasive plants and fire, while improving habitat for threatened, endangered, and at-risk species (TER-S), in the context of global change. The project had six primary technical objectives, with associated tasks (Figure 1):

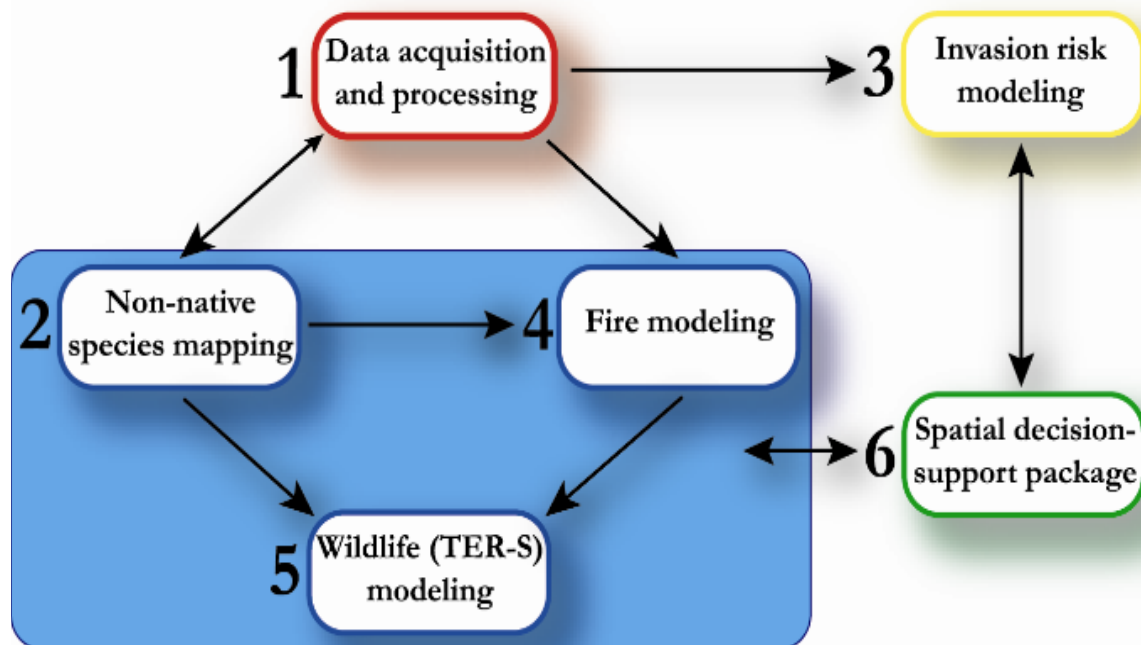


Figure 1: Relationships among the six, original primary technical objectives. Objective five was not pursued with SERDP funding.

OBJECTIVE 1: Develop empirical remote sensing-based models of the distribution and biomass of non-native invasive plants in the Sonoran Desert and surrounding ecoregions. Target species included: African buffelgrass (*Pennisetum ciliare*), red brome (*Bromus rubens*), Sahara mustard (*Brassica tournefortii*), Mediterranean grass (*Schismus* spp.), and arugula (*Eruca vesicaria sativa*).

Tasks and subtasks associated with Objective 1.

| Task # | Task or <i>Subtask</i> | Completion date |
|--------|--|-----------------|
| 1 | Design sampling scheme | 10/2010 |
| 2 | Field sampling efforts | 04/2012 |
| 2.1 | <i>Field sampling efforts (phase 1)</i> | <i>04/2011</i> |
| 2.2 | <i>Field sampling efforts (phase 2)</i> | <i>04/2012</i> |
| 3 | Acquire and process existing Landsat/MODIS data | 08/2012 |
| 3.1 | <i>Acquire and process existing Landsat/MODIS data (phase 1)</i> | <i>05/2011</i> |
| 3.2 | <i>Acquire and process existing Landsat/MODIS data (phase 2)</i> | <i>08/2012</i> |
| 4 | Acquire and process ancillary spatial distribution data | 04/2012 |
| 4.1 | <i>Acquire and process ancillary spatial distribution data (phase 1)</i> | <i>05/2011</i> |
| 4.2 | <i>Acquire and process ancillary spatial distribution data (phase 2)</i> | <i>04/2012</i> |
| 6 | Non-native mapping (Landsat/MODIS) | 08/2012 |
| 6.1 | <i>Non-native mapping (Landsat/MODIS) (phase 1)</i> | <i>07/2011</i> |
| 6.2 | <i>Non-native mapping (Landsat/MODIS) (phase 2)</i> | <i>08/2012</i> |
| 6.3 | <i>Target-based mapping using WorldView data</i> | <i>08/2015</i> |
| 6.4 | <i>Phenology-based mapping of habitat suitability</i> | <i>08/2015</i> |
| 11 | Acquire new Hyperion-hyperspectral data | 10/2012 |
| 11.1 | <i>Acquire new Hyperion-hyperspectral data (phase 1)</i> | <i>12/2011</i> |
| 11.2 | <i>Acquire new Hyperion-hyperspectral data (phase 2)</i> | <i>10/2012</i> |
| 12 | Non-native mapping (Hyperion-hyperspectral) | 05/2013 |
| 12.1 | <i>Non-native mapping (Hyperion-hyperspectral) (phase 1)</i> | <i>08/2012</i> |
| 12.2 | <i>Non-native mapping (Hyperion-hyperspectral) (phase 2)</i> | <i>12/2013</i> |

OBJECTIVE 2: Model invasion risk from non-native plants under current and projected climate conditions.**Tasks and subtasks associated with Objective 2.**

| Task # | Task or <i>Subtask</i> | Completion date |
|--------|--------------------------|-----------------|
| 5 | Compile AOGCMs | 11/2010 |
| 7 | Construct BEMs | 08/2012 |
| 8 | BEM uncertainty analysis | 11/2012 |

OBJECTIVE 3: Model the impacts of recent and ongoing land use disturbances on non-native plant invasion.**Tasks and subtasks associated with Objective 3.**

| Task # | Task or <i>Subtask</i> | Completion date |
|--------|---|-----------------|
| 9 | Land use models of disturbance and risk | 08/2012 |
| 9.1 | <i>Land use models of disturbance and risk (phase 1)</i> | <i>06/2012</i> |
| 9.2 | <i>Land use models of disturbance and risk (phase 2)</i> | <i>08/2012</i> |
| 13 | Test and refine disturbance models based on Hyperion | 08/2013 |
| 13.1 | <i>Test and refine disturbance models based on Hyperion (phase 1)</i> | <i>11/2012</i> |
| 13.1 | <i>Test and refine disturbance models based on Hyperion (phase 2)</i> | <i>NA</i> |

OBJECTIVE 4: Model the effects of increased fuel loads caused by non-native plant invasion on regional fire risk.

Tasks and subtasks associated with Objective 4.

| Task # | Task or <i>Subtask</i> | Completion date |
|--------|--|-----------------|
| 10 | Fire modeling outputs | 12/2013 |
| 10.1 | <i>Fire modeling outputs (phase 1)</i> | 06/2012 |
| 10.2 | <i>Fire modeling outputs (phase 2)</i> | 12/2013 |

OBJECTIVE 5¹: Model resource use and habitat connectivity for Sonoran pronghorn (*Antilocapra americana sonoriensis*) and other sensitive wildlife species.

OBJECTIVE 6: Integrate the above models in a spatial decision-support package that informs sustainable resource management and recovery of native habitats and species on DOD and adjacent lands.

Tasks and subtasks associated with Objective 6.

| Task # | Task or <i>Subtask</i> | Completion date |
|--------|--|-----------------|
| 14 | Design and develop scenarios for decision support | 06/2014 |
| 14.1 | <i>Design and develop scenarios for decision support (phase 1)</i> | 12/2011 |
| 14.2 | <i>Design and develop scenarios for decision support (phase 2)</i> | 12/2012 |
| 14.3 | <i>Design and develop scenarios for decision support (phase 3)</i> | 06/2014 |
| 15 | Develop collaborative process and stakeholder workshops | 06/2014 |
| 15.1 | <i>Develop collaborative process and stakeholder workshops (phase 1)</i> | 11/2010 |
| 15.2 | <i>Develop collaborative process and stakeholder workshops (phase 2)</i> | 11/2011 |
| 15.3 | <i>Develop collaborative process and stakeholder workshops (phase 3)</i> | 11/2012 |
| 15.4 | <i>Develop collaborative process and stakeholder workshops (phase 4)</i> | 06/2014 |
| 16 | Tool transfer, training, and presentations | 08/2014 |
| 16.1 | <i>Tool transfer, training, and presentations (phase 1)</i> | 12/2010 |
| 16.2 | <i>Tool transfer, training, and presentations (phase 2)</i> | 12/2011 |
| 16.3 | <i>Tool transfer, training, and presentations (phase 3)</i> | 12/2012 |
| 16.4 | <i>Tool transfer, training, and presentations (phase 4)</i> | 08/2014 |

¹ A direct analysis of wildlife populations was not funded by the SERDP Science Advisory Board, and work on originally proposed objective #5 (task #5; Wildlife (TER-S) modeling) was not pursued.

Background

Non-native invasive plants pose a significant threat to human and ecological systems by altering biodiversity, function, and natural disturbance regimes (Mack 2000; Ehrenfeld 2010). Preventing new plant invasions is critical for reducing large-scale ecological change (Lehan et al. 2013). In arid and semi-arid ecosystems, the positive interaction between annual and perennial invasive (native and non-native) grass cover, increased loading of fine-fuels, burning frequency, and fire severity illustrates the potential for plant invasion to substantially alter disturbance patterns, especially regional fire regimes (e.g., Balch et al. 2013). Increases in fire frequency, size, and intensity facilitated by invasive species can promote ongoing invasion, while populations of non-fire adapted native plants are more readily impacted (Brooks et al. 2004). Because disturbances in arid ecosystems involve slow vegetation recovery and a loss of native biodiversity (Steers & Allen 2010), targeted and adaptive management activities will be critical in mitigating the negative consequences of non-native invasive plants (Wang et al. 2014).

In the Sonoran Desert of North America, impacts of non-native plant invasion are of considerable conservation concern because the region is a hotspot of biodiversity, and is subject to heavy influences from climate change (Seager et al. 2007; Diffenbaugh et al. 2008). Native species in the Sonoran Desert are likely to face reduced precipitation and increased inter-annual variability as a result of climate change, and the relative diversity and densities of species, as well as interspecific interactions, could potentially be impacted, leading to no-analog species assemblages (Davis & Shaw 2001; Williams & Jackson 2007). Indeed, extensive turnover in woody plant composition has already been observed in the Southwest, apparently stemming from extreme drought (Breshears et al. 2005). As these impacts demonstrate, global climate change may seriously threaten native species and ecosystems of the Sonoran Desert (Weiss & Overpeck 2005).

Because of the synergy between climate change, invasive species, disturbance, and fire, conservation and vegetation recovery efforts should target key non-native species, likely disturbance areas, and areas with high fire risk in an effort to boost ecosystem resilience (McCarty 2001). Studies of historical fire events in the Southwest identify an increase in the number and probability of large fire events in recent decades (Swetnam 1990; Dickson et al. 2006), and have demonstrated a significant effect of invasive plant species on the frequency, severity, and extent of fire (Esque & Schwalbe 2002; Brooks & Matchett 2006). Furthermore, the combination of non-native plant invasion and fire also degrades critical wildlife habitat (Esque & Schwalbe 2002; Esque et al. 2003; Sánchez-Flores 2007), placing species with narrow habitat requirements, including wildlife such as the endangered Sonoran pronghorn, increasingly at risk. Dramatic environmental change due to the 'invasive grass/fire cycle' (D'Antonio & Vitousek 1992) is therefore well appreciated, but understanding and responding to changing fire risk requires an ability to predict the spatial distribution and abundance of those invasive grasses into the future. The development of robust predictions in turn requires model-based evaluations of the interactions between non-native plant invasion and fire effects, taking into account different climate and land use scenarios, at multiple spatial and temporal scales. In short, the full complexity of the system must be appreciated and taken into account by models and subsequent management recommendation development.

In many cases, biological invasions are facilitated by disturbance. Factors such as fire, military activities, off-road vehicle use, and road construction appear to enhance the availability of resources for establishing organisms, enabling the spread of non-natives (Westbrook et al. 2005). Modeling results indicate that biological invasions in the Desert Southwest are likely to be exacerbated by climate change, perhaps impacting native ecosystems and species (Weiss & Overpeck 2005; Westbrook et al. 2005; Bradley 2009). The synergistic relationship between these drivers of environmental change may impact both native and, by feedback, non-native species. Understanding these linkages is a critical step toward the development of useful predictive models and management strategies that can effectively benefit

rare and sensitive species by adequately addressing biological invasions, disturbance, climate change, and their interaction.

The ecology and phenology of target non-native invasive species

Non-native plants that have been shown to boost fire frequency in the Sonoran Desert of southwestern Arizona include, but are not limited to: African buffelgrass (*Pennisetum ciliare*²; hereafter *Pennisetum*), red brome (*Bromus rubens*³; hereafter *Bromus*), Sahara mustard (*Brassica tournefortii*; hereafter *Brassica*), Mediterranean grass (*Schismus* spp.; hereafter *Schismus*), and arugula (*Eruca sativa*; hereafter *Eruca*) (Tellman 2002; Weiss & Overpeck 2005; Swetnam & Betancourt 2010). Lehmann lovegrass (*Eragrostis lehmanniana*; hereafter *Eragrostis*) is a non-native invasive perennial grass introduced to Sonoran Desert grasslands from South Africa. It has transformed desert grasslands in Arizona producing 2 to 4 times the annual biomass of native grasses and responds positively to livestock grazing and fire (Van Devender et al. 1997).

Each of these species has been considered to be expanding rapidly in population size and distribution in the region (Tellman 2002). These species are largely characterized by early winter germination, high viable seed loads, and multiple dispersal mechanisms; in combination, these traits result in a competitive advantage over native plants (Table 1). These non-natives can rapidly establish on disturbed sites, forming dense stands that displace native plants and increase flammable biomass (Van Devender et al. 1997). In less disturbed sites, the species can colonize via dispersal from wind, vehicles, and water.

Table 1: Attributes of non-native invasive plant species targeted by this study.

| Genus | Type | Ecological amplitude ¹ | Typical growth period | Dispersal mechanism |
|-------------------|--------------|--|--------------------------------|---|
| <i>Pennisetum</i> | Annual grass | Desertscrub, semi-desert grassland, riparian | Summer monsoon | Wind, vehicle tires, animals |
| <i>Bromus</i> | Annual grass | Desertscrub, semi-desert grassland, riparian | Early winter or summer monsoon | Wind, vehicles tires, animals, ag. products |
| <i>Brassica</i> | Annual herb | Sandy and disturbed soils | Early winter | Wind, vehicle tires, animals, water |
| <i>Schismus</i> | Annual grass | Desertscrub | Early winter or summer monsoon | Wind, vehicle tires, animals, water |
| <i>Eruca</i> | Annual herb | Undocumented | Early winter | Vehicle tires |

¹Principal Sonoran Desert ecological types invaded with >20% occurrence of target species

Phenology is of central importance to this research. *Bromus*, *Brassica*, *Schismus*, and *Eruca* are annual grasses and herbs, typically germinating after winter rains (Marushia et al. 2010). *Pennisetum*, a perennial grass, begins growing after the onset of summer monsoon rainfall (Franklin et al. 2006). The green-up characteristics for these plants differ from those of native species, resulting in unique signatures in remotely sensed snapshots of the region. Non-native invasive plants in the Sonoran Desert also often respond to interannual temperature and precipitation variability in an amplified manner not seen for native communities (e.g., Bradley & Mustard 2005). Vegetation indices derived from remote

² The scientific name for African buffelgrass has been updated to *Cenchrus ciliaris*

³ The scientific name for red brome has been updated to *Bromus madritensis*

sensing can pinpoint these phenological differences between invasive and native plant species and thus be used to identify non-natives at a landscape scale.

Remote sensing of plant phenology and invasive species detection

Many invasive plant species can be identified via remote sensing based on annual and interannual phenological differences from native vegetation (Peterson 2005; Bradley & Mustard 2006). Phenological differences between native and non-native species have opened the door to the establishment of remote sensing as an indispensable tool for detecting non-native plant invasions (Lass et al. 2009). Earlier timing of green-up for the non-native relative to native plants has enabled remote mapping of the distribution of the invasive annual cheatgrass (*Bromus tectorum*) (Bradley & Mustard 2006), while responses to precipitation events reveal interannual variability that has been used to map the distribution of cheatgrass (Peterson 2005) and the non-native perennial *Eragrostis* desert environments (Huang & Geiger 2008). The Moderate Resolution Imaging Spectroradiometer (MODIS) and Landsat satellite remote sensing platforms allow repeated Earth observations approximately every 2 to 16 days. When applied to these observations, spectral sampling in the red and shortwave-infrared regions is sensitive to changes in plant chlorophyll, cell structure, and moisture that can be indicative of plant phenology cycles (Cleland et al. 2007; Huang & Geiger 2008). Single- and multi-date airborne hyperspectral remote sensing platforms have been successfully used to map and monitor invasive plant infestations in a number of habitat conditions (Glenn et al. 2005; Asner et al. 2008; Lass et al. 2009; Noujdina & Ustin 2009). Satellite-based hyperspectral systems, such as the EO-1 Hyperion platform, have been used infrequently to map invasive plants (Pengra et al. 2007), but have the potential to provide global measurements of vegetation at unprecedented spectral and temporal resolutions (e.g., NASA HypIRI satellite). These various sources of remote sensing data, increasing in precision and detail, can be applied to phenology-based mapping to produce robust and repeatable methods for identifying invasive plants. Particularly when invasives generate landscape-scale impacts, such as transformation of fire regimes, this type of landscape-scale assessment of their spread potential may be crucial to adaptive land management planning to mitigate threats to native biodiversity.

Land use and plant invasion

Disturbance is known to promote plant invasion (Hobbs & Huenneke 1992). Roads, trails, and ensuing traffic have led to increased invasion of non-native grasses in desert (Gelbard & Belnap 2003; Bradley & Mustard 2006) and prairie ecosystems (Larson 2002); the disturbed margins of routes offer free resources for exploitation by invaders, and human traffic along the pathways can disperse non-native species. The spatial distributions of invasive plants across the Sonoran Desert are likely related to anthropogenic disturbance. The extent and magnitude of disturbance in the region can be measured in a Geographic Information System (GIS) environment (e.g., Bradley & Mustard 2006) and then used in a predictive capacity to assess how different land use and management practices, with relation to disturbance, might enhance or reduce future plant invasion at the landscape scale.

Climate change and ecological forecasting

Terrestrial plants are strongly responsive to climate conditions, particularly precipitation and temperature, and invasive plant species are no exception. As climate conditions change in the Sonoran Desert region, the zones and land quantity susceptible to non-native plant invasion are likely to change as a result. Current climate projections suggest that southwestern US conditions will become drier and more prone to extreme drought during the 21st century (Diffenbaugh et al. 2005; Seager et al. 2007). Due to the life histories of individual species, seasonal changes in precipitation may be more influential on the persistence of many plant species than is the annual rainfall average (Bradley 2009; Bradley et al. 2009). As an example of the complexity of seasonal precipitation projections, the median of 10

Atmosphere-Ocean General Circulation Models (AOGCMs) using the SRESa1b “middle of the road” emission scenario (Nakicenovic & Swart 2000) projects a loss of up to 20% of winter and spring precipitation for southwestern Arizona, with a largely unchanged summer monsoon (Figure 2).

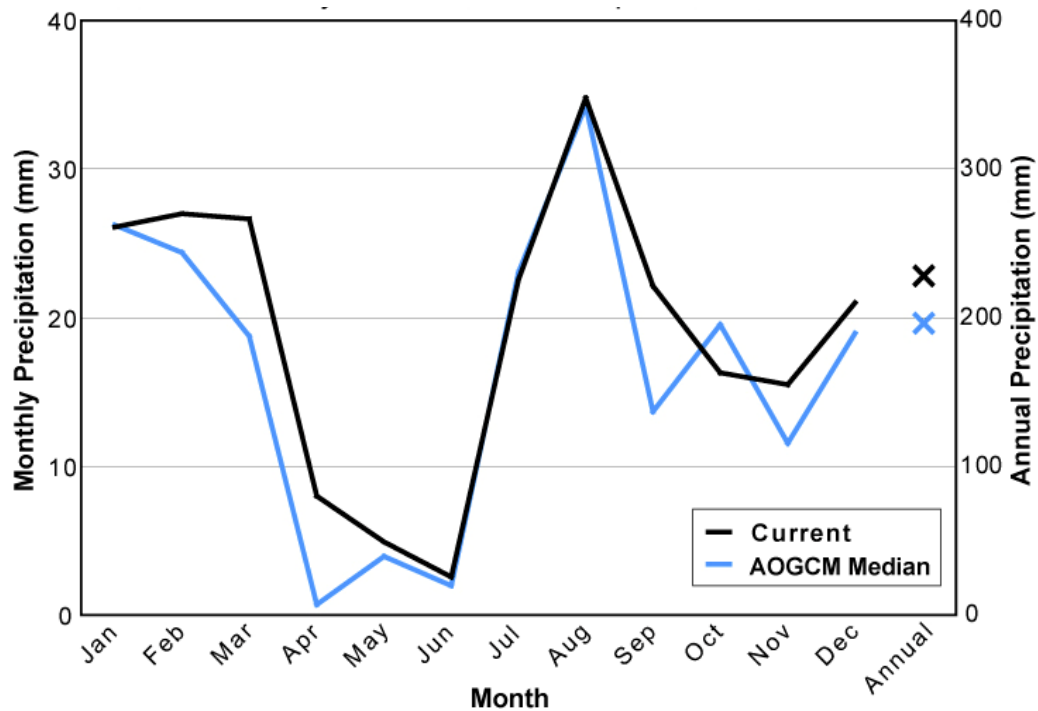


Figure 2: Current (2010) monthly and annual precipitation in southwestern Arizona, and median precipitation projection of 10 AOGCMs for 2100 using the SRESa1b emission scenario.

Understanding the likely response of focal invasive species to forecasted climate changes is essential for developing long-term management strategies that will be robust under future conditions (Bradley et al. 2009). Bioclimatic envelope models (BEMs) are frequently used to describe species’ climatic habitats based on their current regional geographic distribution (e.g., Guisan & Zimmermann 2000; Pearson & Dawson 2003), with the assumption that a species can be currently found in climatic conditions appropriate for it. Climatic habitat is defined as land area with climate conditions suitable for a species’ establishment (Kearney 2006). For invasive plants, the species’ climatic habitat can be considered at risk of invasion. BEMs, with their spatially explicit outputs, can be used to project the spatial distribution of invasion under both current and future climate conditions.

The effects of increased fuel loads and treatments on fire risk

Fire has historically been rare in the Sonoran Desert, where native plant density is generally insufficient to carry fire. This pattern has changed in recent decades, however. Across various vegetation communities of the Southwest, recent increases in fire occurrence and area burned by wildfires have resulted from wet periods (e.g., El Niño Southern Oscillation, or ENSO, events) resulting in high biomass accumulation and therefore rapid fuel buildup, followed by dry periods enhancing flammability of those fuels (La Niña) (Westerling et al. 2006; Swetnam & Betancourt 2010). In Sonoran Desert ecosystems, large, uncharacteristic wildfires are fueled and spread by contiguous beds of non-native plant biomass (Esque & Schwalbe 2002). The result is a vastly altered fire regime for desert regions. As a consequence of human activities and the prevalence of invasive species, more than 68,000 ha of the study area for this research has burned since 2000 (Figure 3). In 2005 alone, seven large fires burned over 52,000 ha of

the BMGR. The conditions leading to that heavy fire season can be examined. The winter of 2004-2005 was one of the wettest periods recently recorded in southwestern Arizona, creating extremely high productivity in annual plants, both native and non-native. In September 2005, the 11,700-ha King Valley fire, likely ignited by munitions testing on YPG, quickly spread to the KNWR. After confronting the vast acreage that burned in this and other recent events, land managers in the region are aware that the presence and spread of non-native, fire adapted grasses and forbs (Bradley & Mustard 2006), including *Pennisetum*, *Bromus*, *Brassica*, *Schismus*, and *Eruca*, create conditions of high fire risk. Since these non-native species are responsive to land use activities (Brown 1994) and can be both promoted and restrained by management activities, well-intentioned, but poorly planned, conservation or restoration efforts could act to benefit invasive plant species, if they do not account for the likely impacts of land use and climate change.

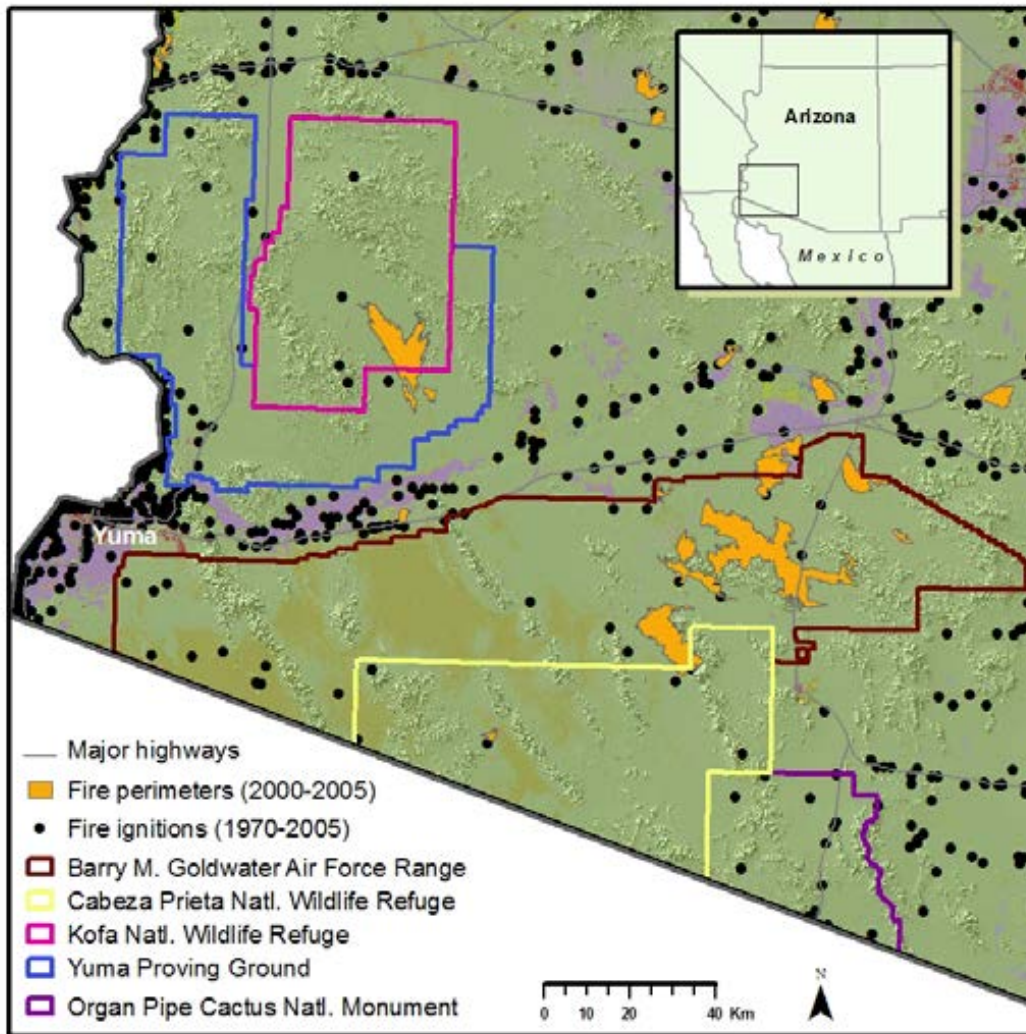


Figure 3: Map of the proposed study extent and historical fire occurrence locations, including focal jurisdictions.

Predicting resource use and connectivity for Sonoran pronghorn and other sensitive species⁴

Wide-ranging wildlife species depend on planning efforts that simultaneously consider the habitat quality and the ecological processes that provide critical resources and motivate animal movement (Dickson et al. 2005). Large and highly mobile wildlife species are commonly used as umbrella or focal species in conservation planning across thousands of square kilometers (Berger 2004; Sawyer et al. 2005; Beier et al. 2006). However, land managers commonly lack the specific information needed to assess key features of sensitive wildlife habitat that facilitate or impede connectivity and maintain habitat quality in population core areas, including vegetation structure, topography, disturbance factors, and anthropogenic barriers or impacts (Dickson et al. 2005; Beier et al. 2006).

The cycle that links plant community composition to fire and ecosystem processes has the potential to dramatically reduce habitat quality and use for the endangered Sonoran pronghorn and other TER-S species with narrow habitat requirements. The Sonoran pronghorn was listed as endangered by the U.S. Fish and Wildlife Service (USFWS) in 1967 and is one of the rarest ungulates in North America. The U.S. segment of the population has shown dramatic recent fluctuations, from a low of approximately 20 animals in 2002, to the current (2008) estimate of 124 animals. Their present range is restricted to southwestern Arizona and northern Mexico, with the US subpopulation occurring primarily on the BMGR, CPNWR, and adjacent OPCNM. From 2003-2006, a successful captive breeding and release effort was established on the CPNWR.

Sonoran pronghorn reproduction and resource use are closely tied to precipitation, which influences forage quantity and quality (Bright & Hervert 2005; Hervert et al. 2005). In addition, pronghorn are attracted to burned or disturbed areas because visibility is increased in such sites due to reduced density of tall shrubs and increased production of native annual forbs (Krausman et al. 2005). Invasive plants also thrive in these disturbed areas, but appear to receive little use by pronghorn. Thus, the individual and synergistic impacts of invasive plants, fire, and climate change on native habitat are likely to impact habitat use and connectivity for Sonoran pronghorn and other desert species in complex ways that are poorly understood.

Embedding landscape models in a decision-support package to translate science to practice

The focal study system is deeply complex. Invasive species spread is responsive to land use, disturbance, and climate change, and directly influences fire regimes. Understanding these linkages sufficiently to develop predictive models is a formidable task. The uncertainties related to climate change adds an additional challenge for DOD and its partners in environmental management, and requires a forward-looking approach for considering complex ecological dynamics in the context of training needs and management priorities. Effective management requires informed predictions about the future, based on scientifically responsible, data-driven and appropriately selected and applied ecological models. Previous spatial decision-support efforts (Sisk et al. 2006; Hampton et al. 2008) have found that the key assumptions and computational complexity of ecological models can be conveyed to non-specialists through the exploration of alternative scenarios in map-based formats and an explicit revision/review process. By engaging decision-makers early, and by harnessing the power of the scientific enterprise to inform, rather than dictate management actions, spatial decision support can facilitate the application of new scientific insight to complex environmental planning and problem solving. Cutting-edge ecological modeling placed into a spatial management framework puts the DOD in a powerful position

⁴ Some material related to wildlife-specific research, as originally proposed for this study, has been retained for context only. Although a direct analysis of wildlife populations was not funded by the SERDP Science Advisory Board, other funds were acquired to pursue wildlife related research tasks, and these leveraged SERDP data (e.g., as model inputs). Nevertheless, work on originally proposed objective #5 (task #5; Wildlife (TER-S) modeling) was not pursued.

to integrate environmental objectives with training needs, and provide leadership on regional responses to global change.

Research Approach

OBJECTIVE 1: Develop empirical remote sensing-based models of the distribution and biomass of non-native invasive plants in the Sonoran Desert and surrounding ecoregions.

Task 1: Design sampling scheme

Study area

The Sonoran Desert region in which we placed this research includes a variety of federal, state and private lands. The majority of the study area was comprised of federal lands, including the YPG, BMGR, KNWR, CPNWR, and OPCNM. We excluded private property, state trust lands, and a small number of Native American tribal lands from the total area available to sample, since these impose different access and permit requirements. Ecoregions in the study area included the Arizona Upland and Lower Colorado River Valley subdivisions of the Sonoran Desert (Brown 1994). These ecoregions contain extensive areas dominated by native and non-native invasive plant species recently impacted by large-scale fire and other disturbances, as well as notably low precipitation (Figure 4). Long-term average annual precipitation (1952-2007) at the YPG and KNWR was 93 mm and 175 mm, respectively (see <http://www.prism.oregonstate.edu/>).

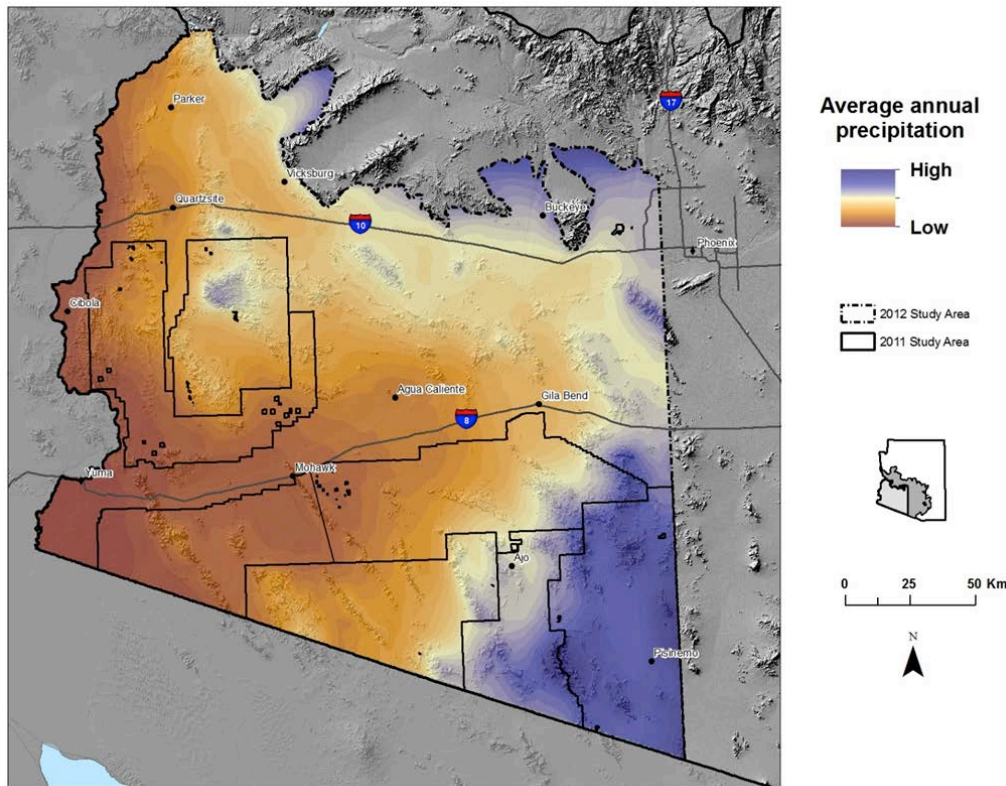


Figure 4: Example of a foundational data layer (average annual precipitation, 1991-2010) used to design a field sampling scheme for the Sonoran Desert.

The study area was characterized by high topographic relief, including mountain ranges separated by expansive desert valleys, plains, and bajadas, as well as numerous jurisdictional boundaries (Figure 5). Field sampling in 2011 covered 66,541 km². In 2012, we narrowed the field sampling area to 31,473 km², focusing on the southwestern portion of the original study area. This shift reduced heterogeneity in environmental conditions, allowing us to focus specifically on areas in and adjacent to BMGR and YPG (referred jointly hereafter as DOD lands), to elevate the power of our analyses, and to increase our ability to detect our target invasive plant species.

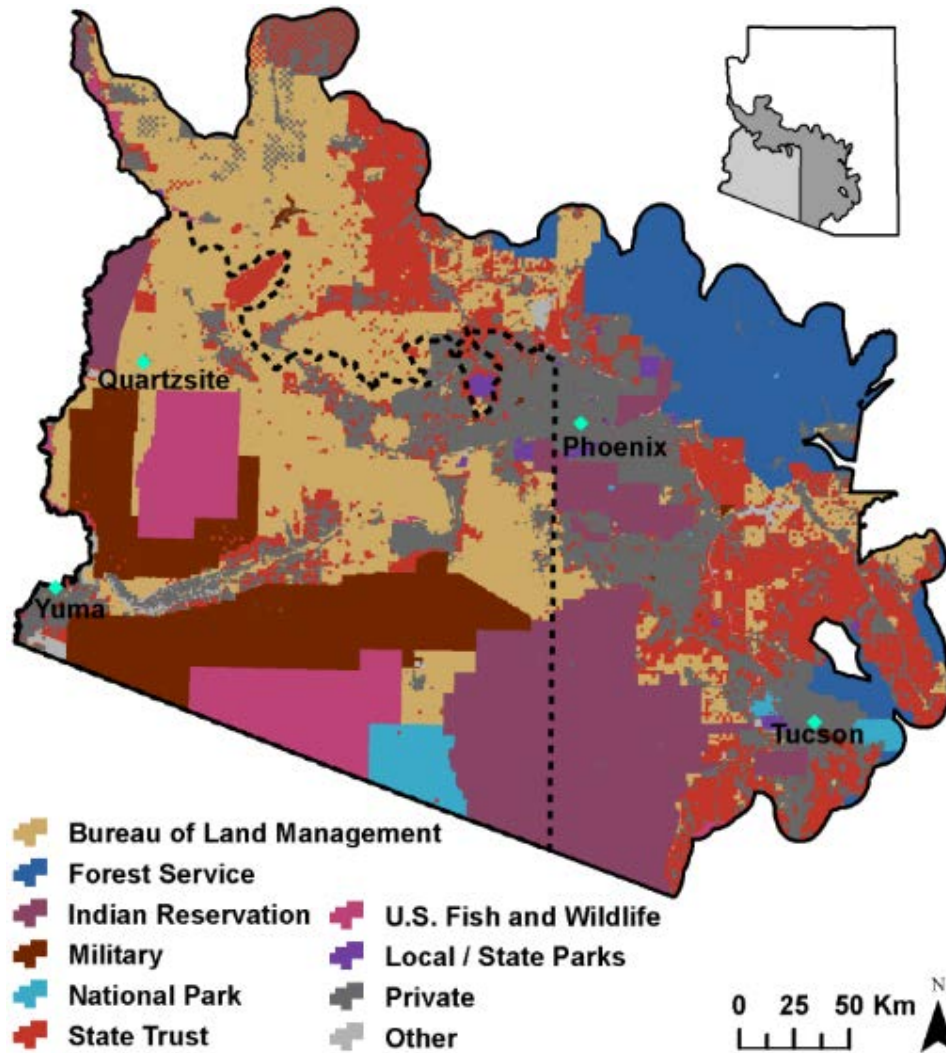


Figure 5: Boundaries of our study area in the Sonoran Desert of Arizona during the 2011 (solid line) and 2012 (dotted line) field seasons.

Suitability modeling to guide targeted sampling

Prior to our field efforts, we targeted five non-native invasive plants (Figure 6), including two annual C₃ grasses: *Bromus* and *Schismus* spp. (*Schismus arabicus* and *Schismus barbatus*; hereafter referred to jointly as *Schismus*); two annual cruciferous forbs: *Brassica* and *Eruca*; and one perennial C₄ grass: *Pennisetum*. Note that in 2012, we narrowed our focus to target only *Brassica*, *Schismus*, and *Eruca* since the 2011 field effort revealed only low incidence of *Bromus* and *Pennisetum* in and around DOD

lands. All five of these invasive species have been linked to increased fire frequency in desert ecosystems (Swetnam and Betancourt 1998, Tellman 2002, Weiss & Overpeck 2005).

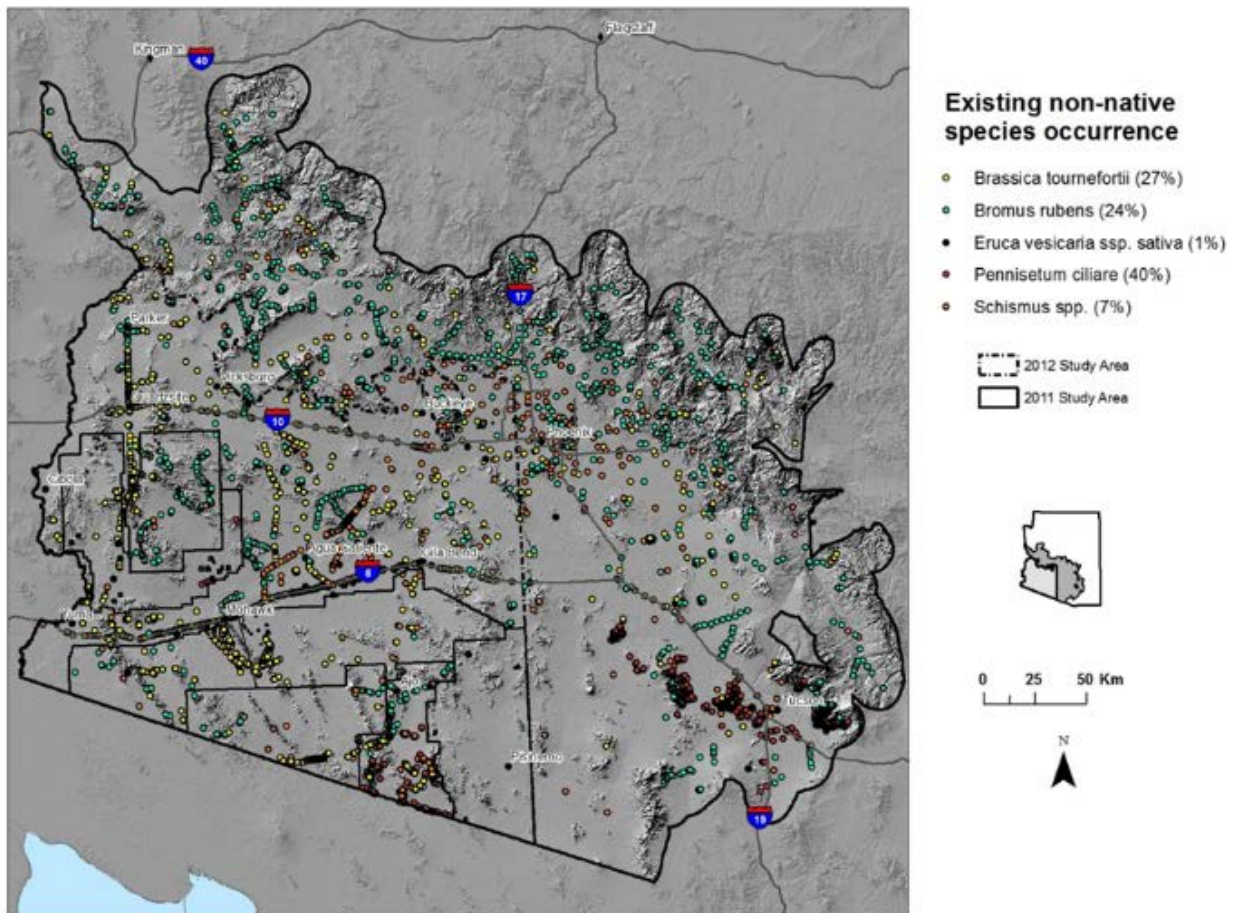


Figure 6: Previously mapped locations of five target species, which were used to guide field efforts in 2011 and 2012.

We designed a stratified sampling scheme to direct our field efforts (Wang et al. 2014; Figure 7). Stratification was based, in part, on predictions of habitat suitability for each target species and constrained to low slopes and proximity to roads in order to improve sampling efficiency and maximize detection rates over the large study area. These slope (<10 degrees) and road proximity (≤ 2 km from nearest road) constraints reduced the amount of effort required to access field locations, enabling us to increase sample size. Additionally, most of our focal species prefer soil conditions on low slopes. The road proximity threshold was based on the influence of roads as facilitators of invasion (e.g., enhanced moisture, fertilization, and dispersal) typical in the Sonoran Desert (Van Devender et al. 1997). We included all access roads visible in acquired data layers for sampling, such as rugged four-wheel-drive and off-highway vehicle roads with access to backcountry locations.

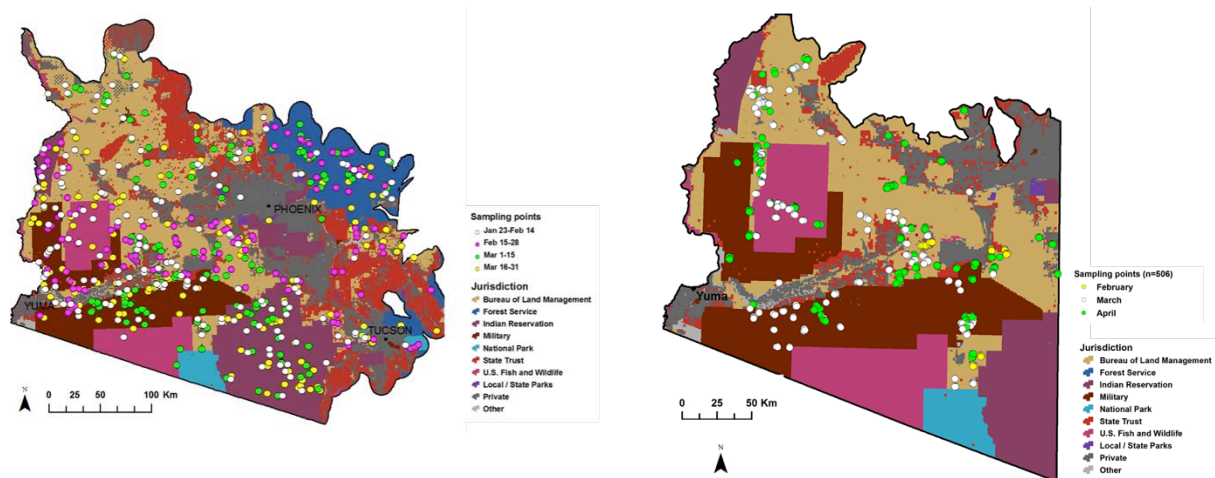


Figure 7: Points and jurisdictions sampled in 2011 (left) and 2012 (right).

To identify plot locations for empirical data collection, habitat suitability models (HSMs) for each target species were developed using the MaxEnt software package (Phillips et al. 2006). This modeling leveraged known locations of invasive plant occurrence, obtained from published and unpublished databases, including the Southwest Environmental Information Network (SEINET; <http://swbiodiversity.org/seinet/index.php>), the Southwest Exotic Mapping Program (SWEMP; <http://sbsc.wr.usgs.gov/research/projects/swepic/swemp/swempA.asp>), multi-year invasive survey data from managers of the BLM and National Park Service (NPS), and unpublished research data from local and regional biologists) (see Figure 6). From these records, we obtained geographic locations ($n=9,713$ total; 2,783 for *Bromus*, 615 for *Schismus*, 1,476 for *Brassica*, 95 for *Eruca*, and 4,744 for *Pennisetum*). Other suitability model inputs included spectral bands of August 2009 Landsat TM imagery (U.S. Geological Survey EROS Data Center, <http://edc.usgs.gov>), four topographic data layers derived from the National Elevation Dataset (NED, <http://ned.usgs.gov/>), average annual, summer and winter precipitation between 2000–2009 derived from the Parameter-elevation Regressions on Independent Slopes Model (PRISM, <http://www.prism.oregonstate.edu/>), and rasterized road data derived from the 2003 Tele Atlas Dynamap Transportation version 5.2 product (Spatial Insights, Inc.). For topographic variables, we smoothed the digital elevation model (DEM) to reduce visually discernible contour and point artifacts and derived slope and aspect variables (sine- and cosine-transformed to represent slope eastness and northness). We developed a weighted representation of suitable habitats using models assigning specific raster cell values (as weights of habitat suitability) to derive an inclusion probability for each sampling location (Stevens Jr and Olsen 2004, Theobald et al. 2007). Locations were balanced spatially and confined to the 90th percentile of predicted habitat suitability, gentle slope (<10 degrees) and road proximity (within 2 km of the nearest road). In other studies, stratification applied ensemble forecasting to combine multiple model outputs into a single projection for reducing individual model errors (Araújo & New 2007; Jones et al. 2010; Le Lay et al. 2010). However in our study, locations with the highest habitat suitability (i.e., 90th percentile) that were completely overlapped by all five HSMs for each species (described below) only covered <5% of the study area, making these areas less representative of habitat conditions across the region. Therefore, we combined multiple models as described below to target suitable habitats suggested by at least one of the five HSMs for each species as potential sampling locations. Each plot was spatially registered to a pixel from the MODIS (250-m resolution) that encompassed five subplots (Figure 8). Each of these subplots was then matched with a Landsat-5 Thematic Mapper (TM) pixel (30-m resolution). In the field, at 25 point-intercept locations within each subplot, we recorded presence of individual target plants as well as other data (see below).

We collected herbaceous biomass of native and non-native plants at nine of 25 point-intercept locations within each subplot.

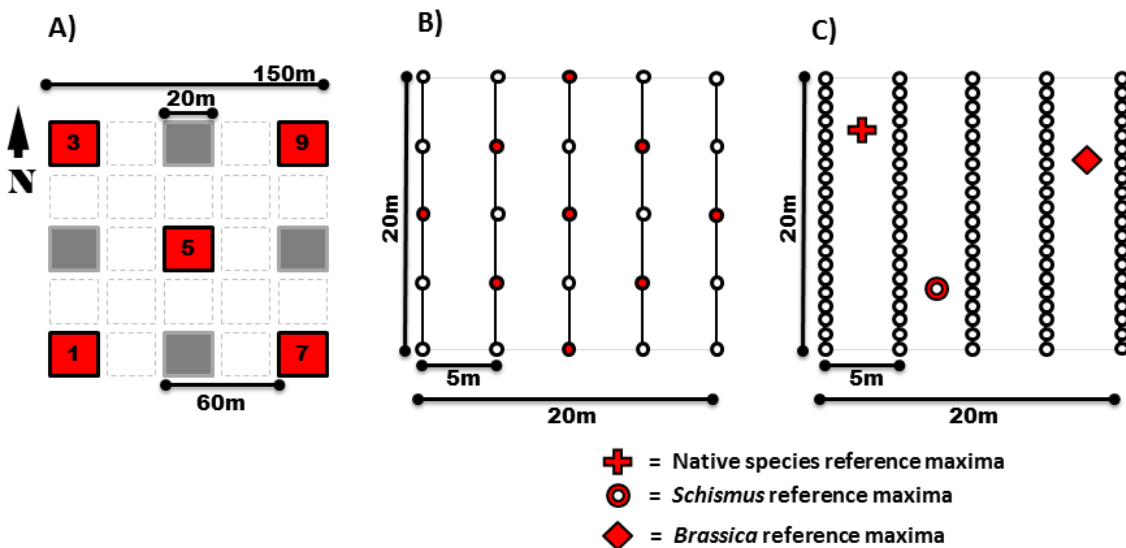


Figure 8: Spatially nested field sampling design used to detect and measure non-native invasive plants. A) 150-m plot nested within a 250-m MODIS pixel includes five nested subplots, each centered within a Landsat TM pixel. Target and alternate subplots are in red and gray, respectively. Subplot sampling varied from 2011 (B) to 2012 (C). B) In 2011, vegetation attributes were measured at 5-m intervals. Red circles indicate locations where biomass was collected. C) In 2012, vegetation attributes were measured at 1-m intervals along five transects, and biomass was estimated using an expedited comparative yield based method, which involved assessing the fraction of reference biomass at all point intercepts. Shown in red are hypothetical locations for reference maxima for native species, *Schismus*, and *Brassica*.

To characterize soil substrate types across the study area, we used the continuous spectral information obtained from six TM bands (bands 1–5 and 7) of eight Landsat image scenes (path/row p36/r37, p36/r38, p37/r36, p37/r37, p37/r38, p38/r36, p38/r37, and p38/r38) from August 2009. Qualitatively, spectral characteristics of soil substrates of high sand content or loose texture soils appeared to be highly related to the presence of three focal species (*Brassica*, *Schismus*, and *Eruca*). We obtained digital numbers for these radiometrically corrected TM images, converted them into spectral reflectance values, and mosaicked images using Environment for Visualizing Images (ENVI) version 4.7.1 (ITT Visual Information Solutions, Inc.). We employed linear spectral unmixing (e.g., Wang et al. 2014) to estimate the proportion of sand substrate per pixel and applied a pixel growing technique (e.g., Chen & Stow 2002) to extract adjacent pixels within two standard deviations of the mean value of seed pixels of pure sand. We used pixel values from the unmixing step to represent the proportion of a pixel dominated by sand and assigned five sandiness categories. We overlaid the sandiness category layer with a buffer range placed around the center pixel of a potential location to assign the sandiness based on a majority count of pixels. We directed our crews to focus, when logistically feasible, on accessible plot locations with high to medium sandiness.

We generated the summer Normalized Difference Vegetation Index (NDVI) for the study area using reflectance information of TM red and near infrared (NIR) bands (NIR-Red/ NIR+Red) to represent patterns of vegetation greenness. To quantify road proximity, we calculated the Euclidian distance from a raster cell to the nearest road. We obtained or derived all variables at a 30-m pixel resolution using ArcGIS version 10.0 (Esri, Inc.).

Using the methods and variables described above, we developed five separate HSMs for each species (total = 25 models) using a maximum entropy algorithm and the MaxEnt software package version 3.3.3e (<http://www.cs.princeton.edu/~schapire/MaxEnt/>) (Elith et al. 2006; Phillips et al. 2006). For HSMs that rely solely on presence-only data and are thus limited to sites that have been comprehensively surveyed, environmental conditions are typically represented by occurrence records and background data describing the entire region, with species occurrence data spatially biased toward locations with easy access. To account for such bias, it is suggested that selection of background sample locations be performed according to the same sampling bias as that identified for species presence records (Phillips et al. 2009). We employed a “bias prior” approach to derive background data based on the density of sampled locations of all focal species across our study area and to estimate relative sampling effort as recommended by Merow et al. (2013). We assigned a raster cell value of 1 to cells with presence records of focal species to represent sampling intensity and a “no data” value for the remaining cells (Syfert et al. 2013). Five separate HSMs were constructed for each target species, to investigate the influence of combined environmental variables. Detailed information about the specification for each model and the relationship between models can be found in Table 2.

Table 2: Description of the variables included in habitat suitability models 1-5. An ‘X’ indicates that the given variable set was included in the predictor set for the model. Only one of mean summer or mean winter precipitation was used in models 4 and 5, depending on the species (summer precipitation for *Pennisetum*, winter precipitation for all other species).

| Variable type | Description | Model number | | | | |
|---------------------------|---|--------------|---|---|---|---|
| | | 1 | 2 | 3 | 4 | 5 |
| Topography | Elevation, slope, eastness, and northness | X | X | X | X | X |
| Spectral bands | TM bands 1-5, 7, and NDVI | X | X | X | X | X |
| Precipitation (2000-2009) | Mean annual precipitation | X | X | | | |
| | Mean summer precipitation (7-81 mm)* | | | | X | X |
| | Mean winter precipitation (10-103 mm)** | | | | X | X |
| Road proximity | Euclidean distance to the nearest road | | X | X | | X |

Each of the 25 resulting models included a bias estimate and employed the hinge algorithm (a piece-wise linear regression) to produce ten replicates at the convergence threshold of 10^{25} (i.e., where model training terminated in terms of log loss per iteration). We used 60% of the total available occurrence data for model training and the remaining 40% for testing (Elith et al. 2006; Phillips & Dudík 2008). We evaluated the contribution of each variable by randomly permuting the values of that variable among the presence and background training points and measuring the resulting decrease in training area under the receiver operating characteristic (ROC) curve (AUC) (Phillips 2005). A large decrease indicated a strong dependence on that particular variable. As another assessment of variable importance, we omitted each variable in turn and then used it in isolation (Phillips 2005). The use of training and test gain provided an assessment of the amount to which the variable, when omitted or used alone, affected model gain. By contrast, the use of AUC provided information on how the variable influenced the model in predicting presence in the data.

To evaluate model performance, we used three threshold independent assessment measures. This enabled us to avoid using arbitrary binary threshold presence/absence when the assumption for the threshold could not be validated. We constructed null models using random points to confirm that our HSMs for each species had significantly higher values of training AUC than did random models ($\alpha = 0.05$) (Raes & ter Steege 2007). We used AUC values of > 0.70 to determine acceptable model performance

(Swets 1988; Hosmer Jr & Lemeshow 2004). We calculated the point biserial correlation (COR) as a Pearson's correlation coefficient r between predicted suitability and presence/pseudo-absence of the test data to examine the relationship between predicted suitability and the probability of presence of each focal species ($\alpha = 0.05$) (Phillips & Dudík 2008).

Winter precipitation in 2010-2011 was below average across the region, and subsequent winter germination, cover, and biomass of both natives and invasives were consequently low. Modifications to our sampling protocols in 2012 were intended to increase sample size and target species detections, and to improve biomass sampling efforts. In addition, 2012 sampling efforts targeted areas where *Brassica*, *Schismus*, and *Eruca* were known or likely to occur. We developed new habitat suitability models using the data collected in 2011 to supplement primary source data used for landscape stratification, and the 70th percentile of suitability based on these new models was targeted in 2012. We further restricted areas for sampling using the relative NDVI of MODIS imagery obtained in 2012: that is, we limited sampling to areas in which the maximum spring NDVI divided by the mean spring NDVI between 2001 and 2010 exceeded the 60th percentile. This calculation identified locations that had very high relative vegetation 'green-up,' compared with average greenness, in indication of particularly strong herbaceous growth during a very wet growing season. Plots were further stratified to target locations with greater than average MODIS NDVI acquired in early 2012. This focused sampling on areas that had received sufficient precipitation in winter 2011/spring 2012 to initiate germination and seedling growth, and is important in the target system because there is high spatial variation in individual desert precipitation events.

We used more of a 'clustered' sampling design in 2012 to increase our sample size by reducing travel time among sampling locations (Figure 7). Despite potential bias introduced by sampling at clustered locations, certain statistical estimators can provide unbiased estimates of abundance and density for species with low abundance in local populations (Philippi 2005; Sullivan et al. 2008). To perform this sampling, we first identified a pool of 2,500 stratified random, spatially balanced sampling locations. We then constrained this pool of potential sampling locations to clusters of 4-5 locations within 450-650 m of one another. Each location relied on the same plot and subplot configuration used in 2011, and field methods were similar between years (Figure 8). Crews sampled an average of five clustered plots per day, maintaining a minimal travel distance between daily clusters of 10-20 km. Within five subplots at each plot, biomass was collected at zero, one, or two subplots. We used a modified 'comparative yield method' to estimate biomass production (Haydock & Shaw 1975). That is, at each subplot, we rapidly identified the presence of our target species (non-native herbaceous cover types) as well as native herbaceous cover types (e.g., perennial grass, annual grass, forb). We then systematically evaluated the maximum biomass of each herbaceous cover type within the subplot by clipping biomass of the target species and native herbaceous species within a 0.25 m² hoop (BLM 1996; Despain & Smith 1997) at the two respective locations, and labeled these values as reference maxima for each cover. Samples were oven dried and weighed to obtain dry weights of maximum herbaceous biomass for native and non-native plants. We used point intercept sampling at 1-m intervals along five 20-m transects to record the presence of each target species and herbaceous cover type. Herbaceous cover was ranked as a fraction, in increments of 25%, of the reference maximum for that cover type. Subplot herbaceous biomass was estimated by multiplying the percentage of intercepts of each herbaceous cover type by the mean biomass rank for that cover type, summed over all cover types within a subplot. A schematic of the layout of the subplot with three example reference maxima is given in Figure 8C.

Relating habitat suitability models to field detections in 2011

We used a generalized linear model (GLM) that assessed detection (as a binary presence/absence outcome for each focal species at each subplot) and habitat suitability, as predicted by each HSM. We

modeled the detection of each focal species with a binomial distribution and a logit link function in the R statistical package version 3.0.2 (<http://www.r-project.org>). This analysis provided an indication of how well the HSM-informed stratification identified sampling locations where species detections were more likely. To assess model fit, we calculated the difference in values of Akaike's Information Criterion (Δ AIC; Burnham & Anderson 2002) between a detection model that included predicted habitat suitability and an intercept-only model. Suitability models with Δ AIC >10 were considered good approximations of the data (Burnham & Anderson 2002).

Task 2: Field sampling efforts

To match our field data to the spatial resolution of the remote sensing platforms we sought to use for occurrence modeling, we adopted a nested plot design creating approximate alignment between sampled locations and satellite image pixels (Kalkhan et al. 2007, Wang et al. 2014). We spatially geo-registered each plot with a MODIS image pixel (250 x 250 m) and geo-registered each of five nested subplots with a Landsat TM image pixel (30 x 30 m; Figure 8A). This process precisely matched field data with the pixel location and resolution of both sensor types (i.e. MODIS and TM) used for developing time-series and phenology-based models of non-native invasive plant occurrence (Olsson et al. In prep.). Co-registered and multi-scaled plots were used to reduce error introduced by mismatches of scale and location between field and remote sensing data (Xu et al. 2009). In the field, crews used the geographic coordinates of the pixel corner of subplots and navigated to the corner using a Magellan MobileMapper 6 Global Positioning System (GPS) receiver. At point intercepts within subplots, placed along five transects at every five meters, we recorded species name and substrate at each point intercept for both native and non-native invasive plants, as well as presence/absence of our focal species and disturbance types.

Task 3: Acquire and process existing satellite data

A major goal of this research was to assess satellite image trajectory-based invasive plant detection and mapping approaches. We investigated two particular approaches to do this: a multi-temporal multispectral approach based on Landsat Thematic Mapper (TM) and MODIS, and a multi-temporal hyperspectral approach designed to test the feasibility of the future planned Hyperspectral Infrared Imager (HypSIIRI) mission. Testing of the hyperspectral approach was the second of two Go/No-Go decision points for this project (see below). In light of our decision to not proceed with this approach (No-Go), we performed an alternative task (focused on use of WV2 imagery; see below) with the potential to be more relevant to DOD and adjacent land managers, given ongoing and mounting challenges faced by National Aeronautics and Space Administration's (NASA) Earth Observation program.

We acquired all available cloud-free Landsat TM and MODIS composite vegetation index (VI) data (MODQ13A1) for the study area for the time period from January 1, 2000, to June 1, 2012. Vis, such as NDVI are correlated with photosynthetic activity and are sensitive to differences in plant production, leaf area index, and phenology cycles (Steltzer & Welker 2006; Pennington & Collins 2007). We derived models at the 30-m and 250-m resolution for Landsat TM and MODIS-based models, respectively. The models were based on common treatment of dynamic (e.g., satellite imagery) and static (e.g., topography) data. Spatial data were derived from three data sources: MODIS satellite imagery, Landsat TM satellite imagery, and NED 30-m data products. MODIS satellite imagery was used to derive phenology estimates for each season (winter/summer) and year, whereas TM and NED datasets were used as static layers to account for albedo and topography, which were consistent over our period of study (Crist 1985).

The WV2 satellite remote sensing system is a relatively new, high spatial resolution (2.4 m pixels) sensor that produces 8-band multispectral imagery (Kruse & Perry 2013). WV2 has the capacity

to enable detection of small populations of desert plants due to its high spatial and spectral resolution and bands in the red (630 to 690 nm), red edge (705 to 745 nm), and near-infrared (770 to 895 nm and 860 to 1040 nm) spectral regions. Vegetation classification potential of WV2 imagery has been demonstrated for forested environments, where the high spatial resolution allowed classification accuracies of 98% (Ozdemir & Karnieli 2011; Garrity et al. 2013). Latif et al. (2012) and Immitzer et al. (2012) used the high spectral resolution of WV2 imagery to successfully differentiate tree species (overall accuracy of 82%), although producer's accuracy (or the probability that pixel classifications correctly represented ground cover) at the species level ranged from 33% to 92% (Immitzer et al. 2012). Other demonstrated uses of WV2 data have included increased classification accuracy for tree species differentiation in a savanna ecosystem (Cho et al. 2012), delineation of cover types in urban areas (Zhang & Kerekes 2011; Longbotham et al. 2012; Pu & Landry 2012), and coral reef detection in marine environments (Botha et al. 2013). The utility of WV2 imagery for mapping invasive plants is likely to be powerful in hot desert environments, where invasive species can exhibit large interannual variability in distribution and abundance.

Because they were tied directly to the development of non-native mapping steps and products, additional, specific data acquisition and processing steps are detailed in Task 6 below.

Task 4: Acquire and process ancillary spatial distribution data

Ancillary spatial data associated with this task are described in Task 3 above, as well as steps taken in non-native mapping efforts (Task 6).

Task 6: Non-native mapping (Landsat/MODIS/WV2)

We applied a range of methods to different efforts to model and map the distribution of our non-native target species. Here we detail five distinct efforts.

A comparison of Landsat TM and MODIS vegetation indices for estimating phenology⁵

For this mapping effort, our primary objective was to identify the best available VI and image data source to estimate annual and seasonal vegetation phenology in areas of steep terrain, testing our approach on areas occupied by sensitive species of wildlife. We also explored image-processing methods to reduce atmospheric and terrain impacts on TM data and determined relationships between 2007 and 2008 weather patterns and VI variability.

A time series of VI values for the full 2008 calendar year was used to estimate phenologic cycles and periods of increased plant productivity (green-up) for single image dates relative to average annual vegetation conditions. Pixel values indicate either a greener than average (positive departure from the annual average) or less green (negative departures) per-day quantity for locations on the ground. Departures from average (DA) values provide a standardized scale to quantitatively compare different VI for characterizing vegetation green-up and senescence periods.

A total of 13 cloud-free TM images and 23 MODIS 16-day VI were downloaded from the USGS Global Visualization Viewer (<http://glovis.usgs.gov/>). An atmospheric correction was applied to TM images using ENVI v4.5 software and the Fast Line-of-sight Atmospheric Analysis of Spectral Hypercubes (FLAASH) model (ITT Visual Data Solutions 2008) prior to deriving VI. This processing corrects for upwelling path radiance scattered from adjacent pixels. We compared corrected and uncorrected red and NIR TM bands used to derive VI for invariant sand targets (pixels) on relatively level terrain.

⁵ These methods have been peer-reviewed and published in Sesnie, S. E., B. G. Dickson, S. S. Rosenstock, and J. M. Rundall. 2012. A comparison of Landsat TM and MODIS vegetation indices for estimating forage phenology in desert bighorn sheep (*Ovis canadensis nelsoni*) habitat in the Sonoran Desert, USA. *International Journal of Remote Sensing* 33:276-286.

To examine terrain effects on VI, we identified areas potentially shaded at some times and locations unlikely to be shaded by surrounding terrain at any time of the year using NDVI and EVI values to obtain the percentage departure value of pixels. Although the amount of plant production differs among sites, temporal patterns in plant phenology, driven by seasonal rainfall and day length influencing the amount of photosynthetically active vegetation, are expected to be similar. Thus, low-productivity sites characteristic of arid lands will be likely to show positive departures from the annual average VI values when even minor increases in green vegetation occur (Van Leeuwen et al. 2010). DA values were calculated as follows:

$$DA = \frac{VI_s}{VI_m}$$

where VI_s is the VI value for a single image date, and VI_m is the mean pixel value for the time series. DA is calculated for a particular image date in the series multiplied by 100 to estimate each pixel's percentage departure from the annual average (Beck & Gessler 2008).

We developed a hillshade model using a 30-m DEM and spatial analyst extension in ArcGIS v. 9.3. The model predicts shade based on the predicted shadows cast at the lowest sun elevation angle (28.7°) and highest solar azimuth (151.7°), to match a January 2008 TM image date. Areas greater than 5 ha in size with a hillshade value of 0 (shaded areas) were used to identify and extract shaded VI pixels from all image dates. To identify unshaded pixels, 100 random points were distributed across the study area on slopes <1%. Each point was buffered with a 1500 m radius polygon. Polygons located over areas of contiguously low slope angle ($n = 27$) were used to identify non-shaded VI pixels from the image time series. To assess the sensitivity of VI to topographic relief, quantitative comparisons were made between (1) mean NDVI and EVI DA' values extracted from shaded areas at each image date and (2) mean VI values extracted from each shaded area during the month of January, when sun angle was lowest. Data were evaluated for normality using a Kolmogorov–Smirnov test and compared using nonparametric Mann–Whitney rank sum or t -tests ($\alpha = 0.05$) using the SigmaPlot v. 11 statistics software package (Systat Software 2008). MODIS-based VIs were also compared by examining residual DA values for each month on both shaded and unshaded terrain. The absolute difference between EVI and NDVI departure values in shaded areas were compared to the absolute difference between the two VIs in unshaded areas using a Mann–Whitney test.

Temperature and precipitation data collected between January 2007 and December 2008 were used to determine linkages between VI and periods of increased desert vegetation productivity and green-up.

Use of WorldView-2 high spatial resolution imagery to detect desert invasive plants⁶

For this analysis, our objectives were to: (a) examine the utility of WV2 data for mapping small populations of *Brassica* in the Sonoran Desert study region, and (b) compare WV2 classification performance with the more readily available Landsat Enhanced Thematic Mapper Plus (ETM+) imagery. Through this comparison, we evaluated whether higher spatial and spectral resolution imagery could improve detection of small populations of invasive plants in desert environments. Importantly, this new effort was approved by Strategic Environmental Research and Development Program (SERDP) program staff in place of subtask 12.2.

⁶ These methods have been peer-reviewed and published in Sankey, T., B. Dickson, S. Sesnie, O. Wang, A. Olsson, and L. Zachmann. 2014. WorldView-2 high spatial resolution improves desert invasive plant detection. *Photogrammetric Engineering and Remote Sensing* 80:885-893.

Field Data Application

Field data on the presence or absence, cover, and biomass of *Brassica* was collected at multiple sampling locations between February and April 2012. Prior to field sampling, the study area was stratified as described above, based on a species distribution model for *Brassica* and a prediction of habitat suitability. The approach used specific raster cell values (i.e., weights of habitat suitability) to determine the inclusion probability of a location to be sampled (Stevens Jr & Olsen 2004; Theobald et al. 2007).

At each sampling subplot, we navigated to the southwest corner. The entire subplot was searched systematically to determine the presence or absence of the target plant species, *Brassica*. Next, the point intercept method was used to record the presence or absence of the target species and three other herbaceous cover types: perennial grass, annual grass, and forb. The point intercept method was employed at 1 m intervals, resulting in a total of 100 points per plot, which were then directly converted into percent cover estimates of the target species and the three herbaceous cover types at the 30 m plot scale.

Image Preprocessing

To evaluate non-natives in our study area, images from both WV2 and ETM+ satellite sensors were collected during the peak winter growing season period for native and non-native annual plants. Ten WV2 scenes from the study area were selected. The swath width of each WV2 scene is 16.4 km. The scenes were acquired between 04 to 10 February 04 2012 and delivered in calibrated radiance in 2.4 m resolution with ~5 m geometric accuracy. Multispectral bands were delineated: coastal (0.477 μm), blue (0.477 μm), green (0.546 μm), yellow (0.607 μm), red (0.658 μm), red edge (0.723 μm), near-infrared 1 (0.831 μm), and near-infrared 2 (0.908 μm). One ETM+ scene (Path 38 and Row 37) from 23 February 2012 was used, encompassing all of the WV2 scenes, with all bands except band 6. To preprocess images, both the WV2 and ETM+ data were corrected for atmospheric effects using the FLAASH module in ENVI image processing software v. 4.8 (ITT Industries Inc., 2008, Boulder, Colorado) and projected in UTM Zone 11N and NAD 1983 projection and datum. The WV2 images were orthorectified using a 10-m DEM (www.ned.usgs.gov). All images were co-registered to orthorectified 2007 NAIP digital imagery. All Root-Mean-Square error (RMSE) were < 1 pixel).

Calculation of NDVI

WV2 data have two near-infrared bands: band 7 (0.831 μm) and band 8 (0.908 μm). Each near-infrared band allows the calculations of an estimate of NDVI (hereafter referred to NDVI-B7 and NDVI-B8, respectively). NDVI-B7 and NDVI-B8 were calculated using the following equations for both WV2 and the resampled WV2. ETM+ NDVI was also calculated using the bands 3 and 4:

$$NDVI = \frac{B5 - B7}{B5 + B7}$$

$$NDVI = \frac{B5 - B8}{B5 + B8}$$

MTMF Classification

Mixture-Tuned Matched Filtering (MTMF) is a spectral mixture analysis technique which estimates the relative proportion or abundance of a target cover type within each pixel (Root et al. 2004; Hunt Jr & Parker Williams 2006; Mladinich et al. 2006). Spectral mixture analysis techniques are especially useful in arid and semi-arid environments, where a mixture of bare ground and vegetation is common within pixels (Noujdina & Ustin 2009; Sankey et al. 2010). Linear spectral mixture analysis produces a mixture

representing a linear combination of the cover types weighted by the coverage of each cover type in a pixel (Rencz 1999). Compared to linear spectral unmixing models, MTMF suppresses background noise and provides a measure of false positive detection of target cover (Boardman 1998), which can occur frequently in remote sensing of arid and semi-arid vegetation (Okin et al. 2013).

To estimate sub-pixel *Brassica* abundance and map its presence/absence, all images from our study area were forward transformed using the Minimum Noise Fraction (MNF) rotation and classified using the MTMF technique in ENVI software. The MTMF classification was performed with: (a) WV2 imagery in their original pixel size (hereafter referred to as WV2), (b) WV2 data resampled to a 30-m pixel size (hereafter referred to as resampled WV2), and (c) ETM+ imagery.

An advantage of the MTMF technique is that it requires endmember (EM) training spectra for target species as inputs, but does not require training spectra for background or non-target species. EM spectra for *Brassica* was derived from field measurements of healthy green *Brassica* plant canopy reflectance (350 to 2500 nm) using an ASD, Inc. FieldSpec 3Max spectrometer. Reflectance was measured via a series of five assessments (25 replicates per measurement) per plant using a bare fiberoptic cable with a 25° field of view at 45 cm above plants with dense, closed canopies. Reflectance was calibrated between samples using a non-calibrated diffuse white reference panel (ASD, Inc., Boulder, Colorado). Spectrometer measurements were acquired under clear sky conditions within one hour of solar noon on 24 February 2012. The mean value for all *Brassica* reflectance spectra was used as a single composite EM.

The MTMF classification produces two images that can be used together to classify a target cover: (a) matched filtering (MF) scores that estimate the target cover abundance within each pixel, and (b) infeasibility values which represent the likelihood of false positives in the MF scores. An MF score near 0 indicates background noise, while a score of 1 corresponds to approximately 100% cover of the target spectrum within a pixel. MF scores have been used to directly estimate sub-pixel target cover abundance, and have demonstrated correlation with field-based estimates of target canopy cover (R^2 ranging from 0.32 to 0.69) (Williams & Hunt 2002; Mundt et al. 2007; Mitchell & Glenn 2009; Sankey & Glenn 2011). MF, however, tends to underestimate abundance and present a complex mathematical problem (Mitchell & Glenn 2009) because unconstrained estimates within pixels can result in negative target cover values as well as values greater than 100%, representing a disconnect with field-based cover estimates ranging from 1 to 100%. There is in addition no automated method to combine the MF scores with the infeasibility values to reduce false positives in MF.

For these reasons, a user-defined approach was used to produce a final map of target cover (Mundt et al. 2007). The relationship between the MF scores and infeasibility values for all images was examined using a regression approach (Sankey et al. 2010). The best fit regression model was chosen for each image type based on its statistical significance ($\alpha = 0.05$ for all variables), the value of the coefficient of determination (R^2), and model simplicity (i.e., fewer variables were preferred over more complex models with small increases in R^2). Three quadratic polynomial regression models were chosen to combine the MF scores and the infeasibility values in the WV2, resampled WV2, and ETM+ images, respectively:

$$Y = 2.34 + 22.59*MF + 103.72 *MF^2$$

$$Y = 2.39 + 28.53*MF + 507.84* MF^2$$

$$Y = 0.64 - 0.97*MF + 0.05* MF^2$$

where the infeasibility values were the response variable and the MF scores, and quadratic terms were the predictor variables. After the regression models were fit to each image, all pixels that fell below one

positive standard deviation above the regression curve and had MF scores of 0 to 1 were classified as *Brassica* presence, with other pixels classified as *Brassica* absence. This approach allowed exclusion of negative and >1 MF scores, which fall outside the field-based estimates of canopy cover and indicate target cover absence. The regression curve provides an objective and quantitative approach for determining a threshold in the infeasibility values. The positive standard deviation above the regression curve increases true positive detection by raising the upper limit of the infeasibility values while still limiting unacceptably large infeasibility values and keeping the MF scores within the 0 to 1 range (Sankey et al. 2010). No minimum threshold was necessary for the low infeasibility values. Using these methods, three separate binary maps of *Brassica* presence/absence were produced: one at 2.4m resolution and two at 30 m resolution.

Accuracy Assessment

Field data were used to assess the accuracy of the binary classifications of *Brassica* presence/absence (Story & Congalton 1986). The binary map at 2.4 m resolution was compared to field point data gathered along the line transects. Of a total of 27,100 field points, 700 points (equally divided between presence and absence) were randomly selected over the entire area encompassing the images, ensuring that the selected points were spatially independent to minimize spatial autocorrelation. The field-mapped points were buffered with a 30 m radius to re-enforce a minimum distance between the selected points, because (a) point intercept sampling was used at intervals of only 1 m, and neighboring points could be highly spatially autocorrelated, (b) GPS horizontal errors ranged up to 6.7 m, and (c) the WV2 data geometric accuracy was 5 m with RMSE <1 pixel. The buffering ensured that absence points with no target species present within a distance of two pixels were selected as absence pixels. The two binary maps at 30 m resolution were compared to a set of similarly selected random points of *Brassica* presence ($n = 370$) and absence ($n = 524$) within the 30 m plots.

MF scores were also correlated with the field-based *Brassica* percent cover estimates using a simple linear regression. Only the resampled WV2 and ETM+ MF scores were analyzed, since *Brassica* percent cover estimates were made at the 30 m plot scale. *Brassica* percent cover estimates were divided into three bins with 10 percent incremental increase (i.e., 1 to 10%, 10 to 20% and >20%) to determine if a potential detection threshold existed.

Last, the maximum biomass references for *Brassica* and native herbaceous cover measured at the point locations were correlated with the WV2 NDVI estimates, while the *Brassica* biomass and total herbaceous biomass estimates at the 30 m plot scale were correlated with NDVI estimates from the resampled WV2 and ETM+.

Target-based mapping using field-based spectra and WorldView imagery

We recently developed new methods using WorldView-2 that data were effective for mapping *Brassica* in the Sonoran Desert (Sankey et al. 2014). We extended these methods to another highly invasive non-native plant, *Eragrostis*, in the spatial context of semidesert grasslands on Buenos Aires National Wildlife Refuge (BANWR) located in southern Arizona (Figure 9).

Eragrostis has replaced native grasses and formed extensive areas of high biomass on BANWR exceeding 1200 kg/ha (Sesnie, unpublished data). Our specific objectives were to 1) collect target invasive plant field spectra and WorldView-2 (WV2) imagery over areas of high and low target species abundance, 2) develop spectral mixture analysis techniques for mapping target species, and 3) compare detection methods using field- and image-collected spectra to intensively sampled field plot and cover data to assess accuracy.

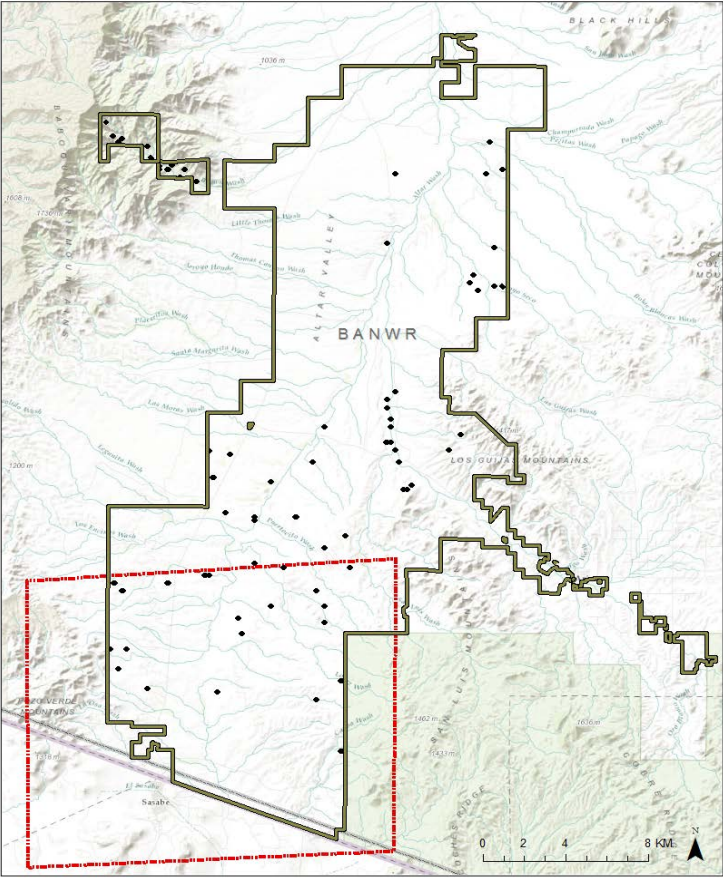


Figure 9: Focal area (red boundary) for detection of *Eragrostis* detection using WorldView-2 on BANWR (black boundary). 2013 sample plots are represented as black dots.

Analysis approach

Combining surface reflectance from satellite imagery and target spectra have been found to reduce uncertainty of vegetation classification (Asner & Green 2001). We tested two techniques to detect and map *Eragrostis* with WV2 reflectance and species reflectance data. One technique used spectra collected in the field with an ASD FieldSpec3 and the other used image-collected spectra from plot locations with high target species cover $\geq 45\%$. Previous studies have applied sub-pixel classification techniques, such as the MTMF with coarser resolution data such as Landsat TM and ETM+ (Root et al. 2004, Mladinich et al. 2006, Williams & Hunt 2002). These techniques have not been widely applied to a new generation of high-spatial and moderate spectral resolution satellite sensors. We combined field spectra with high spatial and spectral resolution WV2 imagery and advanced target detection method of MTMF (see above) to map invasive plants. One of the MTMF products is the MF scores, which estimate the target cover abundance within each pixel. MF scores have previously been shown to provide a direct estimate of sub-pixel target cover abundance and correlated with field-based estimates of target canopy cover (Williams & Hunt 2002, Mitchell & Glenn 2009).

Image acquisition

We used WV2 sensor satellite imagery data acquired 29 Sept 2013 at the basic 1B level of calibrated radiance during the peak summer growing season with no cloud cover. Multispectral bands were used in this study: coastal (0.427 μm), blue (0.478 μm), green (0.546 μm), yellow (0.608 μm), red (0.659 μm) red edge (0.724 μm) near-infrared 1 (0.831 μm) and near-infrared 2 (0.908 μm). The image was

orthorectified (ERDAS 2013; $RMS \leq 0.5$) and we applied radiometric calibration and atmospheric correction using FLAASH with the ENVI 5.2 (Exelis Visual Information Solutions, Boulder, Colorado) convert at sensor reflectance to surface reflectance values. This step was used to assure that target species spectral reflectance values in the WV2 image match those collected from plants on the ground as closely as possible. A potential disadvantage of WV2 sensor is that it does not collect data in spectral regions sensitive to aerosols and water vapor that are now integrated into the WV3 sensor for atmospheric correction, similar to other satellite sensor technologies such as Landsat 8 and MODIS (Roy et al. 2014).

Field plot data collection

Plant canopy cover measurements on plots (2012-2014) followed peer-reviewed techniques described in the NPS Sonoran Desert Network (SODN) Terrestrial Vegetation and Soil Monitoring Protocol and Standard Operating Procedures that incorporate fuels and other fire related measurements (Hubbard et al. 2012). Vegetation plots measured in 2013 also follow NPS protocols. Point intercept methods were used to measure species, height and cover for trees, grasses, forbs, shrubs and subshrubs on plots. A total of six 20-m transects spaced 10-m apart were used to record plant genus and species at each 0.5 m interval along a tape ($n = 240$ intercepts/plot, Figure 10). Percent plant canopy cover by species was estimated on each plot using number of intercepts per species $\div 240 * 100$. For remote sensing applications, a data processing script was developed to use point intercepts from the tallest of three height strata (0.0 – 0.50 m, 0.50 – 2.0 m, >2.0 m) with a plant species recorded to estimate percent overstory plant canopy cover. All plot and plant species data were processed using the R statistics package v. 3.1.2 (R Core Team 2015). All plots were georeferenced with a Trimble GeoXT with GPSCorrect and differentially corrected to within 1-m horizontal accuracy using GPS Pathfinder Office software v. 5.6 (Trimble Navigation Ltd. 2013).

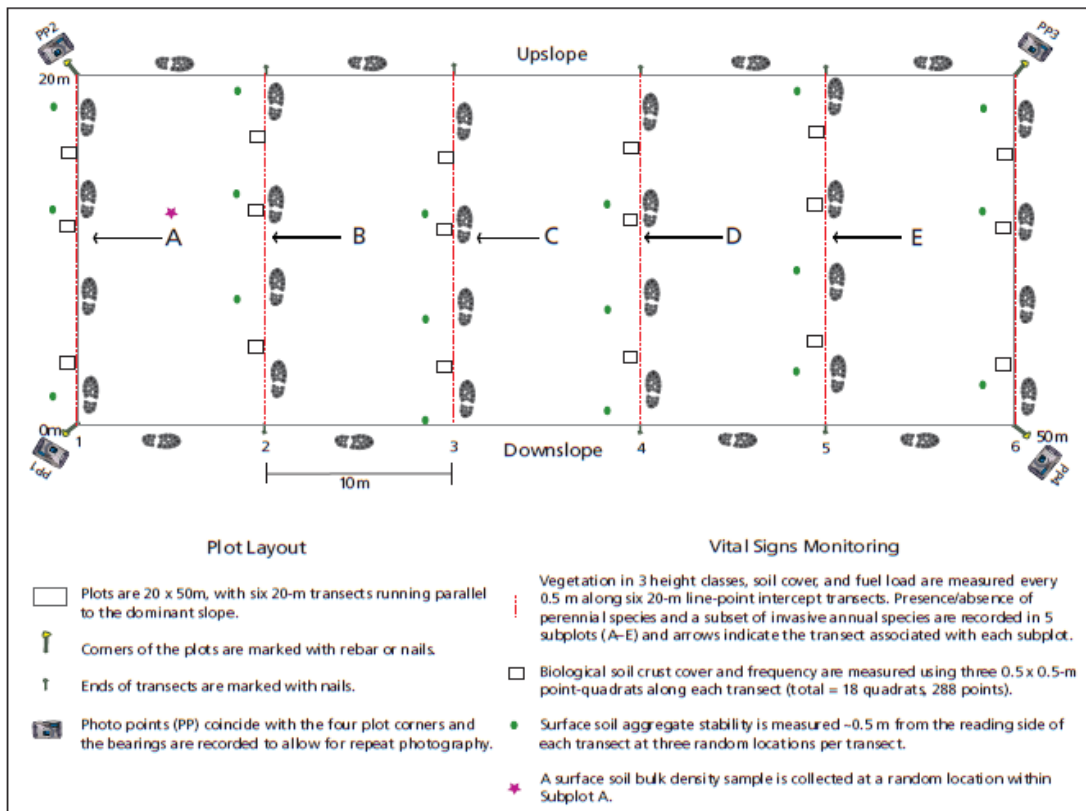


Figure 10: Vegetation plot sampling methods from Hubbard et al. (2012).

Field spectra collection

Field-based *in-situ* spectral radiance measurements from target *Eragrostis* and non-target classes were collected with bare fiber, between 10am – 1pm, within one meter of the target object throughout BANWR with the Analytical Spectral Device (ASD) FieldSpec 3 Max portable spectrometer during August 2014 (Figure 11a). Its wavelengths range from 350 - 2500 nm, collecting across the VIS/NIR/SWIR spectrum, with a sampling interval 1.4 nm for the spectral region 350 – 1000 nm and 2.0 nm for spectral region 1000 – 2500 nm, and a spectral resolution of 3-10 nm (ASD, 2008). Reflectance was calibrated between samples using a non-calibrated diffuse white reference panel. We calculated relative reflectance for each class in ViewSpec Pro 6.2 (ASD, Inc. Boulder, CO) with 5 measurements of 2 acquisitions of each object's radiance values. This process calculated the mean spectral reading for each of 8 classes and converted them to reflectance values. The mean value for all Lehman and each non-target species was used as the composite EMs. These reflectance spectra were taken into ENVI 5.2, converted to a spectral library, convolved to WV-2 reflectance spectra, which reduce the available band wavelengths to 350 – 950 nm (Figure 11b). These wavelengths provided the basis for field-collected spectra EMs for WV2 image classification.

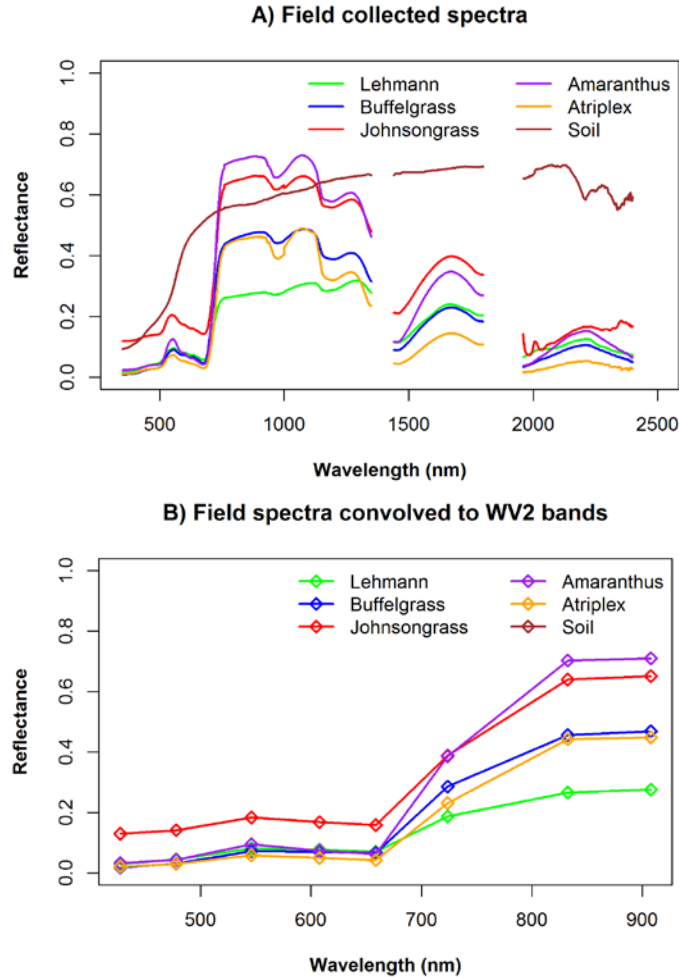


Figure 11: To integrate field-collected spectra with a data sensor, spectra must be convolved (or cleaned and fit) to that sensor's bands. A) Field collected target and non-target spectra prior to convolve and B) field collected target and non-target spectra convolved to WorldView-2 imagery.

Image-based spectra collection

Image-collected spectra or EM pixels representative of species targets (e.g. *Eragrostis*) were selected from field plots with high percent cover. To select EMs and reduce temporal variability between field plot data and image acquisition date we subset the plots sampled in 2013 to match the WV2 image date. For this subset of plots, we used plant cover data summarized by life form to select those with high herbaceous cover ($\geq 60\%$), and low tree, shrub and subshrub cover, 0%, 10%, 10% respectively. Only remaining plots with $>45\%$ *Eragrostis* canopy cover were selected as EMs. Associated field plot photos were reviewed to confirm features, density of target species and stages of green-up of the species of interest.

Phenology-based mapping of habitat suitability using Google Earth Engine

Our original objective was to develop a phenology-based model of occurrence (in which the presence of a target species at a given location is predicted solely as a function of phenology variables) as an input to a model of habitat suitability ('landscape risk') for each species. The habitat suitability model was to be conditioned on landscape and climatic, but not phenology, variables. However, the use of phenology variables alone failed to produce occurrence models that were strong enough to support the hierarchical modeling procedure described above. Thus, we decided to fit a single occurrence model for each species that considered meteorological, geomorphological, and vegetation and surface reflectance variables simultaneously. While it is possible to bias suitability (potential habitat) by using remotely sensed data that reflect the unique spectral or temporal characteristics of the target species (Bradley et al. 2012), we believe that the coarse spatial resolution ($\sim 250\text{m}$) of inputs, in addition to the way in which we derived the vegetation and surface reflectance variables, has alleviated this concern.

Because our models capture variables related to process (e.g., drought, or the rate of greenup in a given season) in addition to pattern (e.g., topographic position), the occurrence models produced in this phase of work can be used to generate predictions in high-risk (wet) years as well as low-risk (dry) years. It is our expectation that such an approach can be used to monitor the development of vegetation and potentially hazardous conditions in any given year and to evaluate landscape risk across years.

Combined (2011-2012) field data

Every record ($N = 742$) in the combined (2011-2012) sampling dataset represents an individual plot and contains information on the occurrence of our invasive targets. We focused on two species in particular, i.e., *Brassica* and *Schismus*, because detections of the other species were too sparse to permit robust predictive modeling (see Table 3).

Table 3: Number and percentage of detections of five focal species by plot and subplot sampled in the Sonoran Desert during our 2011-2012 field season.

| Species | 2011 Detections | | 2012 Detections | |
|-------------------|------------------|----------------------|------------------|----------------------|
| | Plot ($n=238$) | Subplot ($n=1171$) | Plot ($n=506$) | Subplot ($n=2530$) |
| <i>Schismus</i> | 133 (56%) | 505 (43%) | 473 (93%) | 2020 (80%) |
| <i>Brassica</i> | 113 (47%) | 329 (28%) | 260 (51%) | 748 (30%) |
| <i>Bromus</i> | 15 (6%) | 54 (5%) | 11 (2%) | 13 (0.5%) |
| <i>Eruca</i> | 14 (6%) | 32 (3%) | 26 (5%) | 77 (3%) |
| <i>Pennisetum</i> | 21 (9%) | 46 (4%) | 3 (0.6%) | 3 (0.1%) |

Classification models

Records in the combined sampling dataset also contain a large suite of environmental and remotely sensed attributes (hereafter ‘features’). These features served as predictors in the models described below, and were generated by ‘reducing’ time-series of imagery to summary statistics, for every occurrence record. Reductions were performed on image collections available in Google Earth Engine (EE; <http://earthengine.google.org/>). See Hansen et al. (2013) for an example of using EE for processing. The complete set of features selected as predictors is shown in Table 4.

Table 4: Features used to predict the occurrence and cover of the invasive targets. The total number of features in each category is indicated parenthetically in the group column.

| Group | Dataset | Bands/variables | Filters* | Reduction(s)** | Citation/source |
|---|--|---|---|--|---|
| Meteorological variables (9 features) | The Gridded Surface Meteorological (GRIDMET) dataset (daily) | Precipitation, minimum and maximum temperature, and potential evapotranspiration | 1983-2012 (the 30-year window leading up to and through the sampling effort) AND the 1st day of the week AND winter season | Mean and variance | (Abatzoglou 2013) https://earthengine.google.org/#detail/IDAHO_EPSCOR%2FGRIDMET |
| | The Palmer Drought Severity Index (PDSI) dataset | Not applicable | 1983-2012 AND winter season | Anomaly*** | (Abatzoglou et al. 2014) https://earthengine.google.org/#detail/IDAHO_EPSCOR%2FPDSI |
| Geomorphological variables (10 features) | The MODerate-resolution Imaging Spectroradiometer (MODIS) Albedo product | Visible, near-infrared, and shortwave white-sky albedo | Winter season | Mean and variance | (USGS LP DAAC) https://earthengine.google.org/#detail/MODIS%2FMCD43B3 |
| | Shuttle Radar Topography Mission (SRTM, see Farr et al. 2007) digital elevation data | Elevation, slope, aspect (i.e., northness), and multi-scale TPI (sensu Theobald et al. <i>In review</i>) | Not applicable | Not applicable | https://earthengine.google.org/#detail/USGS%2FSRTMGL1_003 |
| Vegetation indices and surface reflectance data (96 features) | MODIS Vegetation Indices products (16-day composite) | NDVI and EVI. Blue, red, near-infrared, and shortwave reflectances. | Sampling year (for anomalies calculations) - The month preceding data collection - The two months bounding the data collection event (before and after) - The 8-month window leading up to the data collection event | - Mean and variance - Anomalies**** - Max (for the first two filters) - Mean, min, max, and variance, as well as slope and intercept (for the final filter) | (USGS LP DAAC) https://earthengine.google.org/#detail/MODIS%2FMOD13A1 |

* The winter season was defined as December to March. Summer was defined as July to mid-September.

** All temporal reductions of image collections were followed with spatial reductions using the footprint of each plot.

*** The 30-year mean PDSI subtracted from PDSI at the time of sampling.

**** The mean and variance of selected bands in the year in which sampling occurred, divided by the mean for the entire series (15 years).

We completed both Random Forest (Breiman 2001) and Support Vector Machine (SVM; Cortes & Vapnik 1995) classifiers. Models were tuned and trained using the caret package in R (Kuhn 2008).

Each model was tuned to a training partition (70%) of the full dataset using repeated 10-fold cross-validation. Final models were applied to the testing data partition (30%) to generate more accurate estimates of out-of-sample error rates (see model evaluation). The model selected as the best model (using the H measure; Hand 2009) in the training stage of model development was then re-fit against the full dataset in EE using the hyperparameter values identified during the tuning process. This EE classifier was then used to generate spatially-explicit predictions of the occurrence of each of the invasive targets. The element of 'landscape risk' was embedded by making the same prediction in both a highly productive, wet as well as an unproductive, dry growing season.

Model Evaluation

The predicted occurrence probabilities can be reclassified to one of two classes (present/absent) depending on whether the predicted probability (for a given plot or pixel) is greater or lower than a specified threshold (described in more detail below). How false positives are balanced against false negatives depends on the cost/consequence of either error type. The ROC curve visualizes and quantifies the impact of the choice of threshold on the false-positive / false-negative rate tradeoff. In the context of plant invasions, false negatives are more consequential than false positives (Smith et al. 1999). Thus, we created a cost function for each occurrence model by assuming a cost of 1 for false-positive cases and a cost of 2 for false-negative cases.

An optimal ROC curve would go through the point (FPR, TPR) = (0, 1). In other words, model predictions would contain no false positives and all true positives. In real-world circumstances, classifiers are rarely this perfect and, as such, the closer to the optimal point the better. The ROC is summarized into a single value by calculating the area of the convex shape below the ROC curve (the area under the curve; AUC). The closer ROC gets to the optimal point (perfect prediction) the closer AUC gets to 1.

The AUC of a classifier is equivalent to the probability that the classifier will rank a randomly chosen positive instance higher than a randomly chose negative instance (Fawcett 2006). Conventionally, AUC values of 0.5 indicate that the modeled occurrence values are no better than randomly selected values. AUC scores of 0.6 - 0.7 indicate a poor fit of the model to the data, whereas values of 0.7 - 0.8, 0.8 - 0.9, and 0.9 - 1.0 indicate a fair, good, and excellent fit, respectively. We used these breaks as a rough guide to the performance of the occurrence models we obtained from the data.

A spatially weighted ensemble and MODIS phenology-based approach for mapping Sonoran Desert invasive annual plants

We used Random Forests (Breiman 2001) to predict the likelihood of presence of *Brassica* and *Schismus* based on static and dynamic data. Predictions were initially derived with field data collected in 2011 and subsequently with data collected in 2012 where 2011 data served as an independent validation dataset. *Brassica* and *Schismus* were the only species used for these predictions because target detection rates for *Bromus*, *Eruca*, and *Pennisetum* were insufficient for modeling via this approach.

To account for non-stationarity in the influence of predictor variables on likelihood of *Brassica* and *Schismus* detection across the study area, we developed a new method, Spatially Weighted Ensemble (SWE) modeling (Olsson et al. In prep.). SWE is an ensemble model aggregation technique whereby contributing models are combined using spatially varying weights. In arid ecosystems, leaf phenology is highly dependent on precipitation patterns, yet precipitation in arid lands is highly variable, resulting in high heterogeneity of green-up regionally (Figure 12). This is an extremely important consideration because although the invasion-phenology hypothesis suggests that local differences in phenology may be indicative of invasion, the regional asynchrony in precipitation and resulting heterogeneity in green-up may mask those differences (Wolkovich & Cleland 2010).

We introduce SWE as a method to overcome this challenge and therefore a potentially important technique for use in other arid systems, as well. To implement the SWE, we developed a number of “local” models that have been trained using a spatial subset of the field data and, by logical extension, are “tuned” to the local discriminating conditions of that spatial subset. The spatial layout of plots within the spatial subset is used to derive an interpolated surface for each local model, described as an area of influence. The local models are then combined using linear combination but with spatially varying weights. The weights of each local model are normalized at each cell such that the sum of weights is equal to one, and these weights are used to combine model values in a linear weighted sum. We tested a variety of spatial interpolations and weighting schemes, including a hybrid between spatial weights and performance-based weights. Performance-based weighting integrates multiple contributing models into an ensemble wherein the weights are augmented by each model’s performance on a validation dataset, thus using intrinsic validation to guide weighting.

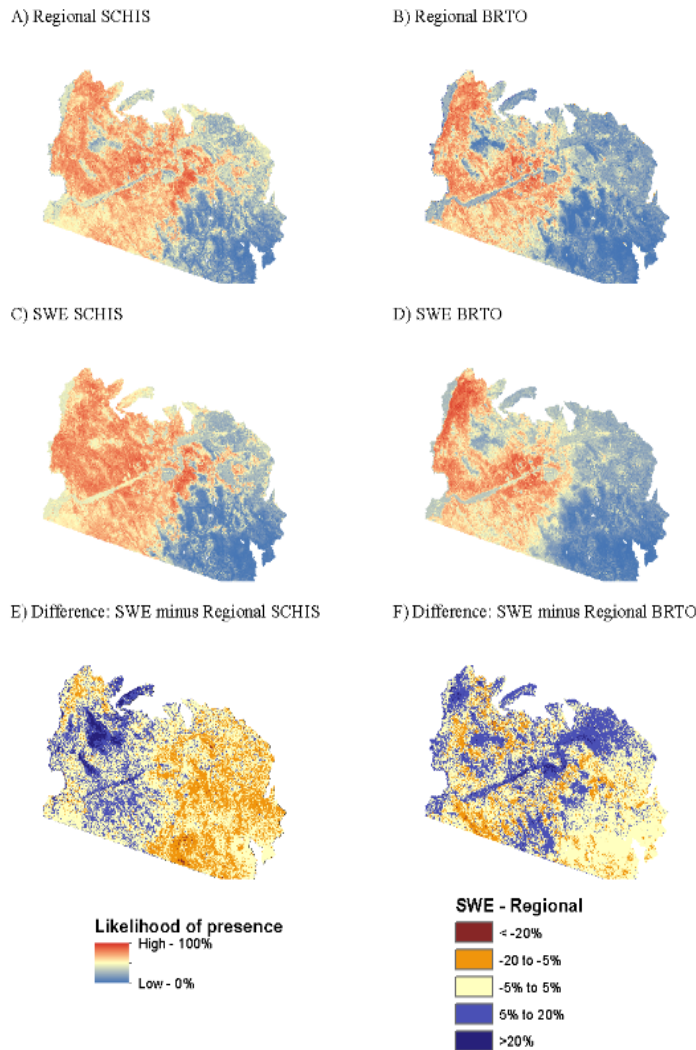


Figure 12: Regional and SWE models of *Schismus* (A, C) and *Brassica* (B, D) likelihood as well as the difference between SWE and Regional predictions (E, F). The difference images highlight areas where the models agree (pale colors) and disagree (warm colors indicate Regional model predicts higher than SWE; cool colors indicate otherwise).

MODIS scenes were pre-processed to remove poor quality data (such as cloud-covered images), and smoothing splines were used to interpolate missing data on a cell-by-cell basis (Scharlemann et al. 2008). We then used NDVI to derive phenology as per Sesnie et al. (2012). For the Landsat TM 30 m models, we obtained all cloud-free Level 1B Landsat TM scenes in existence for path 37, row 37 and path 38, row 37 between January 1, 2000, and June 13, 2011. We calculated NDVI from the NIR and red bands, following Tucker (1978). Beginning in November, 2011, Landsat TM imagery was taken offline. For this reason, we did not acquire new Landsat TM imagery for models based on field data collected in 2012. We derived seasonal estimates of leaf phenology based on NDVI by determining the timing and amplitude of maximum and minimum NDVI for the summer season (June through November) and winter/spring seasons (December to May). Static predictor variables incorporated into the model were derived for topography from 30 m NED DEMs (Hutchinson 1982). Finally, a reference satellite image covering the entire area was derived from Landsat TM imagery from six Landsat TM scenes from WRS2 path/rows 36/37, 36/38, 37/37, 37/38, 38/37, 38/38 for August of 2009. All DEM- and TM-based variables were resampled to 50 m, aggregated to 250 m, and snapped to a MODIS scene for the MODIS model and retained at 30 m for the Landsat TM models. For the Landsat TM analysis, we derived models for *Schismus* and *Brassica* for Landsat p38/r37 and p37/r37 separately using Random Forests. We derived models for *Schismus* and *Brassica* for the full study area using Random Forests and compared this with our SWE modeling approach. Analysis was performed in R 2.15.

Go/No-Go decision point #1:

Within Task 6, and to address the first of two Go/No-Go decision points identified by SERDP program staff, we performed an interim assessment of our methods in order to demonstrate the ability to use remote sensing (multi-temporal satellite data) to differentiate non-native from native species. The specific Action Item was to: *Provide a white paper that includes criteria for success for demonstrating the ability to use remote sensing (multi-temporal satellite data) to differentiate non-native from native species. Include indicating how you will account for inter-annual variation in plant phenology when applying these technologies to detect invasive species.* Our white paper was submitted 9/6/2011.

Task 11: Acquire new Hyperion-hyperspectral data (phase 1)⁷

On June 15, 2009, the USGS Earth Resources Observation and Science (EROS) center began accepting EO-1 Data Acquisition Requests (DARs) at no cost (<http://eo1.usgs.gov/>). We submitted monthly Data Acquisition Requests (DARs) for two sites within the study area: one within YPG and another within BMGR-W in four one-month acquisition windows between January 1 and April 30, 2012 (Figure 13). These four months were selected with the objective of capturing the phenology of each site during the 2012 winter growing season. Based on MODIS time series NDVI, our objective would easily have been met given these criteria and provided hyperspectral imagery spanning the peak spring growing season. MODIS NDVI time series for both locations indicated that peak NDVI most frequently occurred between February 1 and April 30, although the maximum NDVI of both sites occurred in late January 2005 (but remained high through February) (Figure 14). We had anticipated capturing early green-up, peak greenness, and senescence by acquiring Hyperion hyperspectral scenes in locations where large patches of both *Schismus* and *Brassica* were sampled in 2011. Clusters of plots in those locations had been identified based on 2011 Landsat and MODIS models and were located in proximity to the DAR centers. Complete scene extents of DARs would be unknown, although we hoped the scene center of each DAR would be close to our request.

⁷ Phase 2 was not pursued.

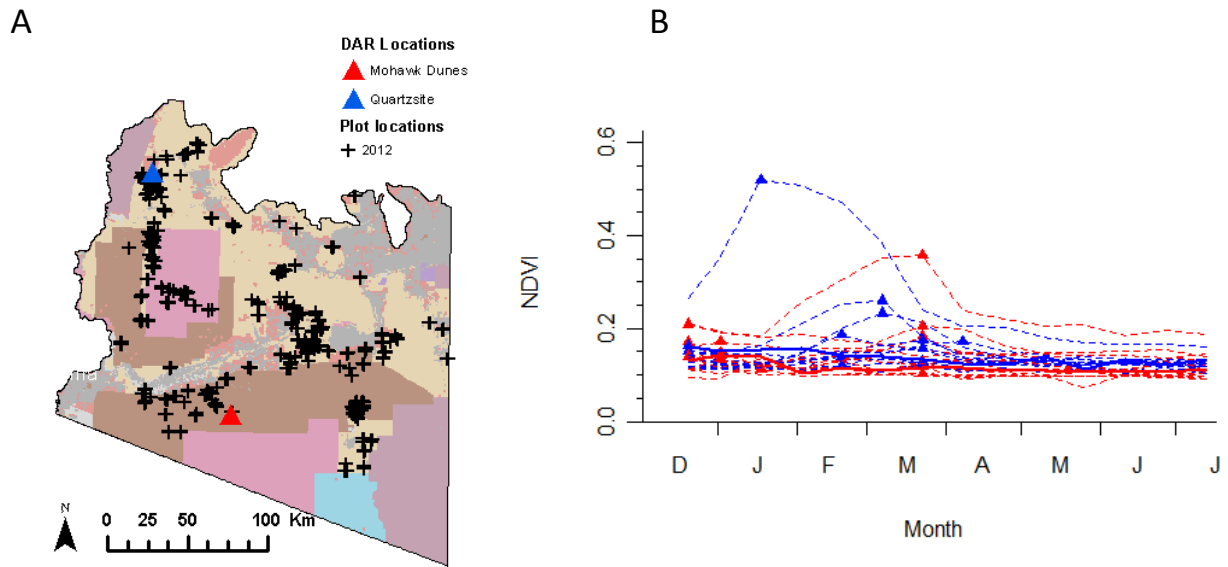


Figure 13: Location of Data Acquisition Request (DAR) positions (A) and yearly winter MODIS NDVI time series from 2000 to 2011 for DAR positions (B). Red and blue triangles signify Mohawk Dunes (in BMGR) and Quartzsite (north of YPG) locations in both graphs with respect to plots visited in 2012. Maximum NDVI for each year is indicated in the graph (B) as a single triangle symbol for each site. 2012 NDVI is indicated by solid red and blue lines, respectively. Notably, maximum NDVI for both locations were below 0.2 throughout early 2012 and declined from January 1 through June 1.

Unfortunately, only one of the ten DARs for Hyperion imagery was fulfilled (Figure 15). A DAR may not be fulfilled if images for higher priority targets are being acquired. In our case, two targets with higher priority may have usurped our request: the CEOS (Committee on Earth Observation Satellites) calibration sites at Frenchman Flat and Ivanpah Playa, and the requests for acquisitions coordinated with the 2012 GOES-R (Geostationary Operational Environmental Satellite R-Series) calibration/validation campaign that included White Sands and the Sonoran Desert.

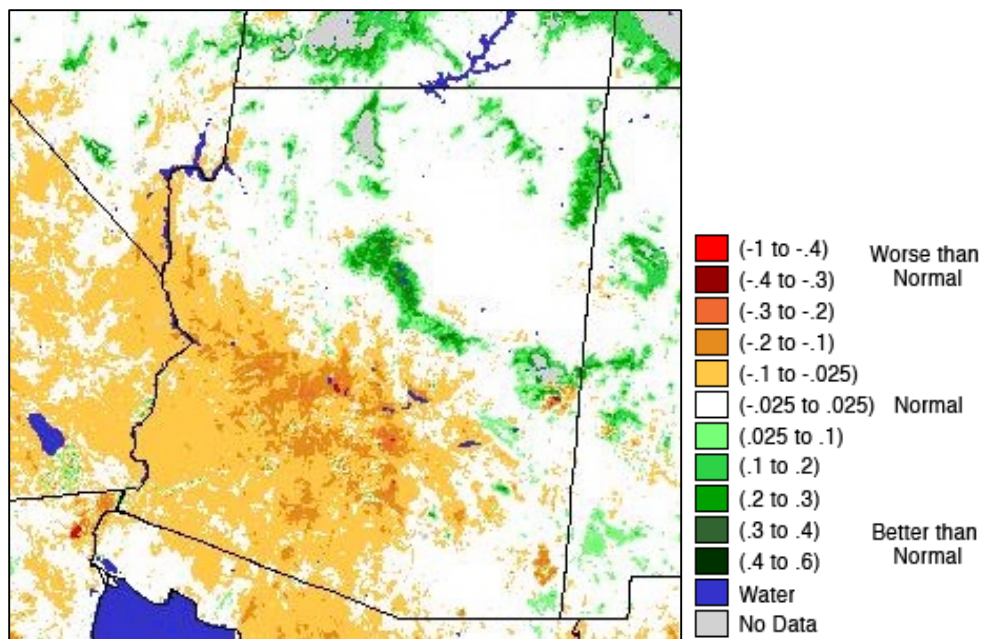


Figure 14: Difference in MODIS NDVI values from 2012 vs. 2011, using image dates from peak spring (March) production period. Warm colors (yellow, orange, red) indicate areas with NDVI that was lower in 2012 than for the same date range in 2011.

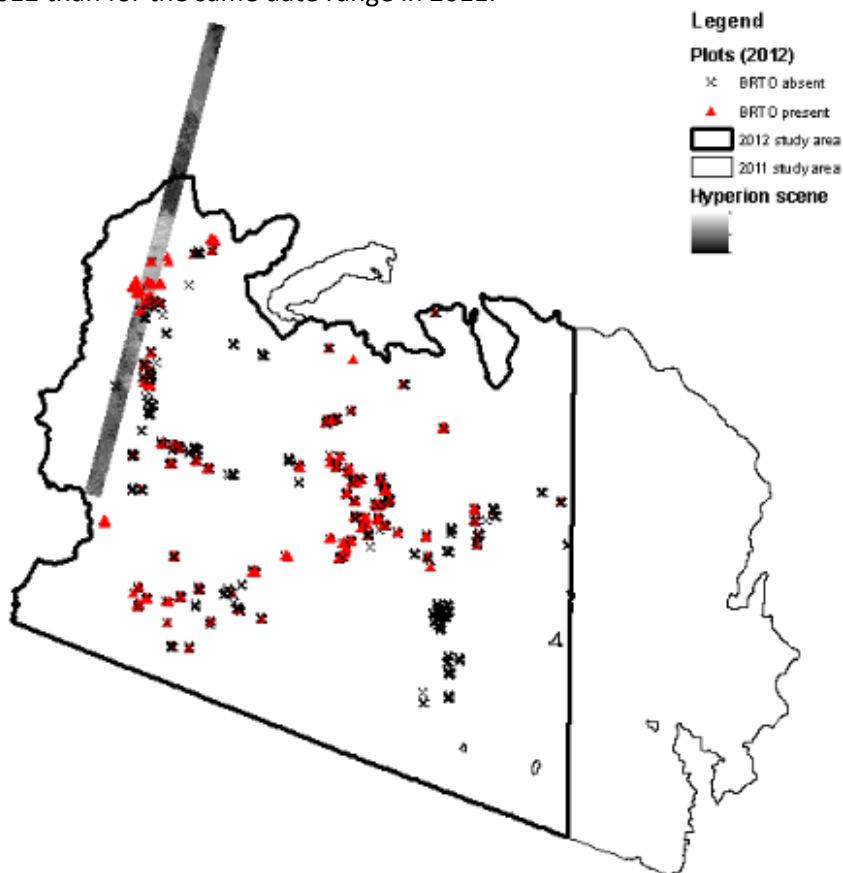


Figure 15: Location and extent of Hyperion scene acquired on March 6, 2012, in relation to study area and plots visited in 2012.

Task 12: Non-native mapping (Hyperion-hyperspectral) (phase 1)⁸

The one fulfilled DAR resulted in a single scene that covered a total of 21 of our plots and 105 subplots, all of which were visited in the field between February and April 2012. Within the boundaries of that one scene, 21 plots and 99 subplots contained *Brassica* and 25 plots and 111 subplots contained *Schismus*. Maximum *Brassica* cover within the scene was 30% at the subplot level and averaged 13.8% among all subplots containing *Brassica*. Maximum *Schismus* cover within the scene was 18% and averaged 6.1% among all subplots with some *Schismus*. Three other target invasive species, *Pennisetum*, *Bromus*, and *Eruca*, were not found at plots within the scene. The abundance of both *Brassica* and *Schismus* in the scene is best characterized as low (i.e., all below 25% cover), even where most abundant.

Hyperion is an experimental satellite sensor with known signal processing errors from excessive ‘striping,’ bad reflectance detectors, and ‘bad’ bands that can degrade spectral data (Datt et al. 2003). Correcting Hyperion radiometric data typically involves removing bands with significant striping (Figure 16). We acquired a Level 1B processed Hyperion scene, which lacks geometric information. Destriping requires the scene to be in its native, un-georectified state. We destriped the image by applying a linear correction to each image column based on a normalization of cross-track means of each band. We used a Landsat TM Level 1B image (Scene LT50380372011059PAC01, path 38, row 37, acquired February 28, 2011) as a reference and geometrically corrected the Hyperion scene (33 ground control points, Mean RMSE 0.58, standard deviation 0.33) (Figure 16). We applied the FLAASH algorithm to convert the scene from exoatmospheric radiance to surface reflectance. One hundred and four bad bands contained no data and were eliminated (bands 1-7, 58-78, 80-82, 120-132, 165-182, 185-187, and 221-224).

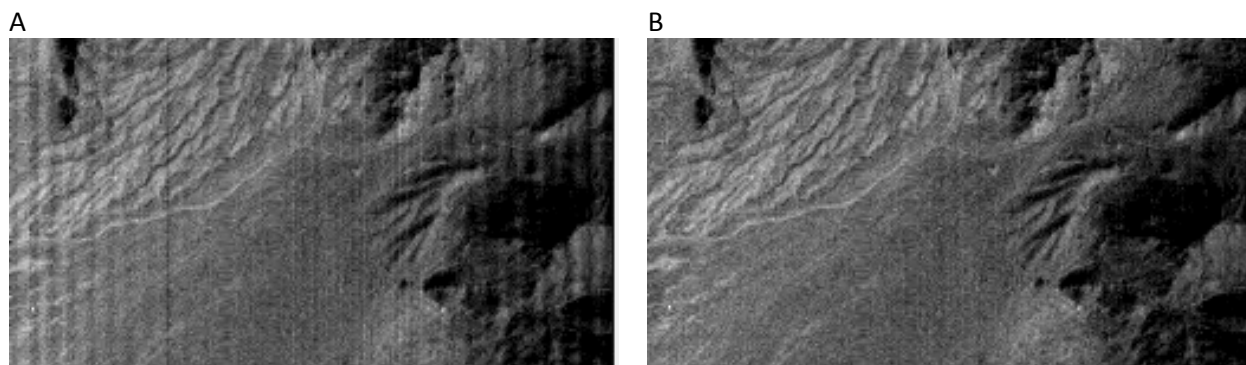


Figure 16: Example of original Hyperion band 9 (A) and de-striped Hyperion band 9 (B).

We applied a MNF transformation to reduce the dimensionality of the hyperspectral data and order bands by decreasing variance (Green et al. 1988). We then applied an inverse transformation of the MNF using the remaining coherent bands and used this as the final Hyperion product for vegetation analysis. Each of these methods is commonly applied to hyperspectral data, which have narrowly defined spectral bands that are more highly attenuated by atmosphere.

To map pixels within the scene containing the target species, we used MTMF to compute the similarity of each pixel to a reference spectrum representing the purest spectra of each target invasive plant, as determined from field samples (Boardman 1998). MTMF estimates the subpixel abundance of a reference material or cover based on pixels values from the MNF-transformed scene. For MTMF to be effective, a pure or semi-pure reference spectrum must be obtained. We selected the pixel within the scene containing the maximum cover of the target species. Ideally, this would be from areas sampled

⁸ Phase 2 was not pursued.

with close to 100% cover by each species. In the absence of pure targets, reference spectra can be obtained in the field or inferred from within the scene at field plot locations. Target spectra were obtained in the field using an ASD Fieldspec3 Spectrometer during February of 2012. Spectra included representative samples from both actively growing and desiccated specimens of our target species. Reconciling these spectra with atmospherically-corrected Hyperion was critical to our ability to use field spectra for scene-based target detection. However, the poor date match of Hyperion data precluded us from utilizing the field spectra, since the hyperspectral satellite image and ground reflectance spectra were collected over 30 days apart (Congalton & Green 1999). This mismatch was compounded by the fact that there is tremendous variability in the field-collected spectra for these species, due in part to our inability to locate large, dense patches of *Schismus* and *Brassica*.

Reference spectra can also be inferred from within the scene using techniques from convex geometry. We used the sequential maximum angle convex cone (SMACC) method to derive EMs, or pure constituents of the scene (Gruninger et al. 2004). Ideally, our target species were distinct EMs but matching a SMACC-derived EM with our target species is not straightforward because the exact EMs selected by SMACC depends on the scene, the number of EMs specified, and other parameters. To identify the best possible EM, we derived 30 EMs using SMACC, then regressed the subplot cover with the SMACC estimates of each end member and selected the EM with the best model fit (i.e., the 'winner'). Using the winning EM from the linear model, we mapped *Schismus* and *Brassica* simply as the proportion of each pixel identified as the winning EM. Analysis was done in ENVI 4.7.

After the development of the above methods, we evaluated our second of two Go/No-Go decision point, as suggested by SERDP program staff, namely to *provide a white paper that includes criteria for success for demonstrating the ability to use remote sensing (Hyperion hyperspectral data) to differentiate nonnative from native species. Include indicating how you will account for inter-annual variation in plant phenology when applying these technologies to detect invasive species.* Our methods (and results) were detailed in our Interim Progress Report, submitted September 9, 2012.

Comparison of simulated HypsIRI with two multispectral sensors for invasive species mapping⁹

We used an AVIRIS scene from 05 November 2003, available from the AVIRIS archives (scene IDf031105t01p00r05c_sc01) for our area of interest. The scene had a spatial resolution of 3.2 meters. We atmospherically corrected the scene using FLAASH (Matthew et al. 2003) and aggregated (pixel averaged) to 15m, 30m, and 60m spatial resolutions. Additionally, we acquired hand-digitized polygons of *Pennisetum* patch boundaries from 2002 based on Olsson and Morisette (2014).

Simulated scenes

We derived ASTER and Landsat TM scenes using spectral convolution of AVIRIS with spectral filters for ASTER and Landsat TM (filter vendor Green Shimada, 1997). HYSPIRI was unaltered from the source dataset because the HYSPIRI spectral filter response shapes are unknown. AVIRIS is similar in spectral characteristics to the proposed HYSPIRI VSWIR instrument. The two sensors both have 0.01 um bandwidths at 0.01 um increments from 0.40 um to 2.50 um, and each have a nominal SNR of 400:1 in the SWIR. Two HYSPIRI bands centered at 0.38 um and 0.39 um were missing from our simulated scenes because they are not acquired with AVIRIS.

⁹ The below methods have been peer-reviewed and published in Olsson, A. D., and J. T. Morisette. 2014. Comparison of simulated HypsIRI with two multispectral sensors for invasive species mapping. Photogrammetric Engineering and Remote Sensing 80:217-227.

Reference map of *Pennisetum* cover

The AVIRIS scene was transformed with a MNF transformation, and we then applied mixed-tuned MF (Boardman 1998) to the corrected AVIRIS scene to map *Pennisetum* cover based on areas known to contain dense *Pennisetum*. *Pennisetum* patches had been mapped by Olsson et al. (2012a) using 0.3 m resolution aerial photography from 2002. A reference spectrum in the MNF-transformed image was derived using areas of dense *Pennisetum*, chosen based on high estimates of *Pennisetum* cover according to 2002 images. Eleven reference pixels were selected from the dense cores of the three largest patches as they appeared in historical imagery. Pixels judged to be most pure were selected to minimize contamination by substrate

We used previously digitized patch polygons ('reference polygons') to create a binary classification of *Pennisetum* at the 3.2m (10.2 m²) pixel size. We used the mixed-turned MTMF filtering output as a predictor variable and the digitized polygon dataset as the dependent variable to construct a logistic regression model of *Pennisetum*. We then iteratively altered the threshold to establish a binary model that fit our expert knowledge. This threshold was the criterion for a binary classification of *Pennisetum* for all cells in the study area. Our approach reduced overprediction associated with north-facing slopes and higher elevations, which are less suitable for *Pennisetum* because it is cold intolerant. These features support greater herbaceous plant cover than native Arizona Upland, giving them the potential to produce a signal that may confound identification of *Pennisetum*, which also supports greater herbaceous plant cover.

Based on these methods, we considered the MTMF threshold-based binary classification the reference image for the rest of our analyses. The binary reference image was resampled to 15, 30, and 60m pixel sizes using simple linear aggregation, resulting in pixel values between 0 and 1. These values represented the percentage of *Pennisetum* cover within each of 15, 30, or 60 m cells.

Predicting *Pennisetum* abundance in all scenes

We obtained the noise equivalent reflectance (NE $\delta\rho$) for Landsat TM and ASTER and added random noise to AVIRIS-based reflectance images. NE $\delta\rho$ values for Landsat TM bands 1-5 and 7 were 0.16, 0.21, 0.23, 0.22, 0.25, and 0.37%, respectively (Mika 1997). For ASTER, we used the stated NE $\delta\rho$ values from the ASTER Users Handbook: 0.05% for VNIR and 0.13% for SWIR (Abrams et al. 2002). For HypsIRI, we used the stated 0.02% NE $\delta\rho$ target for all bands (JPL 2009).

We modeled *Pennisetum* at the 15, 30, and 60 m spatial resolution using Random Forests (Breiman 2001; Lawrence et al. 2006) with noise-added reflectance bands of each of the simulated images as the independent variables. Random Forests uses multiple classification and regression trees (CARTs; Breiman 2001) to perform ensemble classification. A different subset of predictor data is used to train each tree via bootstrapping, and each tree is developed using feature selection at each node. A random subset of predictor variables is selected at each split node in each tree, and an optimal split is selected from that subset (i.e., feature selection). Each split is associated with a node impurity (the Gini coefficient) based on data left out of the training data (i.e., out-of-bag data, which are typically one-third of the data). The importance of each variable is calculated as the mean decrease in the Gini coefficient associated with each variable over all trees in the ensemble. Gini can be summed over all nodes in the tree and over all trees in the forest to provide a measurement of variable importance.

We used 1500 individual trees for each random forest ensemble model, and generated the models using version 4.6-2 of the "randomForest" package in R. We derived continuous models of *Pennisetum* cover for the three sensors at three different resolutions for each sensor. We iteratively removed the least important variable from a model containing the full set of input variables until we had removed all but one variable. We selected the model with the greatest overall model performance based on Cohen's Kappa. From the final (reduced) model for each sensor and resolution, we assessed

variable importance to identify spectral features that HypSIRI might be able to better distinguish than ASTER or Landsat TM.

Accuracy assessment

We normalized the models based on a fixed user's error in order to ensure compatibility between models; lower sensitivity values correspond to a greater number of producer's errors and weaker predictive models. We also compared the performance of models on patches of similar size in order to explore management implications. However, spatial aggregation of pixels at 15, 30, and 60 m results in different pixel areas and indicates different levels of infestation. We use the term 'effective patch size' to define the cover (m^2) of *Pennisetum* within a pixel, recognizing that resolution dictates interpretation such that multiple discrete patches may reside within a pixel and some patches may cross multiple pixel boundaries.

User's accuracy was calculated as a function of effective patch size for models from all three sensors using an incremental analysis for determining thresholds for *Pennisetum* presence while selecting model thresholds for presence that held user's accuracy at 10%. We varied the minimum threshold of *Pennisetum* cover between 1% and 100% and, for each model and cover threshold, we maximized the model threshold such that the user's accuracy of the lowest 5% was at most 10%. By holding user's accuracy constant, we were able to compare the producer's accuracy of different sensors both as a function of cover and as a function of effective patch size. Thus, this predicts the percentage of patches of different sizes that will be identified correctly when 90% of the predicted patches of the same size are, in fact, *Pennisetum*. This is similar to work by Mundt et al. (2006), but differs in two respects: 1) we used a continuous predictive model to avoid the confounding effects of variability in user's accuracy, and 2) we performed accuracy assessment only on the minimum effective patch size. This approach enabled us to compare the ability of each model to detect patches of a given size while holding the user's error rate constant.

OBJECTIVE 2: Model invasion risk from non-native plants under current and projected climate conditions.

Task 5: Compile AOGCMs

We obtained data representing global current and projected future climate from WorldClim (<http://www.worldclim.org>) as interpolated climate surface layers of mean monthly temperature and precipitation at 2.5 arcminutes spatial resolution. Current climate data for the period of 1950-2000 are available through WorldClim as interpolated layers of monthly averages of mean, minimum, and maximum monthly temperature and mean monthly precipitation (Hijmans et al. 2005). Future climate layers compiled through WorldClim are based on atmosphere ocean general circulation models (AOGCMs) from the 5th IPCC report and are downscaled using the WorldClim 1.4 current climate data as a baseline (Hijmans et al. 2005). We chose climate model projections based on those that predicted regional temperature and precipitation with the lowest error (Rupp et al. 2013). We selected AOGCMs based on their performance as assessed by Rupp et al. (2013) and availability of relative concentration pathways (RCPs) in Worldclim. We included AOGCM projections based on RCP4.5 and RCP8.5. RCP4.5 is the 'medium-low' pathway in the 5th report and is characterized by a stabilization of radiative forcing at 4.2 W m^{-2} by 2100, which corresponds to atmospheric CO_2 concentrations of 650 ppm (Stocker et al. 2013). RCP8.5 is the 'high' pathway and projects a stabilization of radiative forcing at 8.3 W m^{-2} by 2100, which corresponds to atmospheric CO_2 concentrations of 900 ppm (Stocker et al. 2013). Climate projections were based on five AOGCMs from the following modeling groups: National Center of Atmospheric Research (CCSM4), National Centre of Meteorological Research (CNRM-CM5), Met Office Hadley Center (HadGEM2-ES), Atmosphere and Ocean Research Institute, National Institute for

Environmental Studies, and Japan Agency for Marine-Earth Science and Technology (MIROC5), and Norwegian Climate Center (NorESM1-M).

Task 7: Construct BEMs

Many techniques for bioclimatic envelope modeling (BEM) have been developed. BEMs are used to understand the relationship between the geographic location where species occur and the climatic conditions at those locations (Franklin 2009). A model of suitable climate can then be projected back into geographic space to identify the spatial extents of potential for invasive plant establishment or abundance. Suitable climate conditions can also be projected spatially based on the geographic distribution of future climate associated with climate change. For *Bromus* and *Brassica*, we used two BEM methods (MaxEnt and Bioclim) to predict the current and future geographic distributions of presence and high abundance.

For our analysis, we selected two target invasives for future spread prediction modeling, based on their abundance and impact in our study area. In order to predict future distributions of *Brassica* and *Bromus*, we first assembled all available data describing their current distributions. Next, we developed risk layers to predict their likely future distributions in southern Arizona. Using average minimum and maximum yearly temperatures and quarterly precipitation, we employed Mahalanobis Distance (Tsoar et al. 2007) and MaxEnt (Phillips & Dudík 2008) to model climatic suitability for abundance and for presence in the study area (Hijmans et al. 2005). Finally, we projected climatic suitability under climate change scenarios for both invasive species using climate conditions predicted by seven climate models for mid- and late century (Ramirez & Jarvis 2010).

Occurrence data

Current distribution data inputs were acquired from regional management databases, including the SWEMP (<http://www.invasiveweeds.com/mapping>), the California Invasive Plant Council (<http://www.cal-ipc.org/>), and the NPS, as well as roadside survey data collected by our team in March 2011 and 2012. Out of that dataset, we identified point locations with known high abundance based on high recorded biomass or cover. This resulted in an abundance dataset and a presence dataset. Presence points are used to predict site suitability for establishment based on environmental characteristics, while abundance data enable prediction of risk of future abundance and associated fire risk.

Presence data for *Bromus* and *Brassica* were compiled from regional datasets (CalFlora (<http://www.calflora.org/>) and Cal-IPC (<http://www.cal-ipc.org/>)), surveys by managers with the Bureau of Land Management (BLM) and the Mojave Desert Network Parks, records from local and regional biologists, and herbaria, and supplemented with two field surveys (in 2011-2012) focused on roadsides only in southern Nevada, southern California, and Arizona. For both species, some abundance data were available from land managers and herbarium records as percent cover values and from field surveys as qualitative descriptions of relative abundance at each site. We transformed these data into two groups for each species: presence and high abundance. We classified locations as high abundance if the species had at least 10% cover, was described qualitatively as having continuous ground cover, or if the target species was observed in abundance beyond the road corridor. We included all available presence data, including points with high abundance, in the presence datasets. Records for both species were restricted to the southwestern USA (i.e., the region from which *Bromus* and *Brassica* are problematic invaders). Therefore, we limited the extents of our study regions using a convex hull around the presence locations of each species. Absence data comparable in extent to the presence/high abundance data were not available for either species. To remove duplicate entries and reduce sampling bias, we resampled each of the four datasets to include only one point per 2.5 arcminute climate grid cell. If more than one point

within a grid cell had abundance data, the maximum abundance value was retained. Maps of the resulting distribution data are presented in Figure 17.

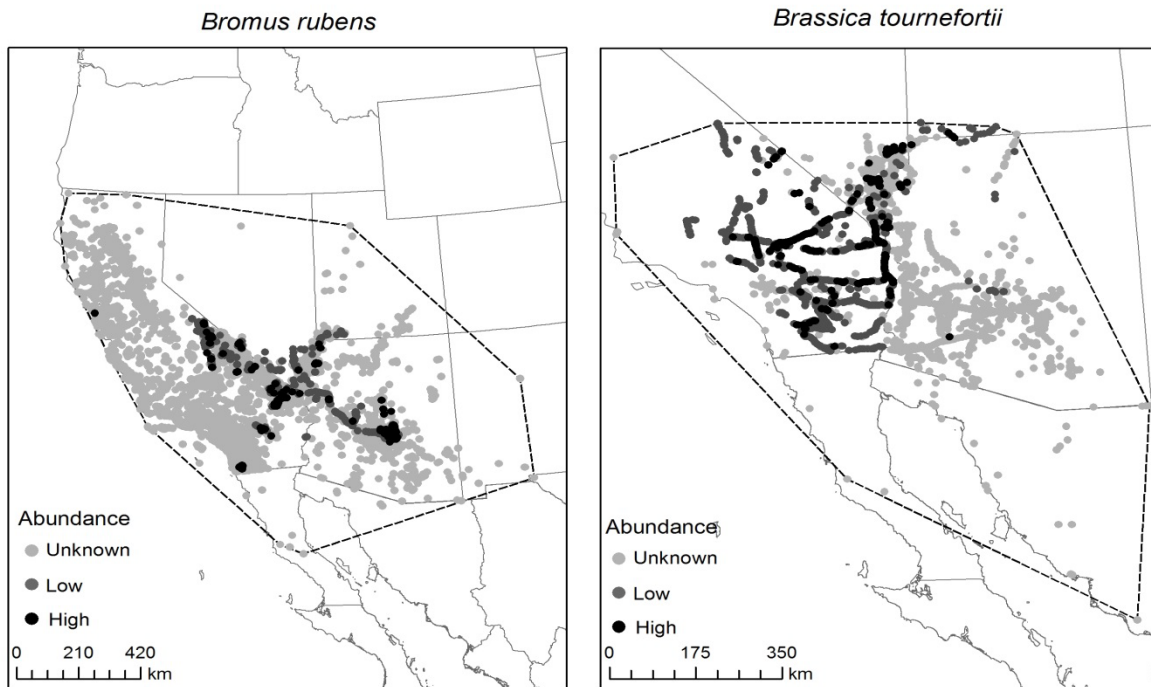


Figure 17: Spatial locations of data collection for each species. We classified locations as high abundance if the species was recorded as having least 10% cover, was described as having continuous ground cover, or was observed in abundance beyond the road corridor. Points are shown as low abundance if they do not meet these criteria but have some description of abundance associated with them. Points lacking a description of abundance level are considered unknown. At the 2.5 arcminute resolution, we compiled 110 high abundance occurrences for *B. rubens* and 218 for *B. tournefortii*. 243 points were classified as low abundance for *B. rubens* and 565 for *B. tournefortii*. Unknown abundance was found for 2950 *B. rubens* points and 1072 *B. tournefortii* points. Dashed line reflects a convex hull modeled using the most peripheral presence locations of each species.

Analytical methods

First, we used MaxEnt (Version 3.3.3k), an implementation of maximum entropy modeling (Phillips et al. 2006), to model climatic suitability for the two coverage groups: presence and high abundance. MaxEnt relies on presence-only data, but generates pseudo-absences drawn from the study area to construct probabilistic relationships between climate and species distribution. Therefore, MaxEnt is sensitive to the extent of the area from which pseudo-absences are drawn (VanDerWal et al. 2009). We used a mask in MaxEnt to select pseudo-absence points only within our study area, defined as a convex hull around each species' occurrences. In order to account for uneven sampling of occurrence points (Kramer-Schadt et al. 2013), we included a bias file for each of the species based on presence of National Parks and distance to roads. We transformed the continuous model into a binary suitable/unsuitable map based on a threshold value that encompassed 95% of the location points. Second, we created Bioclim models of climatic suitability for *Bromus* and *Brassica*. Bioclim identifies thresholds for each climatic predictor that encompass the distribution data (Busby 1991; Pearson and Dawson 2003). We used ArcGIS 10.1 to extract the values of the four climate variables to all of the known locations, and then calculated climatic limits that encompassed 95% of the distribution dataset.

This threshold was created by excluding the climate values associated with the upper and lower 2.5% of presence or high abundance points. We calculated Bioclim climatic suitability as areas identified as suitable by all four climate layers. The MaxEnt and Bioclim results were combined to identify regions that were climatically suitable in either model.

We evaluated MaxEnt model performance based on the AUC values, which are widely applied to determine agreement between predicted species distributions and occurrence records (Fielding and Bell 1997; Pearson et al. 2006; Thuiller 2003). AUC values are based on the ROC, which plots the rate of true positive predictions (sensitivity) against false positive predictions (specificity) with values ranging from 0.5 (no better than random) to 1 (perfect model prediction).

Task 8: BEM uncertainty analysis

After establishing the climate conditions suitable for *Bromus* and *Brassica* based on current climate, we projected those conditions onto future climate models using the same thresholds used to describe current climatic suitability. We repeated this process for the five AOGCM projections, using an ensemble approach to assess model uncertainty. We created ensemble models of future presence and high abundance of *Bromus* and *Brassica* by summing all of the binary climatic suitability maps (i.e., those created by MaxEnt and Bioclim for each AOGCM) to create models ranging from zero (unsuitable in all models) to ten (suitable in all models). Combining models of suitability made with multiple BEMs and AOGCMs reduces the effect of any single model or scenario, and degree of model overlap provides a measure of confidence associated with model agreement (Araújo and New 2007). Still, uncertainty associated with the climate models used in our analyses likely contributed to uncertainty in our modeling results (Knutti et al. 2010). Although our choice and use of multiple climate models attempted to partially remedy this issue, we were unable to precisely quantify all sources of uncertainty. We created separate ensemble models for the two relative concentration pathways (RCP4.5 and RCP8.5).

To identify climatic suitability for invasion by *Bromus* and *Brassica* in the future, we created maps of range shift that show areas of future expansion, maintenance, and contraction. We simplified this analysis by considering any area projected to have suitable climate conditions currently by either MaxEnt or Bioclim as suitable. We created two sets of range shift maps by applying a low and a high threshold for identifying suitability. The low threshold included all areas projected to be suitable by at least one model in the ensemble. The high threshold included all areas projected to be suitable by at least six of ten possible models. We compared current and future suitability to measure the land area of projected contraction, maintenance and expansion of invasion risk by 2050 within the study region defined for each species.

OBJECTIVE 3: Model the impacts of recent and on-going land use disturbances on non-native plant invasion.

Task 9: Land use models of disturbance and risk

To model the effect of land use relative to other site characteristics on *Brassica* establishment (an extension of methods used by Bradley & Mustard (2005)), we first created a map of current *Brassica* presence in southwestern Arizona. This map was constructed using a time series of Landsat data for time periods when the invasive plant showed unique phenology and/or abundant growth across the landscape and could therefore be identified remotely. The resulting map was validated using the field survey data we gathered in 2010-2012 to compare predicted presence/absence of *Brassica* to on-the-ground presence/absence. We used the validated, landscape-scale presence/absence map to test the effect of proximity to disturbance features, including roads, highways, and railroads, as well as physical geographic features, including topography and surface geology, on establishment of *Brassica* (after Bradley & Mustard 2006). One potentially significant source of disturbance could not be included in this

mode: the US Border Patrol employs road dragging as a method of detecting human foot traffic through border regions (i.e., Border Patrol teams drag tires over dirt roads to erase previous tracks in order to detect new tracks laid on the smoothed road). This practice disturbs roadsides, theoretically releasing resources and likely facilitating invasion. However, we did not have access to existing data on locations and quantity of road dragging, and for security reasons we were unable to sample near the US-Mexico border where road dragging is common.

OBJECTIVE 4¹⁰: Model the effects of increased fuel loads caused by non-native plant invasion on regional fire risk.

Task 10: Fire modeling outputs

Modeling and mapping large fire probability

For two different large fire probability scenarios (see below), we used a mixed effects logistic regression model to estimate the relative probability of a large fire given a historical ignition event and conditioned on multiple environmental covariates (fixed effects). We characterized all fires that burned during the study period as either 'large' (i.e. ≥ 20 ha) or 'small' (i.e. < 20 ha) fires. Twenty hectares represents a low-end estimate of large fire size in desert fuels and is a threshold that characteristically identifies years when the annual fuel load is sufficient for fire spread (W. Reaves, pers. comm.). For the period 1989-2010, we used fire occurrence data from two national level datasets (Finney et al. 2011, Short 2013 and Fire Program Analysis, www.fpa.nifc.gov). Using a GIS, a random sample of fires that burned < 20 ha was eliminated from the dataset so as to arrive at a more parsimonious 4:1 ratio of small to large fires (Brillinger et al. 2003).

Approximately two thirds of the desert annuals in our Sonoran study region are winter growing and it is known that they contribute significantly to fuel loads following winters of above-normal precipitation. However, the exact effect of this precipitation on the timing and amount of growth is unpredictable, and may show irregular lagged effects with delayed germination. To account for inter-annual variability in the response of large fires, we included in our models a random effect of moisture anomaly in the three winter growing seasons immediately prior to a given fire year. This approach allowed us to more accurately predict the probability of a large fire between 1989 and 2010, given the fixed effect parameters of interest.

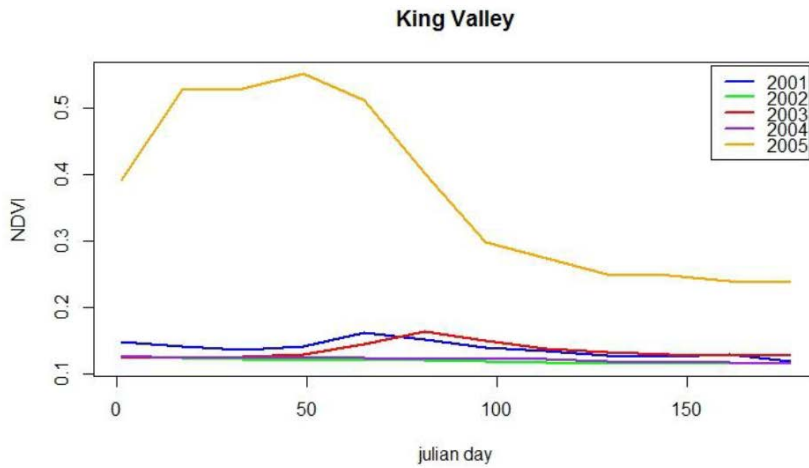
We accounted for the direct effect of fine fuel loads on large fire probability using a time-series analysis and seasonal NDVI summaries. As a spatially and temporally 'dynamic' variable, it can be used to estimate fire risk over large, contiguous extents (Maselli et al. 2003). Yearly maximum NDVI in a given area can be thought of as a proxy for the annual build-up of fuel (Box et al. 1989). Our exploration of NDVI values preceding large fires indicated a strong relationship between yearly NDVI values and large fire occurrence (Figure 18). To estimate yearly maximum NDVI values for 1988–2010 – the period coinciding with our fire occurrence dataset – we obtained Landsat Thematic Mapper (TM) scenes covering our study area ($n = 1114$, temporal resolution = 16 days) from the US Geological Survey (USGS) Global Visualisation Viewer (<http://glovis.usgs.gov>, accessed November 2012). Our model included variables of the year-of-fire maximum NDVI value as well as the maximum NDVI value of the year before the fire.

¹⁰ For Objective 4, methods have been peer-reviewed and published in Gray, M. E., B. G. Dickson, and L. J. Zachmann. 2014. Modelling and mapping dynamic variability in large fire probability in the lower Sonoran Desert of south-western Arizona. *International Journal of Wildland Fire* 23:1108-1118

– AND –

Gray, M. E., and B. G. Dickson. 2015. A new model of landscape-scale fire connectivity applied to resource and fire management in the Sonoran Desert, USA. *Ecological Applications* 25:1099-1113.

A



B

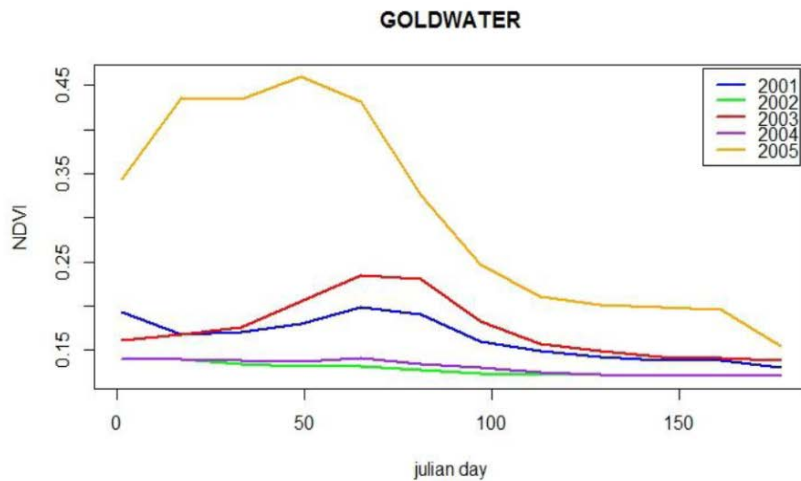


Figure 18: Values of NDVI within the burn perimeter of two large fires that burned in the study area: the King Valley Fire (A) burned in October 2005 and the Goldwater Fire (B) burned in June 2005.

In addition to the dynamic NDVI variable described above, we derived an NDVI-based variable to represent the horizontal spatial structure of perennial vegetation. Similarly, previous research in the Mediterranean region of Spain successfully used Landsat TM to characterize the horizontal heterogeneity of vegetation by taking the standard deviation of Landsat bands in a local window (Vega-García & Chuvieco 2006). Therefore, we approached our work in the context of far-reaching, uniform shrublands and sparsely vegetated areas in the Sonoran Desert, where large interspaces have been observed to amass continuous fine fuels after heavy precipitation. Our variable for perennial vegetation heterogeneity was the standard deviation of maximum NDVI in 1989 – a dry year when NDVI was most likely dominated by perennial growth. Our modelling approach also accounted for multiple terrain variables that directly influence fire spread and indirectly influence vegetation growth and flammability (Syphard et al. 2008). Using a DEM obtained from the USGS (<http://ned.usgs.gov/>, accessed March 2011), we derived estimates of elevation, aspect (in degrees), and terrain roughness (standard deviation of slope; Preisler et al. 2011) within the GIS. We used the cosine transformation of aspect to provide an index that ranged between -1 (180°, south-facing slopes) and 1 (0 or 360°, north-facing slopes).

To account for human accessibility that might differentiate where fires are more or less likely to become large, we used the GIS and 2011 US Census Bureau TIGER line data (<http://www.census.gov/geo/maps-data/data/tiger.html>, accessed November 2011) to estimate a simple road density (km km^{-2}) variable that could serve as a proxy for human accessibility and help to differentiate where fires were more or less likely to become large.

We used a circular moving window operation and focal statistics in a GIS (ArcGIS v10.1, Redlands, CA, USA) to summarize each of the fixed effects within a 20-ha neighborhood around each ignition point. Although this approach was designed to encompass the landscape factors that influence fire size within our large fire threshold, it may not adequately account for the full array of factors that influence fire growth beyond 20 ha. All landscape variables were derived as or converted to raster grids with a 30-m pixel resolution. For all landscape variables except the maximum NDVI, we standardized and rescaled values to a mean of zero and unit variance at the full extent of our study area. We used the 'raster' package (Hijmans & van Etten 2012) in R 2.15.1 (R Development Core Team 2011) to extract landscape variables from each ignition point before statistical analysis. We included the winter precipitation anomaly immediately preceding a fire event and one lag-season precipitation anomaly as crossed random effects (Bolker et al. 2009). Precipitation anomalies, based on 1981–2010 normals, were derived from 800-m gridded data as the percentage of normal precipitation from October through March (Western Regional Climate Center, <http://wrcc.dri.edu/monitor/WWDT/archive.php>, accessed November 2011). For parsimony, and to account for the variance associated with winter precipitation totals, we categorized each random effect into five quantiles. We extracted the year-of-fire and lag-year winter precipitation anomaly from each ignition point before statistical analysis.

We used an information-theoretic approach and multi-model inference (Burnham & Anderson 2002) to identify and contrast environmental variables within a 'full' model. Using Akaike's Information Criterion (AIC), we computed AIC weights to rank and evaluate the weight of evidence in favor of a variable given all possible models (i.e., all possible variable combinations; Burnham & Anderson 2002). We summed the AIC weights across all models in which a given variable (j) occurred and considered a cumulative AIC weight ($w_+(j) \geq 0.50$) to be strong evidence for a response (i.e., probability of a large fire) to that variable (Barbieri & Berger 2004). We used the difference in AIC values to evaluate the performance of the full model against a null (i.e., random) model, and considered a ΔAIC value > 4.0 as a good approximation of the data (Anderson 2007). We used maximum-likelihood to estimate model-averaged regression coefficients and unconditional standard errors. We also computed the variance-covariance matrix of our fixed-effects parameters using the empirical Huber–White 'sandwich' estimator, which relaxed the assumptions of independence between fire locations and known covariance structure. To evaluate model classification accuracy, we computed the area under the ROC curve (AUC; Hosmer et al. 2000). This AUC value provided a likelihood-based measure of discrimination between predicted presences and absences. We considered AUC values > 0.70 as indicative of acceptable discrimination (Hosmer et al. 2000). We used the Hosmer–Lemeshow statistic to evaluate goodness of fit ($\alpha = 0.05$; Hosmer & Lemeshow 2000). We conducted all analyses within the Statistical analysis software (SAS) and R Statistical Programming environments (GLIMMIX procedure in SAS v9.2, SAS Institute, Cary, North Carolina, USA; and R Statistical Package v2.15.1).

We used the model-averaged regression coefficients and GIS to implement the full model and produce probabilistic, spatially explicit maps for two analysis years (1996 and 2005) at a 30-m pixel resolution. We chose these years to illustrate dynamic large fire probability in a moderate fine fuel scenario (1996) and high fine fuel scenario (2005), and we refer to these as moderate and high large fire probability scenarios. For 1996, we reasoned that fuel loads were affected primarily by the wet winter of 1994 and therefore only moderately abundant. Fine fuels were uncharacteristically abundant across the study area in 2005.

Models and maps of fire behavior and hazard

The interagency Landfire Project (www.landfire.gov) and the spatially explicit fire simulation tool FlamMap v5 (Stratton 2004) provide 'off-the-shelf' raster data that we were able to use to establish a baseline of current fuel conditions and potential fire threat. From those baselines, we derived predictive models and maps of fire behavior, hazard (heat per unit area), and rate of spread (m/min) across the full study area. FlamMap computes these potential fire characteristics based on topographic and fuel model features across the landscape for constant weather and fuel moisture conditions. Prediction of fire behavior uses categorical metrics of relative canopy fire behavior, including surface fire, passive canopy fire (torching of individual plants), and active canopy fire (simultaneous torching of multiple plants in a stand) to forecast fire behavior at any given location on the landscape under the assumption that the entire landscape is burning under a specific set of weather conditions. Fire hazard (BTU/ft²), by contrast, is a measure of either the amount of fuel available to a burning fire or a measure of fire intensity at any given location (i.e., pixel) on the analysis landscape under a specific set of weather conditions. These fire model outputs offer a snapshot of relative potential fire threat over extensive areas by reflecting biomass and non-native plant contributions to the fuel bed on an interannual basis. They do not, however, take into account the high levels of vegetation heterogeneity that can be present in the Sonoran Desert region.

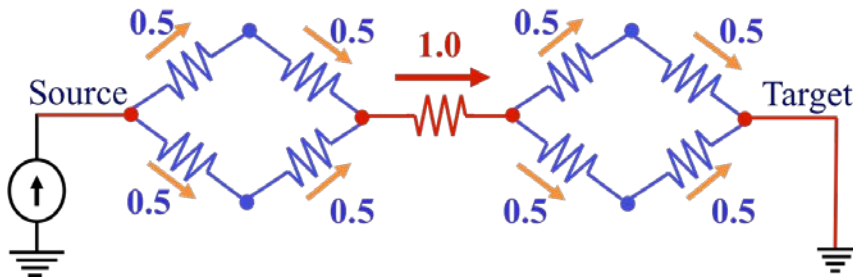
To capture that heterogeneity, our custom-derived fuel and vegetation models draw on estimates of biomass collected in the field or predicted using the methods described above, coupled with freely available 30-m resolution data on existing biophysical and vegetation characteristics provided by Landfire (Rapid Refresh 2008). Landfire-supplied inputs to these models included elevation, slope, aspect, fuel model (Scott & Burgan 2005), and vegetation height, cover, and basal area (of trees).

We parameterized our landscape file for FlamMap simulations using 96th percentile drought weather and fuel moisture conditions measured at the Squaw Lake, CA, Remote Automatic Weather Station (RAWS) (27-year average; Elev: 91 m, 32.91N, 114.49W). Squaw Lake has the most extensive source of climate data from 1986-present and is representative of the lowest mean annual precipitation across the study area (73 mm). Using that low precipitation value enabled a complete, lower estimate of average fuel moisture conditions for fire behavior calculations. In the model, we assumed maximum sustained wind speeds of 20-40 kph and an azimuth of 220 degrees. Live fuel moistures in the models ranged between 2 and 50%. Dynamic wind grids were generated using the Wind Ninja module within FlamMap. We applied the Scott et al. (2001) canopy fire calculation method.

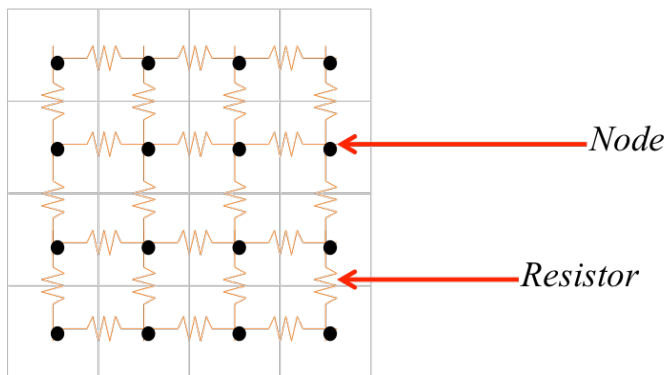
Modeling and mapping fire connectivity

In addition to modeling large fire probability and fire behavior, we modeled fire connectivity across the landscape using circuit theory models. The underlying networks in circuit theory models are analogous to electrical circuits and are mapped as a graph structure of interconnected nodes and resistors that conduct current (McRae et al. 2008) (Figure 19). A resistor's value is given by the probability of movement between its incident nodes and is the inverse of its conductance, making the model a probabilistic analysis of flow (Carroll et al. 2012). Whole landscapes can be modeled as circuit networks (Rayfield et al. 2011). An ecological flow is modeled via a voltage input, or a procession of thousands of 'random walkers.' The voltage begins at a source node and moves randomly through the network until it reaches a target node. The resulting current density at any intermediate node is an estimate of the likelihood of flow passing through that node, en route from source to target.

A



B



C

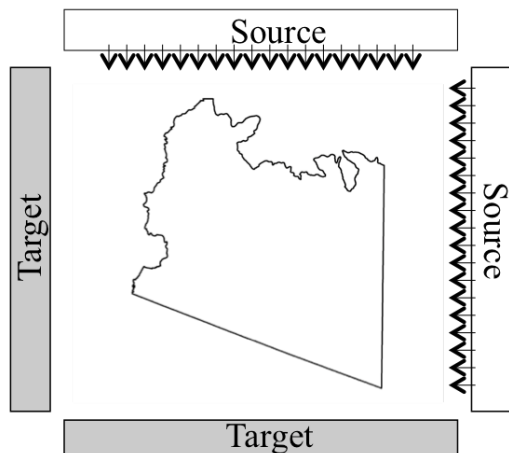


Figure 19: (A) In circuit theory models, a resistor's value is given by the probability of movement between its incident nodes. Fire connectivity is modeled via a voltage input that begins at a source node and moves randomly through the network until it reaches a target node. (B) To model fire connectivity in the Sonoran Desert, the whole study extent was represented as a circuit network by representing landscape grid cells as nodes connected to adjacent nodes by resistors. The resulting current density at any node was an estimate of the net, directionless likelihood of fire. (C) An 'omnidirectional' approach was used to account for overall fire connectivity, by implementing a model with one whole edge of the study extent as source and the opposite edge as target.

Standard statistical models investigating large fire occurrence develop and analyze continuous maps of the conditional probability that an ignition event will become a large fire (e.g., Gray et al. 2014). The probabilities in these models reflect a calculated likelihood that an ignition will result in a fire of at least some predetermined size, but are not able to generate predictions regarding fire spread dynamics beyond the specific location and size threshold. These models therefore offer limited capacity to predict whether a given location on a landscape is going to burn (Thompson & Calkin 2011). Our models are designed to overcome these limitations. In a circuit-network representation, the probabilities influence the strength of resistors, reflecting the probability that individual ignitions will grow and spread to incident nodes. The connectivity model thus treats the conditional probability of large fire as one parameter in defining a landscape conductance to fire spread. That conductance layer also incorporates other spatial controls that act on fire spread in order to reflect the overall probability of fire spread between incident nodes. Since the relative influences of spatial controls on fire vary between landscapes (e.g., Rollins et al. 2002), defining conductance necessarily requires a local- to landscape-scale approach. Our connectivity model therefore treats the conductance layer as an interconnected network, and resulting estimates of fire likelihood account for landscape-specific spread dynamics.

Estimating fire likelihood

The previously described logistic regression model permitted a spatial estimate of annual large fire probability under high fire hazard conditions (i.e. high large fire probability scenario), built on estimates of the maximum NDVI from 2004 and 2005. We used a GIS to generate model inputs and map predictions using a 450-m (20 ha) grid cell size. This grain size corresponded with the large fire threshold, and was thus a good minimum, sufficient grain size to introduce into a circuit network model. Next, we introduced fire spread behavior into the model by including the interaction between wind direction and topography. The maximum effect of wind and topography on fire spread occurs when wind direction is directly aligned with aspect (Whelan 1995). Favorable fire weather brings dry hot winds that interact with topographic features and strongly influence burn patterns. We used the program WindNinja (v2.1.3, Missoula Fire Sciences Laboratory, Missoula, MT) to simulate the effect of terrain on wind flow across the study region. With this program, an initial domain-averaged wind speed and direction are specified, and the program computes the spatial variation in these parameters based on topography and dominant vegetation. To obtain the initial inputs, we generated long-term (1986-2009) monthly averaged wind roses from the Western Regional Climate Center (www.wrcc.dri.edu, accessed February 2012). For the most active fire months in our study region (May-July) and daily burning period, the dominant winds were south-southwest with observed 10-minute average speeds of 12.9 – 20.9 km/h. Since peak winds within 10-minute averages significantly affect fire growth, we used a probable maximum 1-minute speed of 30 km/hr (Crosby & Chandler 2004). We ran simulations for both 180° (south) and 225° (southwest) wind directions and wind speeds of 30 km/hour. Using the GIS, we derived a 450-m resolution grid based on the spatially varying wind direction with respect to aspect.

To employ circuit theory, fire likelihood was estimated using cumulative conductance values, an additive combination of conditional large fire probability and spatially varying winds. When incorporated into a conductance layer, these values created a network of interconnected resistors in the fire connectivity model to reflect the probability of or resistance to fire spread from incident 'ignited' nodes. To estimate fire connectivity, we used Circuitscape (v3.5.8), an open source software program that applies circuit theory to predict current flow across large landscapes (McRae & Shah 2009). We used an 'omnidirectional' approach (Pelletier et al. 2014) to account for overall landscape conductance by implementing a model with one whole edge of the study extent assigned as source and the opposite edge as target. Each edge was one grid cell in width (i.e., 450 m). We repeated this method for each of four source-target pairings (north-south, south-north, east-west, west-east) and each of two conductance scenarios (180° and 225° winds), for a total of eight model runs. The map outputs resulted

in a current density for every grid cell, equivalent to the overall likelihood of fire passing through that cell. Using the GIS, we summed these grid-based model outputs to generate a scenario of overall fire likelihood. This approach differs from fire likelihood estimation methods based on distributed fires across a landscape with individual starting and stopping events (e.g., Finney et al. 2011, Ager et al. 2012). These events are typically drawn from probability distributions of burn duration and fire-season weather, so that the results represent long-term, annualized burn probabilities. Our approach was meant to avoid these assumptions, which are rarely based on sufficient data, and to fully represent all possibilities of fire spread in a year with high fire hazard conditions (i.e., 2005). Note that our definition of large fire size (i.e., 20 ha) corresponded to the modeled resolution, making results conditional on large fire occurrence.

To validate the performance of the fire connectivity model, we used a method that relies on burned area data and makes no assumptions about areas that have not burned. We used 13 years (2000-2012) of MODIS multispectral satellite-based burned area data (500-m pixel resolution; http://modisfire.umd.edu/BA_getdata.html, accessed August 2013) to identify evaluation grid cells. We binned fire likelihood cells into ten quantiles, and calculated the proportion of evaluation cells within each bin. We also calculated the proportion of fire likelihood cells within each bin and considered this the proportion expected by chance. The ratio of observed to expected proportions within each bin indicates a frequency of fire occurrence relative to chance, and lower ranked fire likelihood bins should have a ratio less than one, whereas higher ranked fire likelihood bins should have a ratio increasingly greater than one (Hirzel et al. 2006). We plotted this ratio against the ranked bins and calculated a Spearman rank correlation coefficient (r_s). High positive values of r_s would result from an increasing curve and would indicate that the ratio increases as fire likelihood increases, as should occur if the model adequately predicts observed fire occurrence. We considered values of $r_s > 0.80$ as indicative of exceptional support for the model. Boyce et al. (2002) presented a similar approach with presence-only validation data to assess the ability of resource selection functions to consistently predict habitat use within levels of suitability.

Evaluating fire effects

Taking into account the impact of repeated fire and major vegetation associations in the lower Sonoran Desert, we characterized fire effects based on the degree to which future fire exposure is expected to negatively impact native plant community recovery. This approach relied on the notion that higher productivity and diversity of native plants increases fire resiliency (Wisdom & Chambers 2009), and that repeated fire will differentially impact plant communities based on their fire resiliency (Brooks & Chambers 2011). Differences in plant productivity and diversity were broadly grouped into the two ecological subdivisions of our study area – the Lower Colorado River subdivision and the Arizona Upland subdivision. While these subdivisions were created solely in reference to the vegetation, they parallel other ecological gradients that influence fire resiliency, such as available precipitation (Comrie & Broyles 2002). The Arizona Upland subdivision harbors higher plant productivity and richness and thus was assumed to display higher fire resiliency. We retrieved a shapefile of these subdivisions (www.azconservation.org/downloads; accessed August 2010), which was digitized from the original 1980 map 'Biotic Communities of the Southwest' (Brown et al. 1980). We also used mapped fire perimeters from the Monitoring Trends in Burn Severity project (www.mtbs.gov, accessed November 2011), which provides a consistent and continuous source of mapped fire perimeters > 405 ha, from 1984 to 2011. We used these data to determine whether a specific location had burned within the perimeter of a large fire in the recent past. We merged these two datasets in the GIS and assigned the outputs to relative classes of fire effects based on the association with expected fire resiliency. We assumed that fire would have the least negative effect in unburned extents of the Arizona Upland subdivision, with more negative effects in unburned extents of the Lower Colorado River subdivision or

burned extents of the Arizona Upland subdivision, and the most negative effects in burned extents of the Lower Colorado River subdivision. Since the lower Sonoran Desert is not well adapted to fire and large fire anywhere is expected to have at least moderately negative effects, we assigned these outputs to moderate, high, and very high fire effect classes, respectively.

OBJECTIVE 6: Integrate the above models in a spatial decision-support package that informs sustainable resource management and recovery of native habitats and species on DOD and adjacent lands.

Task 14: Design and develop scenarios for decision support

Stakeholders in the Sonoran Desert face increasing uncertainty in developing near- and longer-term natural resource management objectives due to the synergistic impacts of climate change, plant invasion, and fire risk. A key objective of this project was to generate meaningful data and analysis and to contribute these for decision support to our collaborators. These collaborators include managers, decision makers, and technical staff within the DOD, BLM, Tohono O’odham Nation, U.S. Forest Service, several national monuments, the USFWS, and the Arizona Game and Fish Department (AGFD). To leverage our results for the greatest benefit to these collaborators, we developed and utilized a spatial decision-support system (SDSS) (Sisk et al. 2006). The SDSS was a multi-step process in which we participated in a series of interactions (formal and informal) with decision-makers and land managers to clearly identify congruent collaborator needs and project deliverables; structure management need-driven scenarios with existing and developing SERDP project data; present, review and refine scenarios; develop data and scenario delivery package with supporting documentation; and conduct an inter-agency delivery workshop (Table 5). In combination, these methods enabled us to direct our support toward the greatest needs identified by our partners and to translate results in the most effective way possible, breaking down the pervasive barriers between researchers and end users.

We engaged managers and decision makers through an introductory project meeting (March, 2010) by facilitating ongoing discussions regarding permitting and site selection criteria on their lands, and by conducting a comprehensive Needs Assessment Survey (NAS). The NAS provided a mechanism for collaborators to identify their data and information needs. It also served as a means for gaining insight into the institutional cultures and decision processes typical of the different land management units encompassed by our study area, as well as into the inherent challenges of working with multiple agencies across jurisdictional boundaries. To develop and carry out the survey, we structured and posed multiple questions that were electronically delivered to individuals identified through a series of phone calls with our collaborators. Subsequent interactions with our collaborators helped to guide the development of data and other research products for this project. We synthesized the collaborator responses to the NAS in a summary report, which was delivered electronically to all collaborators that had received the survey.

We developed scenarios based on the NAS synthesis and in-person or telephone communications with collaborators on DOD and adjacent lands to address priorities identified in those communications. Uncertainty exists within both the science and management community about the role of invasive species in promoting fires on DOD lands in the Sonoran Desert. Identification of critical needs has been driven by a desire to reduce that uncertainty and thus has tended to be focused on fire risk and herbaceous fine fuels. While invasive species distributions for their own sake are important to managers, it is important to note that our scenarios highlighted the two risks (invasion and fire) both jointly and independently and thus provided managers information in both contexts.

Table 5. Outreach and information exchange schedule for the project SDSS.

| Period | Outreach task |
|-------------------|---|
| March 2010 | Introductory meeting in Yuma with DOD installation, AGFD, and FWS ecologists; field work to pilot sampling methods |
| May 2010 | Began identification of and contacting of prospective collaborators (i.e., installation staff, land managers, decision makers, and other collaborators within project area) |
| Dec 2010-Jan 2011 | Distributed formal project NAS to multiple collaborators |
| Jan-April 2011 | Phone calls and in-person interactions with project collaborators to a) provide project status, b) establish permits, and c) participate jointly in safety, field training, and sampling site selection |
| May 2011 | Submitted Sonoran Desert Research Program (SDRP) NAS summary to DOD staff and other collaborators |
| Jan-April 2012 | Interfaced with collaborators to a) provide project status and b) establish permits |
| May 2012 | Interfaced with DOD staff, project collaborators, and other project PIs at IPR meeting to a) provide project updates and b) expand discussions on specific information needs and data delivery methods |
| March 2013 | Phone interviews a) report on project status, b) gauge interest in further information on the data products, c) identify times for in-office visits |
| May 2013 | In-stakeholder office meetings where we met with 15 people from five jurisdictions to a) share preliminary data products b) engage and receive feedback from agency personnel on invasives, GIS and data capabilities, and fire. This effort expanded our outreach by 11 new people including managers, biologists, GIS and field staff |
| Nov 2013 | Final workshop |

Task 15: Develop collaborative process and stakeholder workshops

In addition to the formal NAS summary report, our outreach efforts (e.g., data transfer or acquisition, training, and professional presentations) included interactions with resource managers during field visits, permitting processes, the SERDP In-Progress Review (IPR) meeting in May, 2012, and other ongoing activities with core agency collaborators, including Steven Sesnie (now USFWS) and Steven Rosenstock (AGFD). Additionally, we conducted phone interviews with DOD and other adjacent land managers in order to: a) review and refine our understanding of their most pressing needs; b) provide a succinct description of our project status and deliverables and how our products can support their management needs; and c) identify date and setting for a stakeholder results-transfer workshop. Importantly, these interactions allowed us to further structure the SDSS process, ensure all data are

developed and distributed in usable format(s), and to develop scenarios of future climate and land use across the study area.

During the IPR meeting, we shared our initial research findings and interacted with key collaborators (installation staff, land managers, decision makers, and other collaborators within project area) and further discussed their overarching land management challenges and issues, with a focus on those related to invasive species and fire. These discussions often targeted specific research needs and how those needs could be addressed within the context of the technical and data limitations facing installation ecologists and managers. Our goal was to gain insights into which research products would have the greatest utility, as well as the technical aspects of how these products might be applied. Interactions at this meeting also addressed a) installation experiences with and access to pertinent software and computing environments; b) intra-agency support for data used to inform decision making; and c) possible data delivery and tech transfer methods. We engaged in more specific conversations with DOD personnel to establish personal connections that could facilitate subsequent conversations about their technical and information needs and how we might best meet those needs.

Task 16: Tool transfer, training, and presentations

In May of 2013, we conducted in-person visits with managers of multiple jurisdictions (Tohono O’odham Nation, Organ Pipe National Park, BMGR/YPG, Gila Auxiliary AFB, and USFWS Refuges) to discuss our work, its results, and applicability to management priorities of regional stakeholders. These meetings helped us to further pinpoint the needs and questions of these partners relevant to this study.

In November of 2013, we led a full-day workshop at Gila Bend Air Force Auxiliary Field. Attendees represented eight entities. Our presentation outlined the methods used to derive our results, presented maps in a Data Atlas as visual outputs of our fire modeling and invasive species spread modeling, and discussed the implications of environmental factors and year-to-year variability for our modeling approaches and for fire risk and invasive plant distributions. The discussion following this presentation focused on transfer of this information for management purposes.

Results and Discussion

OBJECTIVE 1: Develop empirical remote sensing-based models of the distribution and biomass of non-native invasive plants in the Sonoran Desert and surrounding ecoregions.

Task 2: Field sampling efforts¹¹

We sampled 238 plots (1171 subplots) in 2011 and 506 plots (2530 subplots) in 2012 (Table 3). In 2011, 59% of subplots yielded detection of at least one target species, whereas 84% of subplots in 2012 yielded detection of at least one target species. Detection of *Schismus* nearly doubled from 2011 to 2012, reaching 93% and 80% on plots and subplots, respectively. The proportion of plots and subplots where *Brassica* was detected was consistent across the years, perhaps because low rainfall in both years limited the occurrence of the species. In both sampling years, *Eruca* was detected in clustered populations in highly localized areas.

Considering the design of our sampling effort (Task 1), which was informed by habitat suitability modeling, field-based detections corresponded very well to the stratified habitat suitability and NDVI models in both years, and across all target species (Figure 20; Wang et al. 2014). At least three out of five target non-native species were detected in 74% of subplots in 2011 and 93% in 2012, and these subplots fell within the 70th percentile of at least one of the habitat suitability models. Mean biomass

¹¹ These results have been peer-reviewed and published in Wang, O., L. J. Zachmann, S. E. Sesnie, A. D. Olsson, and B. G. Dickson. 2014. An iterative and targeted sampling design informed by habitat suitability models for detecting focal plant species over extensive areas. PLoS ONE 9:e101196.

extrapolated for subplots in 2011 was 51.3 kg/ha with a maximum of 1,328 kg/ha. The mean biomass extrapolated to subplots in 2012 was 43.9 kg/ha with a maximum of 1,404 kg/ha. Thus, there were both a decline in biomass between the two years and heterogeneity across the sampling region. The sampling distribution of biomass in the two years was strikingly similar, but biomass sample values clustered more around the middle range of biomass values in 2012. Differences may have resulted from the 2011 season following a productive spring in 2010, whereas two successive years of drought preceded the 2012 field season.

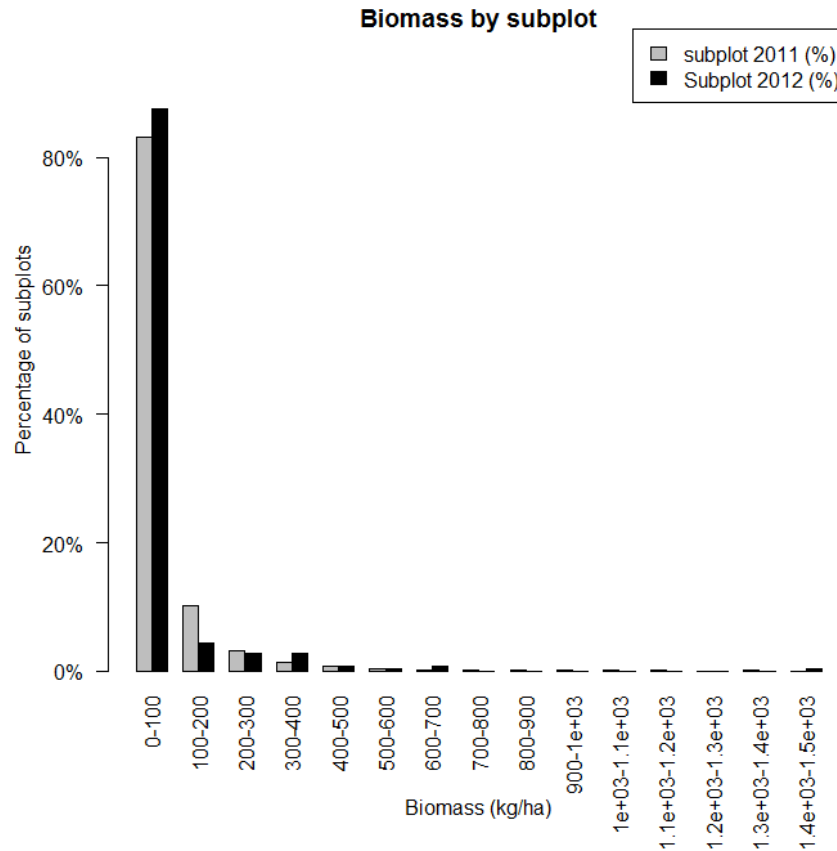


Figure 20: The percentage of subplots containing different amounts of biomass sampled in 2011 and 2012. The number of subplots from which biomass was collected in the two years varied significantly, with 1171 subplots sampled in 2011 and 591 sampled in 2012. This decrease was met with an increase in efficiency in terms of the total number of plots sampled and in the relative biomass collected where biomass sampling did occur.

Characteristics of habitat suitability models and model predictions

Model 4 for the winter annuals and Model 5 for *Pennisetum* predicted highly suitable habitats that coincided with areas of previously identified high *Pennisetum* abundance. The environmental attributes of highly suitable habitats (i.e., 90th percentile) for *Pennisetum* reflected expected habitat conditions in elevation, slope, aspect, annual precipitation, and vegetation type. These models identified seasonal precipitation events for germination and growth of the five target species (appearing on the landscape as green-up), as well as road proximity as important to the dispersal and colonization of *Pennisetum*. In habitat suitability models, the most important variable was elevation for *Brassica*, *Schismus*, and *Eruca*, winter precipitation for *Bromus*, and summer precipitation for *Pennisetum*. For *Brassica*, *Schismus*, and *Eruca*, elevation accounted for 65%, 51%, and 38% of explained variance for Model 4, respectively. Slope was the second most important variable for *Eruca*, accounting for 31% of explained variance. Winter

precipitation was the second most important variable for *Schismus*, accounting for 21% of variance for *Schismus* and 34% for *Bromus*. For *Pennisetum*, summer precipitation in Model 5 accounted for 56% of explained variance.

All 25 HSMs exhibited AUC values that were significantly higher ($p < 0.05$) than null models constructed with random sampling points. All AUC values exceeded 0.70 for training AUC (ranging from 0.73–0.97) and test AUC (ranging from 0.71–0.93). For all HSMs, species presence/pseudo-absence was significantly correlated with predicted habitat suitability with notable variation among species (0.36–0.8 for point biserial correlation (COR), $p < 0.01$ or < 0.0001). COR values were the highest for *Eruca* and *Brassica* and lowest for *Bromus*.

Together, Model 4 for the winter annuals and Model 5 for *Pennisetum* indicated that 81% of the study area was within high predicted habitat suitability (i.e., 70th percentile) for at least one of the five species. For one, two, and three focal species, respectively, 38%, 29%, and 12% of the study area corresponded to the 70th percentile of suitable habitats. Areas with low to medium suitability were spaced out across the study region. In combination, the 25 HSMs predicted 39% of the study area to have low (i.e. 30th percentile) to very high habitat suitability for the five focal species with notable variation among species. Suitable habitats for *Schismus*, *Brassica*, and *Bromus* were common, whereas suitable habitats for *Eruca* and *Pennisetum* were more rare across the study area. Models identified 59%, 64%, and 55% of the study area as exhibiting low to very high suitability for *Brassica*, *Schismus*, and *Bromus*, respectively. Models predicted very low suitability (i.e. below 30th percentile) for 42% and 58% of the study area for *Eruca* and *Pennisetum*, respectively.

Sampled locations in 2011 across ranges of habitat suitability

For 2011, model outputs successfully guided our field data collection efforts, and also identified subplots predicted to harbor very high habitat suitability for one focal species but low to medium suitability for other species. This targeted sampling was directed, for example, at the 28% and 62% of sampled locations that were within the 90th and 70th percentile, respectively, of *Brassica* habitat suitability, and were also within areas of lower suitability for at least one of the other four species. For *Schismus*, 16% and 39% of total locations that were within the 90th and 70th percentile suitability, respectively, fell within lower habitat suitability of at least one of the other four species. Fewer sampled locations were within areas of high habitat suitability for *Bromus* and *Pennisetum*. Our decision to sample in habitats including low to very high predicted suitability values was conservative, providing opportunities to detect unknown populations or unknown areas of species distribution.

Correspondence between detections and habitat suitability models

In 2011, at least one of our five focal species was detected in 184 (77%) plots and 686 (59%) subplots. *Schismus* was most frequently detected, in 56% of plots in 2011 and in 43% of subplots (Table 3). *Brassica*, by contrast, was detected in 47% of the plots and 28% of the subplots and exhibited considerable clustering. *Brassica* was locally more abundant than *Schismus* but less frequently detected. *Bromus*, *Eruca*, and *Pennisetum* were uncommon. Models suggested that sites where *Bromus* and *Pennisetum* were detected were likely at the edge of their suitable habitat. *Eruca* occurred in few clustered populations in highly localized areas.

We observed remarkably high correspondence between models and field data: among the 686 subplots with presence of at least one out of five focal species, 652 (95%) fell within the 70th percentile of at least one of these HSMs. Furthermore, 80% (206) of the 257 subplots where multiple ($n \geq 2$) focal species had been detected fell within the 70th percentile of more than one of these HSMs. *Schismus* and/or *Brassica* was present in 70% of the sampled locations. Ninety percent of the plots and 87% of the subplots where *Brassica* occurred were within the 70th percentile of the *Brassica* HSM. Where *Schismus*

was present, only 54% of plots and 49% of subplots corresponded to the 70th percentile of the *Schismus* HSM, reflecting the greater environmental variability across the distribution of that species.

Four of the five *Bromus* models showed high predicted detection rate (> 0.8) at high habitat suitability (> 0.8). All five *Schismus* models showed positive but less strong relationships, as predicted detection rates ranged from low to medium (0.2–0.6) across low to very high habitat suitability. Predicted detection rates were low (less or near 0.2) across the gradient of habitat suitability for *Eruca* and *Pennisetum* models, consistent with our field data that populations were regionally rare and locally abundant at only a few locations. All models of detection rates outperformed regression intercept models when predicted habitat suitability was included. The average Δ AIC was > 10 (i.e., our threshold of model goodness of fit) for all five models for each focal species (average Δ AIC = 12.8– 229.2). *Brassica* and *Bromus* models showed the strongest fit, whereas *Eruca* and *Pennisetum* models were the weakest.

Both sample size and detection rates in 2012 increased with iterative efficiency adjustments by integration of additional HSM input data, stratification of HSMs and other vegetation indices, and more rigorous sampling location prioritization and targeting. Of those subplots where the focal species were detected in 2012, 93% fell within the 70th percentile of at least one of the HSMs for each species. Detections for *Schismus* and *Brassica* occurred within the 70th percentile of species HSMs at rates of 76–78% of plots and subplots, respectively.

The environmental characteristics of invasion

The advantage to our decision to target a range of recruitment sites with our sampling, working across habitat suitability gradients for each species, was that we were able to obtain a more realistic estimate of the extent of invasion across the study area despite two relatively dry winters preceding sampling. *Brassica* is associated with extremely sandy soils and dunes, whereas *Schismus* was more generally distributed as a minor component of most plant communities represented in our study area. The other three target species were less well-represented in our field data. Since *Eruca* was recently introduced, it may eventually cover a much more extensive range than it currently inhabits (Rorabaugh 2010), and HSMs may be unable to estimate its true fundamental niche. By contrast, *Bromus* and *Pennisetum* appear better suited to Sonoran Desert uplands with higher winter and summer precipitation than are typical of the lower Colorado River subdivision (Brown 1994) so are likely to remain rare in the hottest desert areas with extremely low summer rainfall. During our preliminary sampling in 2010 at locations with great abundance of *Pennisetum* in south-central Arizona, where the mean annual precipitation is 32.3 cm (Olsson et al. 2012b), we detected much higher presence (47%) and cover (11%) (Wang et al., unpublished data).

Detection rates across ranges of habitat suitability

By sampling across habitat suitability ranges in 2011, detection rates for *Schismus* at plot and subplot levels and *Brassica* at plot level outperformed those of another multi-species study that used simulated field detections and multiple field sampling methods (Maxwell et al. 2012). By revising the sampling to be more targeted in 2012, we boosted the sample size still further. Our model outputs identify many suitable locations that *Brassica* could colonize but has not yet reached, or was once abundant but has decreased due to low rainfall. *Eruca* appears to be dispersed along recently abandoned agricultural fields and washes, but models show that it also has the potential to occupy relatively undisturbed locations, such as sandy areas with surrounding rocky terrain. The detection rate for *Schismus* was less variable across the range of habitat suitability, perhaps because this species occupies a broad range of environmental conditions.

Our sampling design yielded high detection for our focal species but was limited in some respects. As is often the case for HSMs, we constructed our models by leveraging available datasets. Those data might not fully represent the distribution of a given species in the study area. Small *Schismus*

plants are often hard to identify, and *Eruca* is still regionally relatively rare. We sampled reasonable distances away from roadsides and across large environmental gradients (i.e., habitat suitability ranges) to capture variation that opportunistic sampling would not have been able to accomplish, reducing non-detection sampling bias.

Additionally, our HSMs provided landscape- to regional-scale habitat suitability information to stratify potential occurrence locations and identify uninhabited areas that are suitable for colonization (Araújo & Peterson 2012). The models may not capture local- or fine-scale variation of colonized habitats. HSMs based on presence-only data cannot account for species absent from highly suitable habitats or present in less suitable habitats due to biotic, historical, or dispersal factors (Pulliam 2000; Holt 2003; Sillero 2011). For example, *Eruca* currently occupies a very low proportion of its predicted suitable habitats, but could expand its distribution during years of increased plant productivity, such as ENSO events.

Extending our designed and targeted sampling framework

Our sampling design allowed us to improve detections for sparse and patchy populations by stratifying locations using HSMs and other ancillary data important to focal species establishment. This approach could easily be applied in other systems and for other focal species. Our framework is particularly relevant to ecosystems where, as in the Sonoran Desert, varied rainfall patterns may facilitate periodic and large increases in non-native invasive plant production and fuel loads followed by dry periods of increased fire risk (i.e., much of the American West). Modeling results can guide the design of management protocols by explicitly linking model-informed sampling to management strategies (Jones et al. 2010).

Several key strategies improved detections rates. First, location selection using strata predicted by HSMs should include a greater range of habitat suitability that covers more local habitat variation. Adding other stratified vegetation indices such as remote sensing-derived phenological metrics in vegetation greenness can enable sampling to be directed toward areas of greater focal species productivity and abundance. Second, implementing a stratified random and spatially confined approach using rigorous criteria can increase sample size. Third, plot prioritization for sampling can be based on vegetation indices from recent remotely-sensed imagery. These data reflect vegetation greenness by annual plants prior to field work and helps to avoid sampling in areas with low or no annual plant production. Finally, targeting specific soil substrate type can help elevate efficiency of sampling for focal species that show strong habitat preferences to particular substrate types. These substrate data can be derived from spectral mixture analysis of high-resolution field spectrometer data, and satellite image classification can guide sampling prioritization.

Task 6: Non-native mapping (Landsat/MODIS/WV2)

A comparison of Landsat TM and MODIS vegetation indices for estimating phenology¹²

Reflectance of invariant targets should remain constant over time. However, reflectance variables emerge over time out of errors due to atmospheric and other noise. The atmospheric correction minimized this variance, resulting in clustering of pixels from three dates in corrected scenes. No additional corrections were applied to MODIS VIs that were pre-processed with the constrained view angle maximum value composite algorithm to reduce atmospheric and terrain effects.

In arid lands, increased plant production is particularly tightly coupled with periods of increased precipitation (Allen 1991). When winter–early spring precipitation is sufficient, annual plants initiate

¹² These results have been peer-reviewed and published in Sesnie, S. E., B. G. Dickson, S. S. Rosenstock, and J. M. Rundall. 2012. A comparison of Landsat TM and MODIS vegetation indices for estimating forage phenology in desert bighorn sheep (*Ovis canadensis nelsoni*) habitat in the Sonoran Desert, USA. *International Journal of Remote Sensing* 33:276-286.

growth between October and November and mature between February and April. Increased precipitation facilitates increased growth. KNWR prior to and during the study period experienced increased monthly rainfall during late fall 2007 and early 2008, characteristic of winter frontal systems that can bring widespread rainfall to the Sonoran Desert (Hanson et al. 1999). Monthly average temperatures were relatively consistent, but precipitation in 2007 and 2008 was highly variable between the years. These conditions typified the high inter-annual variability of rainfall in this region.

The number of available cloud-free Landsat TM image dates was less than the number of MODIS 16-day composited scenes (13 vs. 23). TM presented a less-complete record of plant phenology and productivity. Of the TM-derived VI values, EVI appeared less sensitive to areas of steep rocky terrain shadowed during image acquisition (Figure 21). Departure values greater than 100% of the annual average were considered green-up events or periods of increased plant productivity (Pennington & Collins 2007; Beck & Gessler 2008; Mildrexler et al. 2009; Van Leeuwen et al. 2010). Monthly DA below 100% represents lower productivity periods where annual plants are in an early-germination stage or have undergone senescence. EVI departure values were, in general, more consistent with green-up events corresponding to November to January rainfall during 2007 and 2008 and increased spring temperature in February and March 2008.

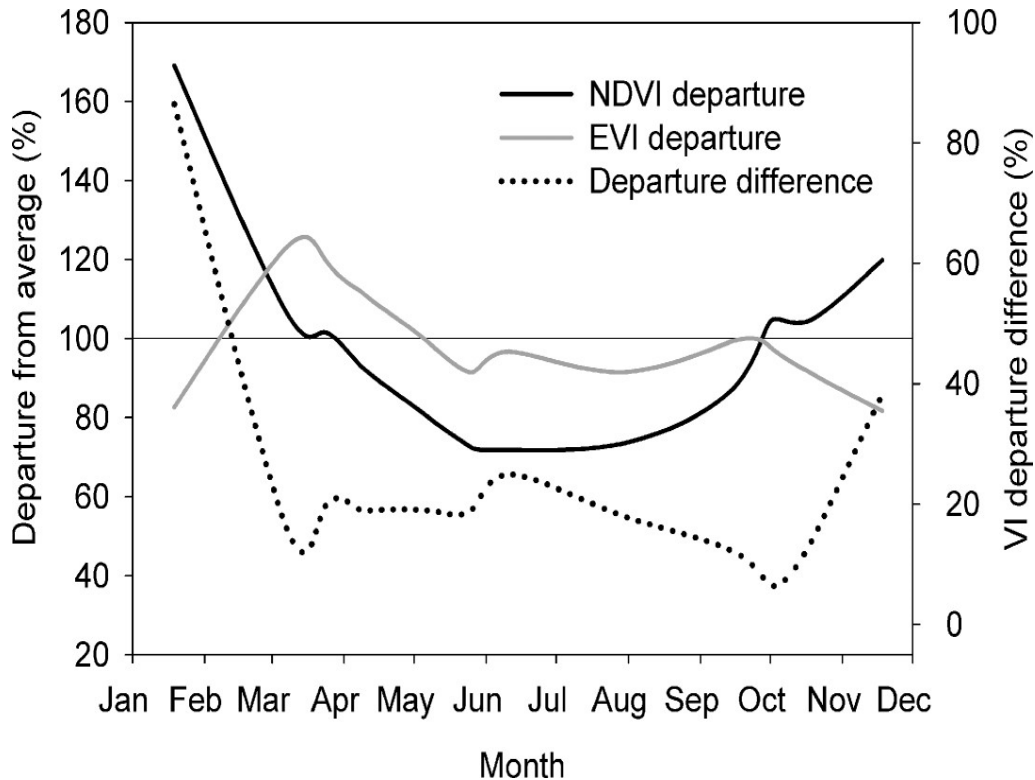


Figure 21: Monthly departure from average Landsat NDVI and EVI values for steep, shaded terrain across the study area. The dotted line (black) represents the percent difference between TM NDVI and EVI values.

Both NDVI and EVI produced inordinately high or low departure values for image dates with a low sun elevation angle ($< 40^\circ$). A comparison of mean VI departure values from pixels within shaded areas showed a significant difference between EVI and NDVI ($U = 213, p < 0.001$) with a median DA of 83 and 170%, respectively, for the month of January.

Northeast-facing slopes and canyon areas with a lower amount of annual solar radiation typically maintain ephemeral herbaceous plants and deciduous shrubs in the study area (pers. obs.). In areas of steep and shaded terrain, MODIS NDVI DA was less sensitive to terrain and shadow effects than was EVI DA. EVI- and NDVI-derived departure values for shaded terrain in mountainous areas also showed a statistically significant difference ($U = 101080.5$, $p < 0.001$) for low sun elevation angle months such as January. In contrast, areas of low topographic variation showed nearly identical MODIS VI departure values, further indicating greater sensitivity of EVI to terrain effects. Areas of steep shaded terrain displayed significantly higher residual departure values than did values from level terrain ($t = 347.0$, $p < 0.001$).

This is particularly important when calculating DA values as a measure of annual and inter-annual green-up events in areas of steep topography. Extremely low EVI departure values ($\geq 20\%$ lower than NDVI DA attributable to terrain and sun angle effects) negatively impacted time series data, erroneously indicating above-average greenness during hotter and drier months of the year that are typically associated with low productivity and senescence of winter annual grasses and forbs. Falsely low EVI values in shaded areas produced low annual average values for these pixels, resulting in higher than expected DA values for summer months.

Use of WorldView-2 high spatial resolution imagery to detect desert invasive plants¹³

For 1,885 subplots located across the study area (2011 and 2012), *Brassica* was detected in a total of 748 (40%). *Brassica* canopy cover averaged 7.5%. Average reference maximum biomass of *Brassica* was 2.19 g/m², but the estimated average *Brassica* biomass at plot scale was only 0.82 g/m². Native herbaceous cover averaged 11%, average reference maxima for native herbaceous biomass was 1.64 g/m², and the average native herbaceous biomass was 1.17 g/m².

Accuracy was quite high for the WV2 MTMF classification using field collected spectra (overall 88%). Producer's values were 86% and 91% accurate for presence and absence, respectively, while user's accuracies were 94% and 79%. The overall accuracy of resampled WV2 MTMF classification was 67%. Under this classification, accuracy of producer's values were 47% and 84% for presence and absence, respectively, and accuracy of users were 70% and 66% for presence and absence, respectively. Finally, the ETM+ MTMF classification had an overall accuracy of 59%. Producer's accuracies in this classification were 0% and 100% for *Brassica* presence and absence, respectively, whereas user's accuracies were 0% and 59%.

MF scores and *Brassica* abundance estimate

Available WV2 scenes overlapped with 136 of the plots for which we were able to gather *Brassica* canopy cover estimates. Target detection rate in these plots was 58%. When WV2 MF scores were correlated with *Brassica* percent cover estimates, the coefficient of determination (R^2) was 0.004 with p -values of 0.473 and 0.011 for MF scores and infeasibility, respectively. When only the pixels with positive MF scores were correlated with *Brassica* canopy cover estimates, the regression coefficient of determination was only 0.06, but MF scores were a significant predictor variable (p -values of 0.002 and 0.264 for MF scores and infeasibility, respectively). The R^2 increased substantially to 0.21 when the predictor variable NDVI-B7 was added to the regression model ($p < 0.001$) and rose to 0.36 when the predictor variable NDVI-B8 ($p < 0.001$) was added.

The relationship between *Brassica* percent cover estimates and ETM+ MF scores was weak but significant (coefficient of determination $R^2 = 0.02$; MF scores $p = 0.04$), and infeasibility values were not significant in this test ($p = 0.51$) ($n = 1,465$). The relationship was strengthened by restricting the analysis

¹³ These results have been peer-reviewed and published in Sankey, T., B. Dickson, S. Sesnie, O. Wang, A. Olsson, and L. Zachmann. 2014. WorldView-2 high spatial resolution improves desert invasive plant detection. *Photogrammetric Engineering and Remote Sensing* 80:885-893.

to plots with *Brassica* canopy cover estimates > 1 percent ($n = 266$) ($R^2 = 0.08$; $p < 0.001$ and 0.74 for MF scores and infeasibility, respectively).

NDVI and *Brassica* biomass

WV2 NDVI-B7 and NDVI-B8 produced R^2 values of only 0.03 ($p < 0.001$) when correlated with *Brassica* biomass measured at point locations in the field. Resampled WV2 NDVI-B7 and NDVI-8 produced an R^2 of 0.16 when regressed against *Brassica* biomass ($p = 0.015$ and 0.010, respectively). Results were similar when the same NDVIs were regressed against total native herbaceous biomass. ETM+ NDVI produced an R^2 of 0.002 ($p = 0.46$) when regressed against *Brassica* biomass.

WV2 imagery and invasive plant detection

Our study provides the first quantitative evaluation of desert invasive plant detection using newly available, high-resolution WV2 data. WV2 data enabled detection of small populations of *Brassica* even in a dry year with relatively low plant productivity. *Brassica* presence/absence mapping with WV2 data produced overall accuracy of 89%. WV2 thematic classification overall accuracy was 82% in a forested environment (Immitzer *et al.*, 2012), 77% in a savanna environment (Cho *et al.* 2012), between 57 to 100% in an urban classification (Zhang & Kerekes 2011), and 63% in an urban tree species classification (Pu & Landry 2012). Producer's accuracies for individual tree species mapped with other studies were 65 to 82% (Cho *et al.* 2012), 33 to 94% (Immitzer *et al.* 2012), and 16 to 75% (Pu & Landry 2012), while producer's accuracy for *Brassica* in this study was 86%.

WV2 data provide a large improvement in accuracies for detecting invasive plant populations in desert environments. WV2 use in this study produced almost 30% greater accuracies than ETM+ classification. This is likely due to the high spatial resolution of WV2 data. Resampling 30-m pixels reduced accuracy by 20%, although the same bands, field spectra, and classification approach were used. The higher spatial resolution of WV2 data provides a key advantage in hot desert environments (Wallace & Thomas 2008; Casady *et al.* 2013) where invasive plant populations can become sparse during dry periods, but rapidly expand in favorable conditions.

At the 30-m plot scale used in this study, average percent cover estimates of *Brassica* and other herbaceous classes were extremely low at (7.5% and 11%). Perhaps unsurprisingly, therefore, ETM+ MTMF classification performed poorly at this level of vegetation abundance, although MTMF is a sub-pixel mapping method specifically developed to enhance target detection (Rencz 1999). The ETM+ MTMF accuracy from this study is similar to a previous Landsat TM-based invasive detection application in the Sonoran Desert, where accuracies ranged between 35 to 65% (Olsson *et al.* 2011). Although ETM+ MTMF overall accuracy was 59% in this study, MF scores were extremely low and MTMF did not detect *Brassica* presence, evidently because the low canopy cover in our study area limited detectability.

WV2 imagery and herbaceous plant biomass

Our research provided the first quantitative evaluation of high resolution WV2 data for estimating invasive and native winter annual biomass in an arid desert environment. These results carry implications for land management strategies, including fire response, a growing concern in this region of the Southwest in recent decades (Esque *et al.* 2013). Timely remote sensing assessment of desert fine fuels may help land managers monitor or mitigate damaging fire events in native vegetation communities of the southwestern US.

WV2 NDVI appears to perform poorly in annual vegetation biomass estimates in arid desert environments during extremely dry periods such as the spring 2012 sampled in this study, when biomass of annual plants is low and their signatures weak. Poor performance might be due to georegistration errors between the images and point locations of biomass data, resulting in mismatched individual pixels with point locations. In light of the high temporal and spatial variability in winter annual biomass

in southwestern desert ecosystems, previous studies propose time-series applications in which pixels are compared to extremely dry years (Wallace & Thomas, 2008) or locations (Casady et al. 2013) to calculate relative winter annual biomass. In future studies, multitemporal WV2 data using the proposed methods may better capture temporal variability in winter annual vegetation biomass. Contrasting image dates of high and low annual productivity periods could produce better results than the moderate and coarse resolution time-series data, given the high spatial resolution and promising results from the binary classification in this study.

Target-based mapping using field-based spectra and WorldView imagery

Field data and Image based spectra analysis

Within our WV2 scene focal area, a total of $n = 114$ plots were measured in 2012-2013, with *Eragrostis* detected on 96 plots. Of those, 21 were collected in 2013, concurrent with the acquisition of the WV2 imagery. Plots without *Eragrostis* were a mix of bare soil and other non-native grasses (including the congeners *Eragrostis chlormelas* and *Eragrostis superb*). Common native grasses include *Boutaloua* spp., *Sporobolus* spp., *Aristida* spp., *Bothriochloa barbinodis* and *Digitaria californica*. Common woody species include *Prosopis velutina*, *Gutierrezia sarothrae*, *Acacia* spp., and *Atriplex canescense*.

Pearson correlation coefficients were used to determine the relationship between MF scores, a measure of detectability, and *Eragrostis* cover from field plot data collected in 2013. Results of the MTMF analysis with the two techniques are summarized in Table 6. Based on visual inspection of spectral plots and similarity among field-collected spectra of the non-target species with the target species (Figure 11), two different sets of non-target species were analyzed. The field-collected *Eragrostis* reflectance with two non-target tree species (*Senegalia*, *Prosopis*) was negatively correlated ($r = -0.103$) with MF score and known *Eragrostis* detections in field plots. A second analysis of the target spectra and six non-target species spectra (*Senegalia*, *Prosopis*, *Hopia*, *Sorghum*, *Amaranthus*, *Atriplex*) showed a slight positive increase in the relationship between the field-collected spectra and MF Score ($r = -0.051$). Image-collected EMs showed a positive correlation between WV2 detection of *Eragrostis* and known *Eragrostis* detections in field plots ($r = 0.59$).

Table 6. Summary of *Eragrostis* canopy cover model performance, based on MTMF.

| Technique | Target spectra | Non-target spectra | Accuracy (r) |
|-------------------------|-------------------|--|--------------|
| Field-collected spectra | <i>Eragrostis</i> | <i>Senegalia</i> , <i>Prosopis</i> | -0.103 |
| | <i>Eragrostis</i> | <i>Senegalia</i> , <i>Prosopis</i> , <i>Hopia</i> , <i>Sorghum</i> , <i>Amaranth</i> , <i>Atriplex</i> | -0.051 |
| Image-collected spectra | <i>Eragrostis</i> | Tree, Dirt road | 0.59 |

The differences between target detection results from image-collected EMs and field-collected EMs suggest several areas for further review. One is the FLAASH atmospheric correction involving radiative transfer algorithm MODTRAN (MODERate spectral resolution atmospheric TRANsmittance) applied to the image prior to analysis. Previous research has shown that while the FLAASH correction can perform better than other atmospheric correction techniques, it can produce errors in the bands most sensitive to green vegetation (Manakos et al 2011, Matthew et al 2003). We calculated surface reflectance using basic MODTRAN assumptions because spectral bands in portions of the electromagnetic spectrum used to assess aerosols, water vapor and other particles typical of

hyperspectral sensors were not available for WV2 imagery (Jensen 2007). This likely resulted in less accurate surface reflectance calculations for the WV2 image and low correspondence with field spectra collected on the ground.

Future applications of the WorldView platform

WV2 2-m resolution and other multispectral sensors are impacted by background soil roughness and albedo contributing to spatial and spectral error (Song et al. 2001, Xu & Huang 2008). Further, we see that the differentiation of our target and non-target species spectra happens in the short-wave infrared (SWIR) and NIR bands. Future use of WV3 imagery, which collects 8 additional SWIR bands along with desert clouds and multiple aerosol bands for atmospheric correction, will allow for more robust image correction and surface reflectance calculation. Importantly, we have ordered WV3 data to be acquired concurrently with our 2015 field plot data and biomass measurements over the BANWR focal area. This timing will help to address the temporal mismatch that may have played a role here where field data and imagery acquisition did not occur concurrently, allowing for levels of green-up to have changed.

Overall, the image-based spectra and WV2 provided the more robust detection of *Eragrostis*. We found a stronger and positive correlation between MF scores and *Eragrostis* cover on plots suggesting that the target detection and MTMF methods used for study can aid in mapping non-native invasive plants. Further work is needed to understand how spatial context and other semidesert grassland vegetation may influence detection results and map accuracy. Moreover, we anticipate that WV2 or WV3 image data collected during years with more widespread green-up will help to reduce omission errors that likely occur for image dates with patchy green-up. Ultimately, field collected spectra may also afford accurate map prediction with improved atmospheric correction techniques. To extend this work, for example, to African buffelgrass, field plots will need to be established in areas with varied levels of buffelgrass cover. As a species that is sometimes treated through physical removal or pesticide spraying, it will be important to coordinate imagery acquisition with field plot measurements.

In addition, the use of object-based analysis is being explored more as an alternative to supervised and unsupervised analyses in remote sensing. Coupled with high spectral and spatial resolution imagery, this approach combines selection of shape and texture of targets, increasing the data to draw upon for detection. This technique classifies features from the imagery rather than single square pixels through multi-resolution segmentation and can be used with multiple bands. The approach has been used with WV2 and produced 94% classification accuracy for wetland reed species (*Phragmites australis*) (Lantz & Wang 2013).

Phenology-based mapping of habitat suitability using Google Earth Engine

Random Forest models outperformed SVM models and were used to predict the occurrence of each target species. The final occurrence models were used, first, to compute the predicted probability of the occurrence of a target at each of the plots in our testing partition and, second, to create a spatially-explicit prediction of its occurrence across the entire study extent. The former application was used to evaluate the expected out-of-box error rate for the model, while the latter was developed to inform management and planning decisions by mapping landscape risk (e.g., occurrence under different climatic conditions).

If presence is considered a positive (1) and absence as a negative (0) result, then Figure 22 illustrates the tradeoff encountered upon specifying a reasonable threshold. If the threshold is increased, the number of false positives decreases, while the number of false negatives increases.

The dashed lines (in Figure 23 and Figure 24, 'a' panels) indicate the location of the false-positive rate/true-positive rate (FPR/TPR) corresponding to a threshold of 0.5. Note that the origin (bottom left; 0, 0) and top right corner (1, 1) are associated with a threshold of 1 and 0, respectively. The cost function and corresponding color of the ROC points ('b' panels in Figures 21 and 22) illustrate that an

optimal false-positive rate and true-positive rate combination is determined by the associated cost. The dashed lines in the 'b' panels of Figures 23 and 24 correspond to an arbitrary threshold of 0.5.

The AUC for the SCHIS model was 0.877, while the AUC for the BRT0 occurrence model was 0.855. Note that the cost associated with the arbitrary threshold of 0.5 shown in Figures 23 and 24 (panel b) is not minimized. The final threshold selected for *Schismus*, based on the cost function and the optimization criteria described above was 0.43. The threshold selected for *Brassica* was 0.38. These can be identified by the inflection point (and greenest circles) in their respective cost function curves.

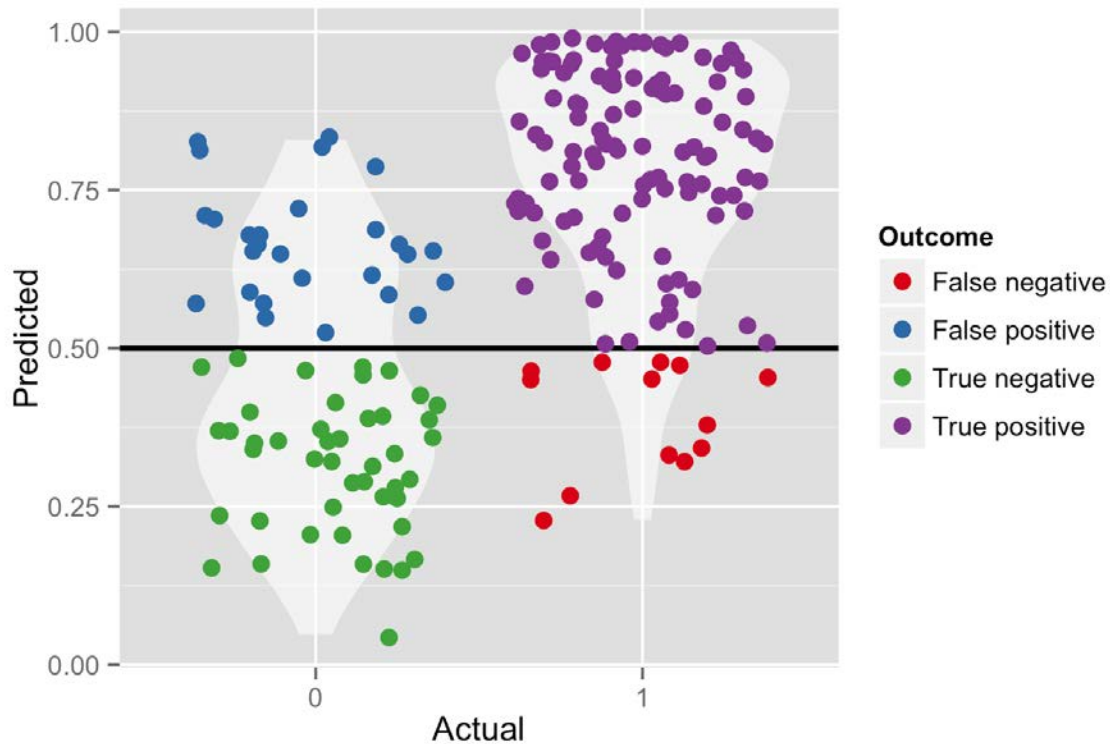


Figure 22: Jitter plot showing the distribution of absence and presence records (0 and 1 along the x-axis, respectively) for *Schismus* on the predicted occurrence probabilities. An arbitrary threshold (the horizontal black line) of 0.5 is displayed for illustration purposes only and does not reflect the threshold selected to reclassify the spatially-explicit predictions described below.

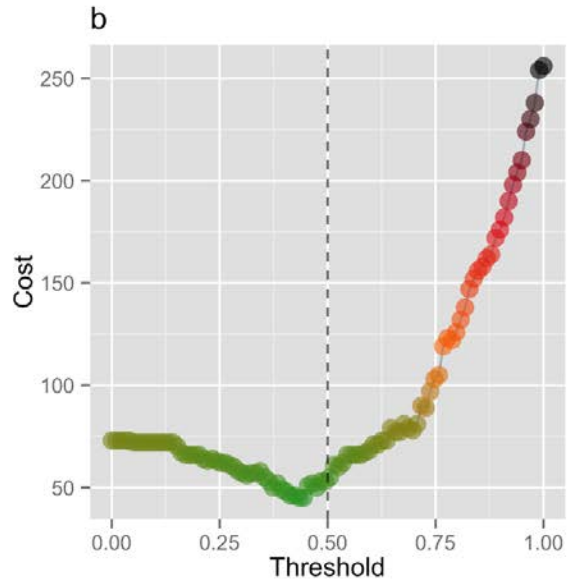
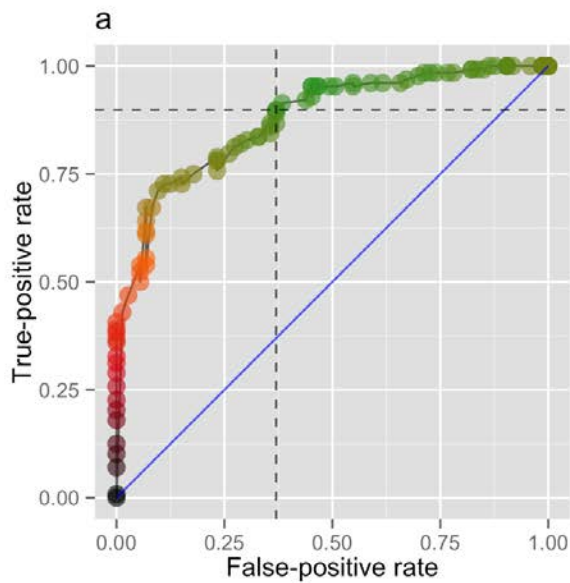


Figure 23: a) ROC curve and b) cost function for the *Schismus* occurrence model. An arbitrary threshold of 0.5 was used here for illustration purposes only. The 1:1 line in blue indicates a hypothetical ROC curve in which a model would perform no better than chance.

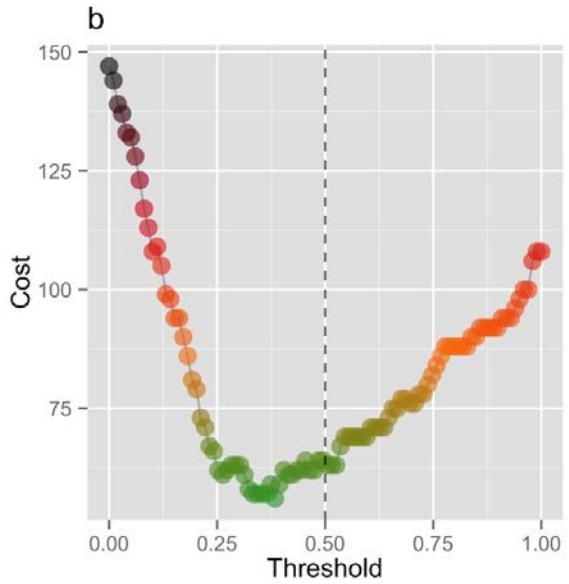
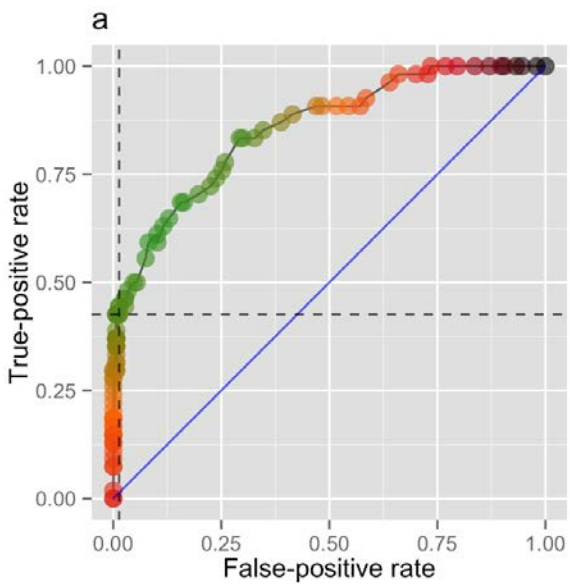


Figure 24: a) ROC curve and b) cost function for the *Brassica* occurrence model. An arbitrary threshold of 0.5 was used here for illustration purposes only. The 1:1 line in blue indicates a hypothetical ROC curve in which a model would perform no better than chance.

Maps of species occurrence and landscape risk

Spatially-explicit maps of the occurrence of each species were derived using the same variables used to fit and evaluate the models. However, because some of the features used in the model are tied to, e.g., climatic conditions in certain time-windows, occurrence could be predicted under different scenarios. Hence, we were able to model landscape risk. Specifically, we predicted occurrence probability both during the last year of the SERDP sampling effort (2012), which was an unproductive, dry year in the Sonoran Desert in Arizona, as well as a productive, wet year (2005). The predicted occurrence probabilities for *Schismus* and *Brassica* are shown in Figure 25 and Figure 26, respectively.

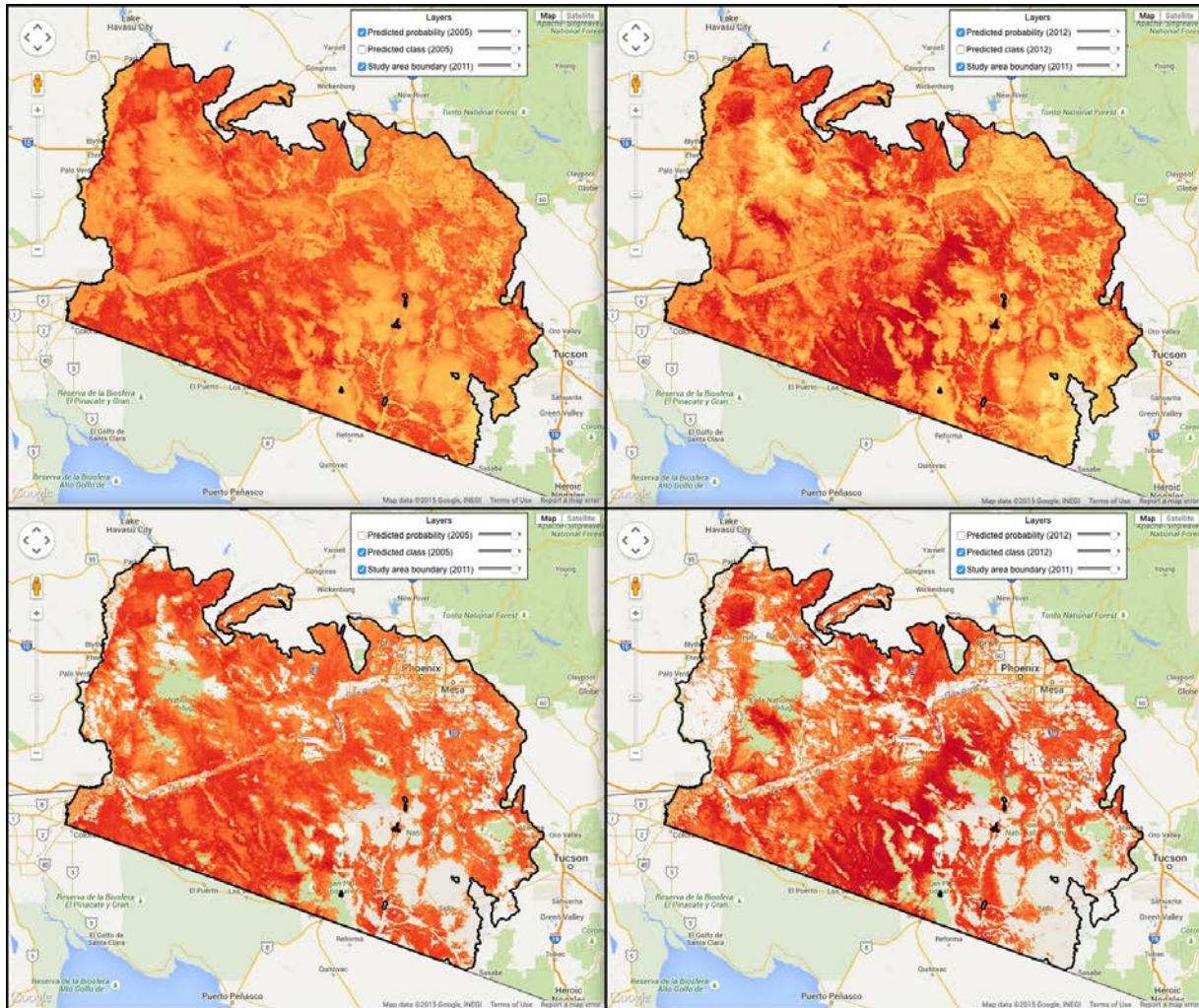


Figure 25: Predicted occurrence probability for *Schismus* in 2005 and 2012 (left and right columns, respectively). Results shown in the maps in the bottom row of the figure have been masked using the threshold identified during the model evaluation step (i.e., 0.43).

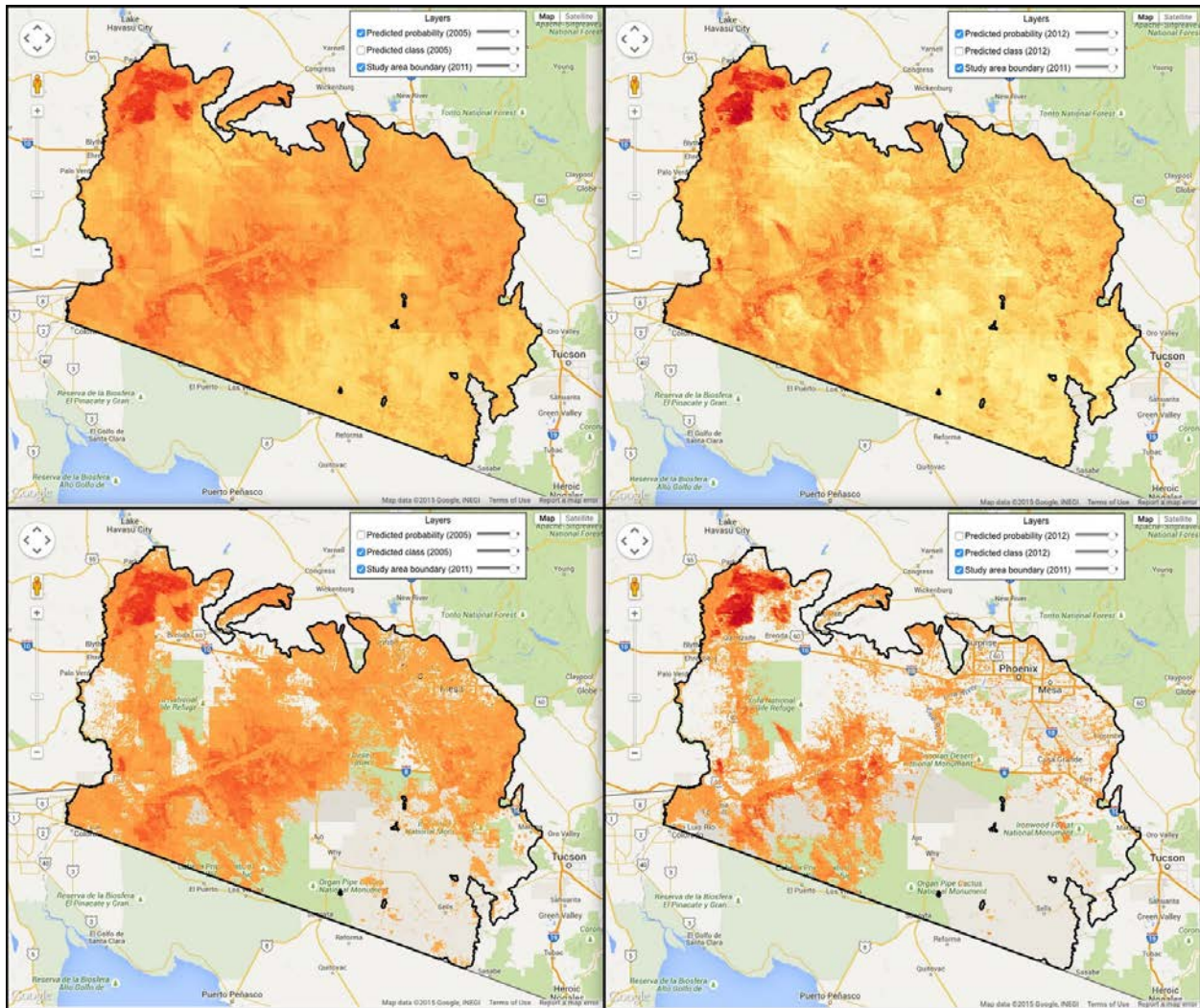


Figure 26: Predicted occurrence probability for *Brassica* in 2005 and 2012 (left and right columns, respectively). Results shown in the maps in the bottom row of the figure have been masked using the threshold identified during the model evaluation step (i.e., 0.38).

Maps of the difference between predicted occurrence probabilities in 2005 and 2012 were also produced. Those results for both *Schismus* and *Brassica* are shown in Figure 27 and Figure 28, respectively.

The models derived for *Schismus* and *Brassica* fall in the 'good' range according to conventions on AUC-related performance measures. The thresholds derived from the cost functions for each species were both < 0.5 , which reflects the relative costs assigned to false-positive vs. false-negative cases *a priori*. Essentially we made the determination that false-negative cases were twice as costly as false-positive cases, since the ecological consequences of *Schismus* and *Brassica* going undetected outweigh the consequences of overestimating their occurrence. The spatial distribution of predicted occurrence probabilities in the bottom row of Figures 23 and 24 reflect the effect of this decision. A different cost specification would have led to slightly different results.

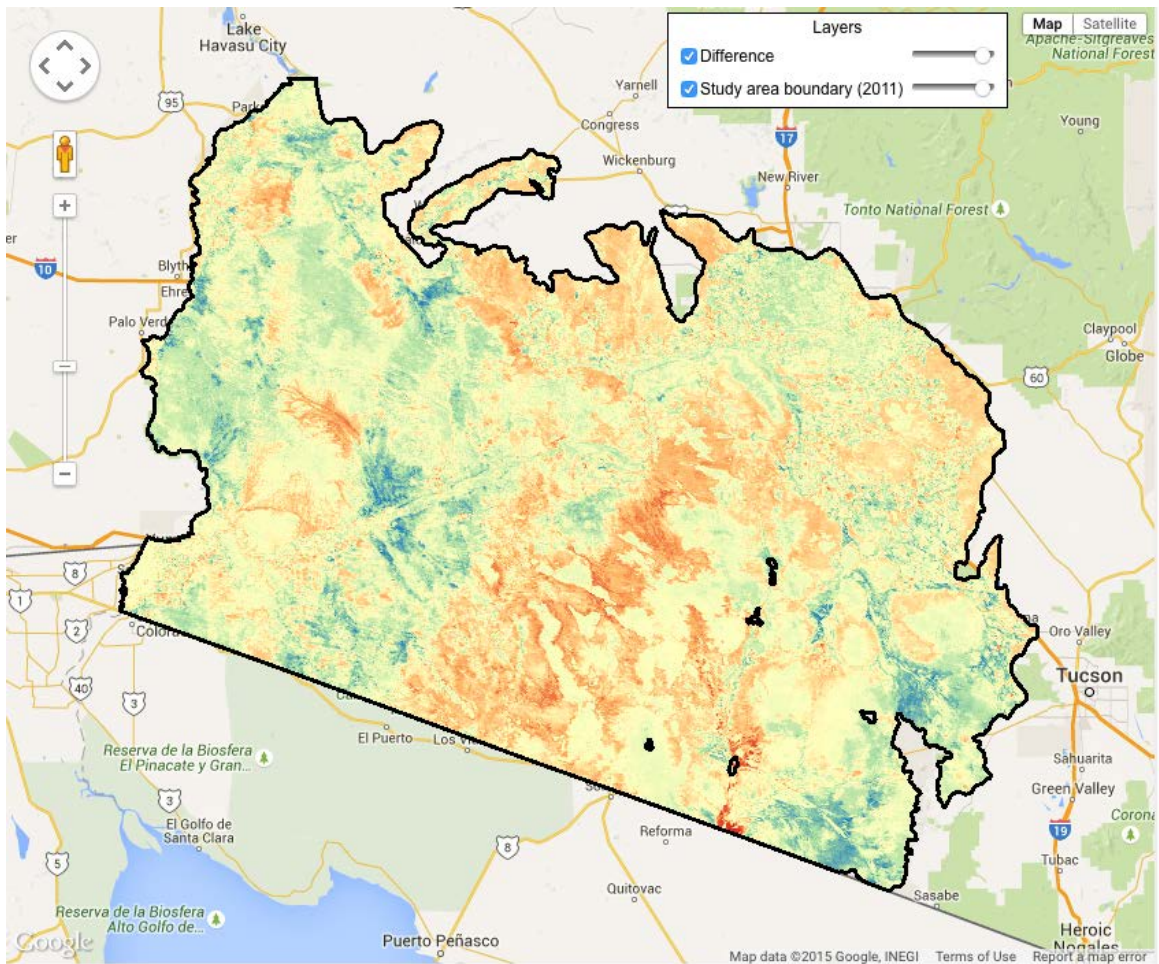


Figure 27: Difference between the predicted occurrence probabilities in 2005 and 2012 for *Schismus*. Blue regions indicate higher predicted occurrence probabilities in 2005 while red regions indicate higher predicted occurrence probabilities in 2012.

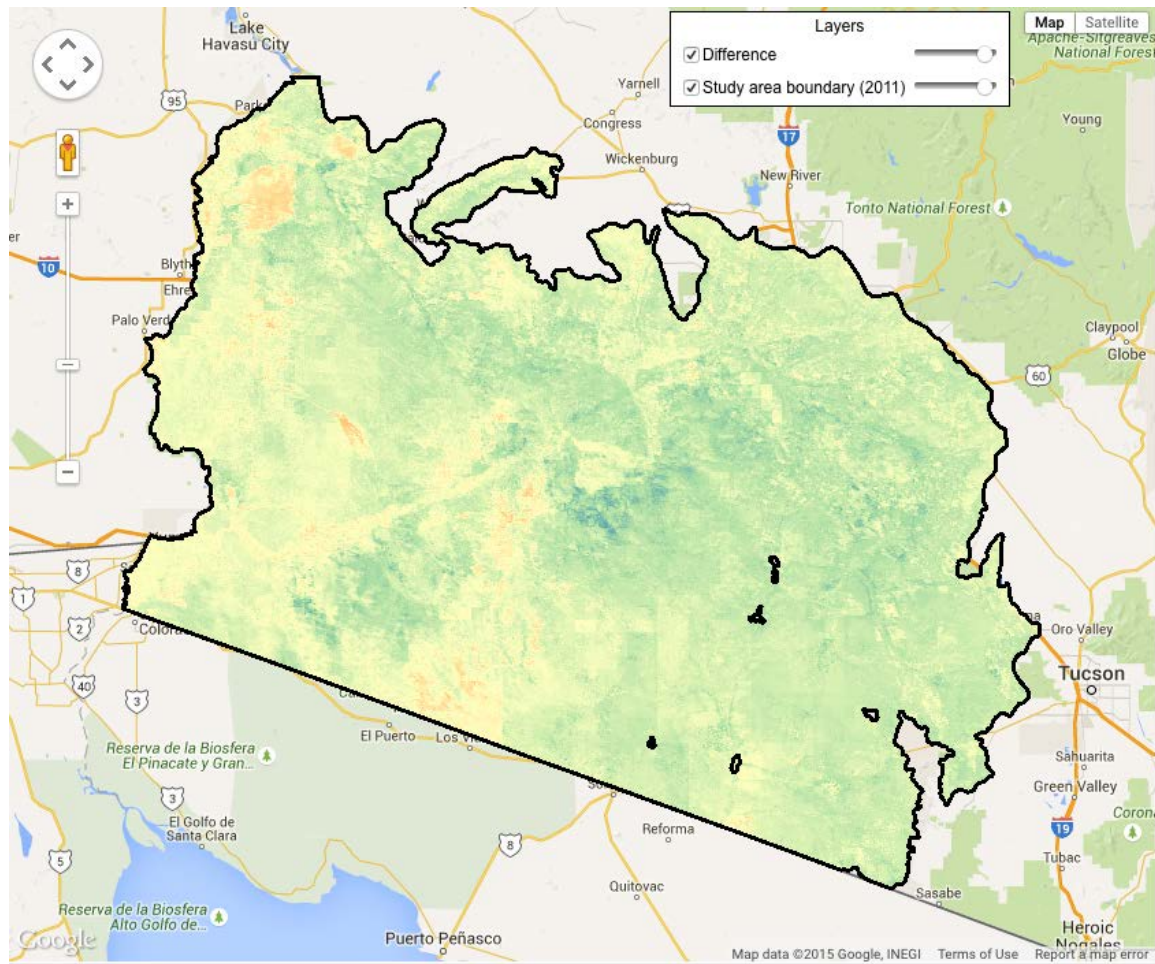


Figure 28: Difference between the predicted occurrence probabilities in 2005 and 2012 for *Brassica*. Blue regions indicate higher predicted occurrence probabilities in 2005 while red regions indicate higher predicted occurrence probabilities in 2012.

Overall, we obtained strong predictive models for the two species for which we had adequate sample sizes. While we did not have the sample sizes required to create similar (and robust) models for the remaining species (i.e., *Bromus*, *Eruca*, and *Pennisetum*), the sampling design can contribute to models in the future if sampling is extended to include additional years or regions. Extending sampling efforts to include areas outside of the 2011 study area extent would be especially critical in detecting *Bromus* and *Pennisetum*, whose ranges do not appear to be centered in the SERDP study area.

As expected based on our observations during the 2011 and 2012 sampling seasons, *Schismus* appears to be more pervasive across the landscape than *Brassica*. The distribution of *Brassica* appears to be more patchy, with well-defined areas of high-occurrence probability (e.g., the areas north of Quartzsite and near Parker, AZ). Interestingly, the spatial distribution of *Schismus* presence appears to be less sensitive to changes in climatic conditions, while the distribution of *Brassica* expands markedly as a function of changing climatic conditions.

The difference in the magnitude of predicted occurrence probabilities between 2005 and 2012 deserves special attention. Specifically, the predicted occurrence probability for *Schismus* is not uniformly higher in the wetter, more productive year as it is (with very few exceptions) for *Brassica*. For instance, wetter, more productive conditions appear to favor *Schismus* southeast of Kofa National Wildlife Refuge (KNWR) while dry, unproductive conditions may slightly favor *Schismus* across much of

the south-central portion of the study area. Overall, *Schismus* maintains a relatively stable and pervasive presence across the landscape and across years.

A spatially weighted ensemble and MODIS phenology-based approach for mapping Sonoran Desert invasive annual plants

SWE models performed better than Regional models for both *Brassica* and *Schismus*, indicating that some factors better distinguish invasive species at a local scale than at a larger scale. Model results and accuracy estimates using Cohen’s kappa coefficients for MODIS- and Landsat-scale models are given in Table 7. Cohen’s Kappa is a statistical measure of agreement between predicted and actual occurrence records on plots and subplots ranging from -1 to +1. Kappa coefficients greater than 0.80 are generally accepted as high accuracy however lower scores can be acceptable depending on objectives (Congalton and Green 1999). Overall prediction accuracy for *Schismus* was low: this species is ubiquitous in the study area but occurs in small populations, showing a high detection rate but low mean cover in 2012. Greater prediction success was obtained for *Brassica* (Table 7).

Table 7. Cohen’s kappa for regional and SWE models of *Schismus* and *Brassica* derived from 2011 field data.

| | <i>Schismus</i> | | <i>Brassica</i> | |
|-----------|-----------------|-------|-----------------|-------|
| | Regional | SWE | Regional | SWE |
| MODIS | 0.435 | 0.429 | 0.561 | 0.576 |
| TM p37r37 | 0.327 | - | 0.446 | - |
| TM p38r37 | 0.449 | - | 0.599 | - |

The differences between Regional and SWE MODIS models were greatest in the northwest, where SWE predicted greater likelihood of *Brassica*, and in the southwest, where SWE predicted less likelihood of *Brassica* (Figure 12). This discrepancy emerges from temporal and spatial variability, reflecting the occurrence of dense stands of *Brassica*, which we observed between 2009-2012, as well as increased cover of *Brassica* in the northwest portion of the study area. Landsat models for *Schismus* followed MODIS models in poor overall performance, but Landsat models for *Brassica* exhibited a different pattern. The model derived from the p38/r37 tile was the best model overall. From the density of *Brassica* observations in both 2011 and 2012, the densest patches of *Brassica* were in the western half of the study area, which is covered by p38/r37; higher densities are easier to model. We surmise that two consecutive dry years (2011 and 2012) resulted in lower overall *Brassica* and *Schismus* cover in 2012 than for 2011, which was likely still responding to the wet year of 2010, which boosted the viable seedbank for both species.

Out of the 236 plots we measured, presence of *Brassica* was observed on 113 plots. Mean κ for the RSM and the full dataset was $\kappa = 0.61$, vs. a mean κ for the training data ($\kappa = 0.56$). The highest mean κ values were associated with the IDW models, but the only models with κ significantly greater than κ of the regional models ($p < 0.0001$) were IDW2, IDW2K, IDW4, and IDW4K. LRM, both WLMs, and all other SWEs were no better than the regional model ($p > 0.09$). The RSM performed significantly better than the LRM WLMs and six of the 10 SWEs (i.e. LIN, LINK, TPS4, TPS4K, TPS5, and TPS5K). IDW4 and IDW4K performed best overall and were equivalent. For simplicity, IDW4 ($\kappa = 0.58$) was selected as the SWE model approach for predictive modeling of *Brassica* occurrence for the entire study area.

The final regional and SWE models using IDW4 were produced using the full set of 236 plots. The SWE predicted areas of greater *Brassica* in the NW and NE portion of the study area and the regional model predicted higher *Brassica* in the SW portion of the study area. Areas known to maintain more extensive populations of *Brassica*, such as the NW corner of the study areas showed as much as 20%

higher occurrence probability in the SWE model. Indeed, Pearson correlation coefficients between *Brassica* canopy cover and occurrence probability were higher for the SWE model in both 2011 (SWE $r = 0.27$, RSM $r = 0.25$) and 2012 (SWE $r = 0.27$, RSM $r = 0.13$). Extremely low *Brassica* cover was measured on field plots in both years because of below average winter and spring precipitation. However, SWE models appeared to show a moderately positive relationship between *Brassica* cover and predicted occurrence for areas with higher canopy cover in 2011 and 2012. Regional model predictions showed little or no relationship with differences in *Brassica* cover on plots.

Elevation and mean NDVI of spring 2004 were the two most important variables for both regional and SWE models, while the relative importance of spring vs. fall predictor variables differed by model type. Fall NDVI phenology metrics were the most prevalent predictors for *Brassica* presence (6 of 12 variables), with three models associated with mean fall NDVI, one with maximum fall NDVI, one related to amplitude, and another related to the mean maximum fall NDVI. Spring NDVI variables were also important (4 of 12 variables) with mean and max spring NDVI from 2001 and 2004 among the top eight. The most important phenology variables were mean and max spring 2004 NDVI, respectively, for the RSM. Variables associated with the timing of maximum spring or fall NDVI were not included in the top 12. The mean variable importance across all SWE LRM also highlighted elevation and mean and maximum NDVI from spring 2004 as the most important variables. Fall variables showed less importance overall, with only four in the top 12 and none in the top six. Five spring NDVI variables were included in the top 12: mean/maximum spring NDVI in 2001 and 2004 and timing of maximum spring 2005 NDVI. Overall, SWE models showed a tendency to select variables for years with relatively moist winter/spring conditions. Another notable difference in variable importance was the inclusion of the Landsat TM PC3 from August of 2009, which distinguished vegetation between eastern and western portions of the study area.

We identified the maximum variable importance for each variable across all models. This enabled us to identify variables with strong local predictive power. The balance of important winter/spring vs. summer/fall phenology variables was higher than both the RSM model and the variable importance means across all SWE LRM. Six of the top 12 variables were based on spring NDVI whereas only three were based on fall NDVI. Additionally, the top 12 variables included three related to the timing of maximum NDVI, all of which are from a different time period (i.e. spring 2001, spring 2005, and fall 2001). The spatial variation of predictor variables with high importance was indicative of how non-stationary factors can be essential to predicting the presence of *Brassica* using phenology metrics. The SWE model outputs indicate that the timing of maximum spring and fall NDVI were important in the western portion of the study area, where extensive areas were by *Brassica* during years with above average rainfall. Conversely, no time-related predictors were important to detecting the presence of *Brassica* in the eastern portion of the study area, where invasions are less extensive.

A cross-comparison of variable importance for regional and SWE models showed that LRM were more likely to be influenced by timing variables and maximum seasonal NDVI. The timing of maximum fall and spring NDVI were of greater importance to SWE models than to the regional model which was more highly influenced by fall phenology and mean and maximum NDVI. The balance of spring and fall phenology timing variables fell above the 1:1 line, indicative of timing variables being more important in local than regional models.

Task 12: Non-native mapping (Hyperion-hyperspectral) (phase 1)

Low image quality and cross-track striping contributed to poor model results when Hyperion-hyperspectral data were used. This was the case for any selected reference spectra; MTMF-based models were contaminated by the excessive striping that is characteristic of Hyperion bands. The low maximum cover of each target species in field data (< 25%) made selection of reference spectra from these data infeasible. Pearson's correlation between individual SMACC-derived EM and *Brassica* cover

ranged from -0.500 to 0.398. The maximum correlation was with EM 26 (Figure 29). EM 26 corresponds with sandy flat areas north of Quartzsite, AZ, consistent with field observations of high abundance of *Brassica* and *Schismus*. This indicates high potential for *Brassica* and *Schismus* to be mapped effectively with hyperspectral imagery, but the sensor quality of Hyperion dramatically degraded our results. Correlation between EMs and *Schismus* ranged from -0.080 to 0.070. Maximum correlation occurred with EM 1.

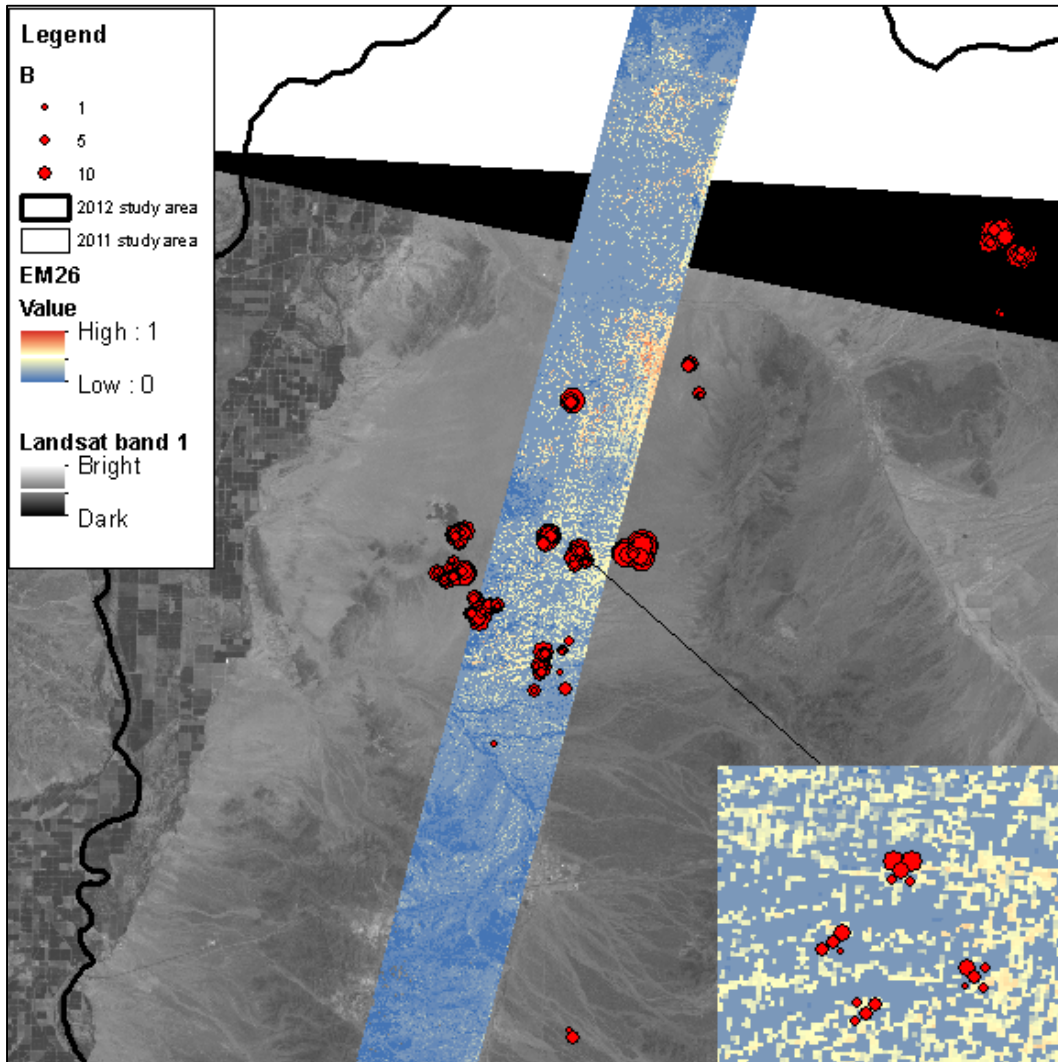


Figure 29: Map of SMACC EM 26, which had the highest correlation with *Brassica* cover on intersection subplots. Percent cover of subplots (red circles) are indicated by larger symbol radii.

In addition to poor image quality, uncertainty in the precise spatial location of image acquisition led to unsatisfactory overlap between the Hyperion image and field data. We were unable to employ methods that would allow us to map target species utilizing the phenologic information potentially contained in multitemporal hyperspectral images, due to a lack of multiple scenes. Given these problems, we did not choose to perform the second phase of non-native target species mapping using Hyperion hyperspectral imagery. Drought conditions alone would have limited our ability to combine Hyperion data with field data, but unreliable timing and geographic location of image acquisition made it still less feasible.

In spite of the problems we encountered with Hyperion imagery, multitemporal HypsIRI appears to be a valuable tool for mapping invasive species of the Sonoran Desert. A recent study showed that *Pennisetum* is easily identified in simulated HypsIRI imagery (AVIRIS airborne hyperspectral imagery) when it is the most abundant constituent of a pixel (Olsson & Morissette 2014). This is reasonable, given the dramatic structural differences between invaded and uninvaded desert pixels; namely, the replacement of bare ground by senesced (and flammable) vegetation. Hyperspectral imagery such as HypsIRI (and Hyperion) can discriminate between these two structural differences due to a cellulose-lignin absorption feature in the shortwave infrared that is characteristic of senesced herbaceous vegetation. *Brassica* and *Schismus* infestations are characterized by high densities of senesced herbaceous vegetation in the arid foresummer (i.e., April through June). This is also the key component that leads to Mojave Desert wildfires where *Bromus* is present (Brooks et al. 2004). Although Landsat TM and other multispectral sensors do have bands in the shortwave-infrared, they do not have the spectral resolution of HypsIRI and other hyperspectral sensors necessary to distinguish the narrow absorption feature associated with cellulose and lignin (Daughtry et al. 2006).

Go/No-Go decision point #2:

In light of the limitations posed by the Hyperion data acquisition process, and considering the uncertain status of the Landsat Data Continuity Mission, we decided not to pursue the second phase of Hyperion-based modeling. Instead, we acquired higher spatial and spectral resolution imagery from the Sistema Para la Observacion de la Tierra (SPOT) and WorldView2 (WV2) satellites across much of the study area during the 2012 field season (Figure 30). This imagery was collected at no cost to our SERDP project through the President’s US Commercial Remote Sensing Space Policy, accessed through the Commercial Image Data Requirement by Co-PI Sesnie with the USFWS. Each of the two satellite platforms provides an image data source that is readily available to federal agencies under current vendor agreements. Image dates from 2012 range from January 16th to April 16th.

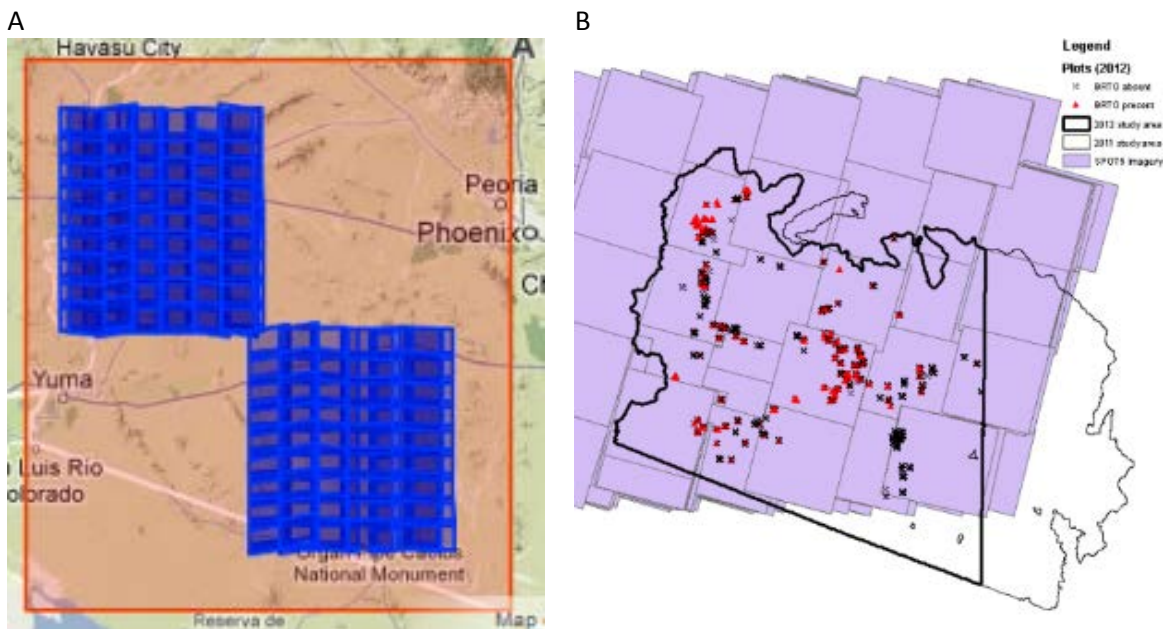


Figure 30: A) Footprint of Wordview 2 images (blue) acquired during the 2012 field season. B) Footprints of SPOT Imagery during the 2012 field season.

WV2 imagery was collected until February 14th over approximately half of the study area in two 1° x 1° consolidated areas. Image data collection was focused on areas sampled during plot measurements taken in 2012. SPOT 10-m data cover green, red, NIR, and shortwave infrared wavelengths that are appropriate for vegetation applications. The WV2 platform is among a new generation of high-resolution commercial satellites producing 2-m multispectral and 0.5-m panchromatic imagery. WV2 multispectral channels cover the visible and NIR spectral range (400 – 1050 nm) with yellow (585 – 625 nm), red edge (705 – 745 nm) and NIR 2 (860 – 1040 nm) bands, for a total of eight bands (Figure 31). WV2 is strategically designed and centered on more narrow spectral channels for vegetation analysis and, prior to this project, has been relatively untested for mapping target invasive species in the study area and elsewhere (Figure 32).

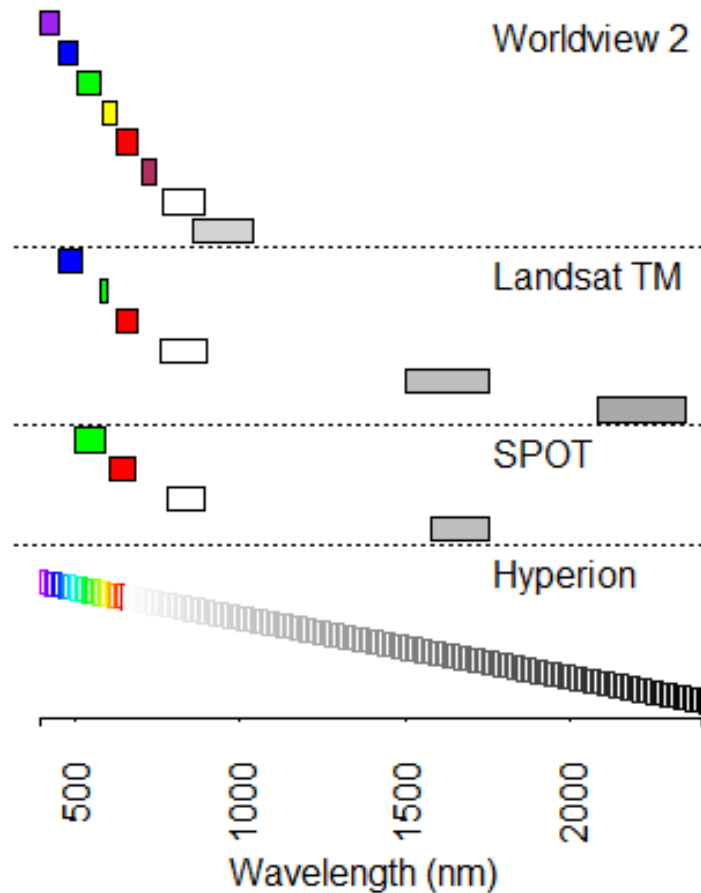


Figure 31: Spectral bands of WorldView-2 , Landsat TM, SPOT5, and Hyperion satellite sensors. The yellow, red edge, and NIR2 bands are unique to WorldView-2 among present-day multispectral sensors.

Given the spatial and spectral characteristics of both SPOT and WV2, our objectives for an alternative to task 11 were to 1) develop and test the potential for mapping target invasive plant distributions using single-date image classification techniques, 2) determine the feasibility of fine-scale mapping of small populations of target species, and 3) explore image fusion and other modeling techniques to potentially improve methods for characterizing fine fuel biomass in the study area. Our collaborators in particular will benefit from research exploring commercial alternatives in light of the current unavailability of Landsat TM and uncertainties surrounding the future of Landsat in general.

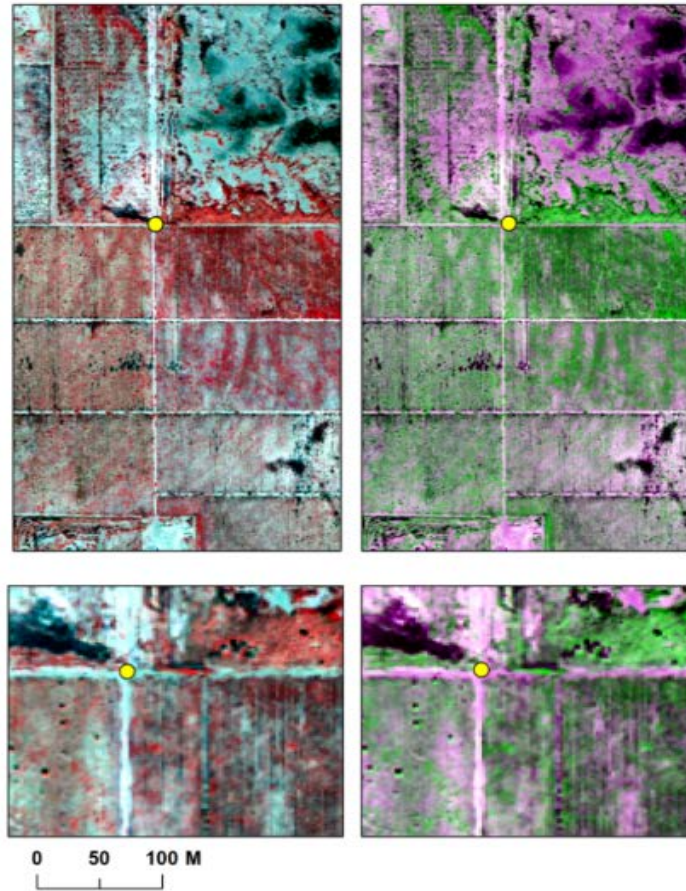


Figure 32: WorldView-2 imagery of abandoned farm fields dominated by *Eruca* located near Sentinel, Arizona. Images are WorldView-2 band combinations 5, 7, and 3 (left) and 4, 8, and 6 (right).

Comparison of simulated HypsIRI with two multispectral sensors for invasive species mapping¹⁴

The area under the ROC curve associated with the AVIRIS¹⁵ MTMF model was 0.932, when contrasted against the reference polygons. This output indicates a very strong estimate of *Pennisetum* abundance. Visual comparisons of aerial photography, digitized polygons, and MTMF and our experience with field work in the area suggested that the AVIRIS model is actually better than the manually interpreted dataset. The threshold we had previously selected was an 82.0% likelihood based on the logistic model, corresponding to a threshold of 0.4 in the MTMF output.

Modeled *Pennisetum* abundance was 1.30% of the study area, inhabiting primarily palo-verde-dominated scrub (0.74% of the study area and 3.94% of the total Sonoran Paloverde-Mixed Cacti Desert

¹⁴ The below results have been peer-reviewed and published in Olsson, A. D., and J. T. Morisette. 2014. Comparison of simulated HypsIRI with two multispectral sensors for invasive species mapping. *Photogrammetric Engineering and Remote Sensing* 80:217-227.

¹⁵ AVIRIS was the actual hyperspectral sensor used for this study, to simulate future data acquired by HypsIRI.

Scrub cover), but also higher elevation scrub (0.24% of the study area and 1.71% of Chihuahuan Mixed Salt Desert Scrub) and higher elevation grassland (0.17% of the study area and 1.95% of the Apacherian-Chihuahuan Piedmont Semi-Desert Grassland and Steppe).

Random Forest models for all sensors and spatial resolutions yielded R^2 values ranging from 0.268 (Landsat TM, 60m) to 0.843 (HyspIRI, 15m). Incremental variable selection identified two narrow bands in the SWIR2 region as the most important variable for all three ASTER and HyspIRI models: 2.205 and 2.207 μm for ASTER and HyspIRI respectively. Aside from the 2.205-2.207- μm emphasis, ASTER and HyspIRI models were strongly linked to SWIR bands. The 60m HyspIRI model, for example, did not include any bands below 1.165 μm in its best model, which included 5 bands in total. The 15m ASTER model was complemented by strong variable importance values in its 2.33 μm and 2.26 μm bands. In fact, the 2.26 μm band was the second or third most important variable for ASTER for all three resolutions. Landsat TM models identified the red band, centered at 0.66 μm in the 15 and 30m models and the SWIR1 band, centered at 0.83 μm in the 60m model.

Model fitness values (R^2) for sensors in their native resolutions were 0.384 (30m Landsat TM), 0.785 (15m ASTER), and 0.637 (60m HyspIRI). HyspIRI was the best model overall at each resolution. For any given effective patch size, the native resolution ASTER model performed better than the HyspIRI model. TM outperformed HyspIRI for patches between 612 m^2 and its GIFOV (900 m^2). HyspIRI outperformed Landsat for all patch sizes of 1440 m^2 or larger. Due to aggregation of smaller patches into larger pixels in the case of HyspIRI and, to a lesser extent, Landsat TM, there was minimal overlap in most patch sizes modeled by ASTER and HyspIRI (144 to 225 m^2), although the differences were striking even in that small range.

The number of bands selected for the final models were relatively low (i.e., seven or below for all but one model), although the best TM models always had five, indicating that only one variable was excluded from the final model. In the case of TM, the dropped variable was always either band 5 or 7, both of which are SWIR bands. In all cases, the remaining SWIR band was either the least or second least important of the remaining five. Considering the high importance of narrow SWIR bands in the well-performing ASTER and HyspIRI models, we surmise that the two TM SWIR bands are simply too broad (wavelength-wise) to bring narrow-band SWIR features associated with *Pennisetum* invasion into focus. The best model overall, both in terms of Cohen's Kappa and in terms of model R^2 , was the HyspIRI 15m model, which utilized just 6 bands. Again, the three most important bands had center wavelengths of 2.12 μm or longer.

OBJECTIVE 2: Model invasion risk from non-native plants under current and projected climate conditions.

Task 7: Construct BEMs for current climate

Brassica and *Bromus* occupy distinct climatic zones, with *Brassica* found in lower elevation, drier sites and *Bromus* in higher elevation sites with slightly more moisture. *Brassica* is currently more likely to achieve high abundance in southern Arizona (Figure 33), while high abundance of *Bromus* is more likely in northern Arizona and Nevada. In the future, reduced moisture in the southwest is likely to reduce the abundance of both invasive plants in southern Arizona (Figure 33), perhaps also reducing annual fire risk associated with these species. Climatic suitability combined with landscape-scale predictors, such as disturbance and soils, can improve hierarchical risk assessments of invasion risk.

There was strong overlap between the two BEMs in projections of current climatic suitability in southern Arizona and California (Figure 33A,B). Model uncertainty (regions where only one of the two models predicted climatic suitability) was highest for *Bromus* abundance in Nevada and northern Arizona and for *Brassica* presence in northern Mexico. Whereas results presented here are based on RCP 4.5 (Figure 33), projections were largely similar when RCP 8.5 was used (Curtis & Bradley 2015).

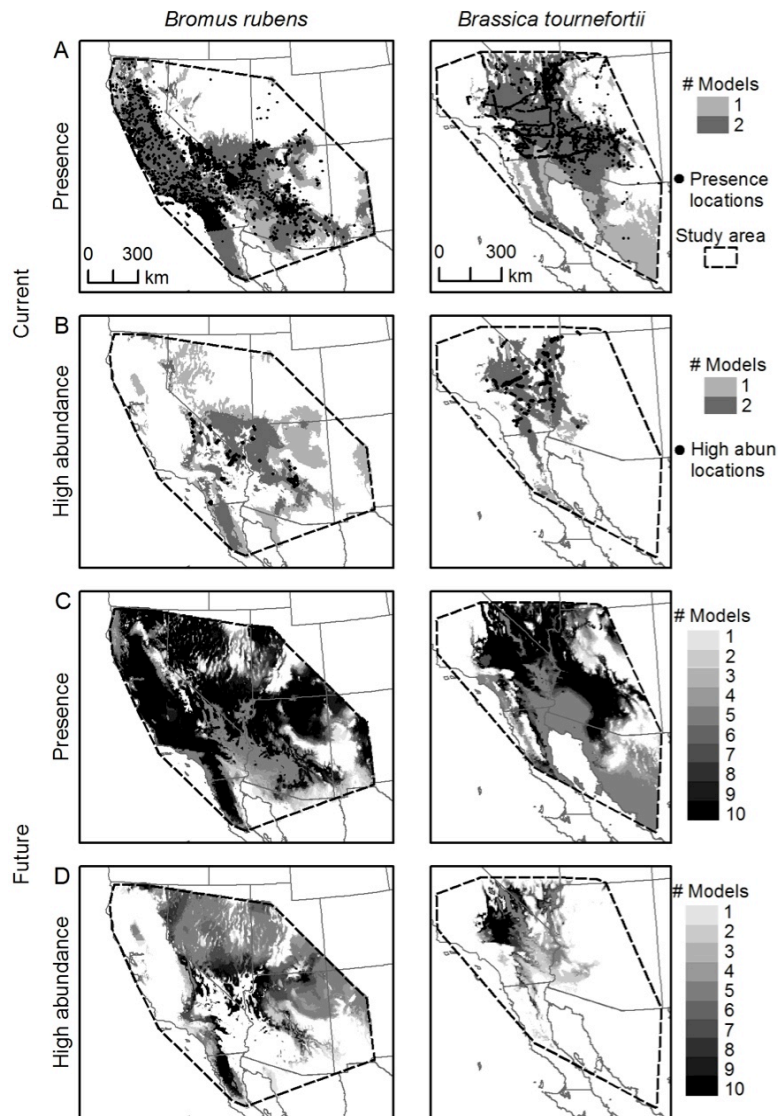


Figure 33: Species distribution models for *Bromus* and *Brassica* within convex hulls of all available distribution data (dashed lines). Point locations indicate where presence (A) and high abundance (B) data were collected. The predicted current climatic suitability for presence (A) and high abundance (B) include the MaxEnt and Bioclim projections and encompass 95% of the original distribution data. Future ensemble models are based on RCP4.5. The future ensemble models for presence (C) and high abundance (D) were created by combining the projections of 10 models: two bioclimate envelope models and five Atmosphere-Ocean General Circulation models. Values indicate how many of the 10 models projected climatic suitability.

Current climatic suitability for *Bromus* and *Brassica* presence extends throughout the study region, consistent with known location points (Figure 33). Suitable climate for *Bromus* high abundance is currently limited to relatively small areas of southern California, Nevada, and Utah and a larger region of

central and northwestern Arizona (Figure 33). Suitable climate for *Brassica* high abundance occurs primarily in southern California (Figure 33). Based on the AUC statistic for MaxEnt models, the projected models performed better than expected by random chance. The smaller suitable range for high abundance (relative to presence) for both species supports previous findings that models of potential establishment overestimate potential impact (Bradley 2013). Based on the MaxEnt models, different climate conditions influences species presence vs. high abundance. For both *Bromus* and *Brassica*, temperature was by far the strongest predictor of presence (minimum temperature for *Bromus* and maximum temperature for *Brassica*). For *Bromus* this result suggests that freezing tolerance may limit the species' survival over winter, which is consistent with experimental studies (Bykova & Sage 2012). For *Brassica*, this result suggests that the species effectively establishes under hot conditions, which is consistent with its measured heat tolerance (Suazo et al. 2012).

In contrast, minimum temperature and spring precipitation were both strong predictors of abundance for *Bromus* and summer precipitation was the strongest predictor of abundance for *Brassica*. Both invasive species are likely to better compete against native species (e.g., Barrows et al. 2009) and have stronger population growth (Beatley 1974, Salo 2004) under wetter conditions. Thus, while temperatures limit the overall range, precipitation appears more likely to influence invader abundance.

Although our presence and abundance datasets for the two species are compiled from all available sources, several portions of their ranges are undersampled. In particular, our data do not extend into Mexico even though the species are not limited by political borders. These spatial biases in the distribution datasets could lead the BEMs to underestimate climatic suitability under current and future climate. Additionally, Worldclim climate data are based on interpolations of weather stations. Although the U.S. is well instrumented, the Southwest is more prone to larger distance gaps between weather stations, which increases uncertainty associated with climate interpolations. As a result, the precision of any given pixel should not be over-interpreted, as climate conditions underlying the BEMs are modeled interpolations rather than precise field measurements.

Task 8: BEM uncertainty analysis under future climate conditions

Projections of future climatic suitability for *Bromus* and *Brassica* presence and abundance under the RCP4.5 emissions pathway are shown in Figure 33C-D, respectively. The model projections based on RCP4.5 vs. RCP8.5 were similar both in overall magnitude of calculated range shift as well as spatial pattern. For simplicity, we present the results from RCP4.5 here and only note the RCP8.5 results in two cases where there is a substantive difference. Most models agreed that large areas will be suitable for *Bromus* presence in the future (Figure 33C). Future suitability for *Bromus* abundance is projected to be greatest in northwest Arizona, southwest Nevada, and Baja California, Mexico based on ensemble model overlap (Figure 33D). Based on the high threshold (six or more models projecting suitability), climatic suitability for *Bromus* presence could expand by 12% along the northern edge of the currently suitable range. However, contraction along the southern edge is also predicted, with areas primarily in Arizona becoming unsuitable. This southern contraction is more prominent throughout southern Arizona and California using the RCP8.5 projections. Using a more inclusive low threshold (one or more models projecting suitability), climatic suitability for *Bromus* presence could expand northward up to 65%. In the model projections, northward expansion is primarily driven by warming temperatures, which is consistent with experimentally derived limitations. Bykova & Sage (2012) show that *Bromus* is sensitive to freezing temperatures and is not as cold tolerant as the related species *Bromus tectorum*.

High abundance of *Bromus* based on the high threshold could decrease by 42%. However, using the more inclusive low threshold, climatic suitability for high abundance could expand northwards by as much as 64%. The large differences in potential future range illustrate uncertainty associated with both differences between BEMs and climate projections. Highest confidence in future range occurs in areas of

model overlap (darker parts of Figure 33). Areas of expansion in southern Nevada, northwestern Arizona, and Baja California, Mexico show the highest model agreement (Figure 33) and are the most likely to see a shift towards high abundance of *Bromus* with climate change. Interestingly, *Bromus* is already present throughout southern Nevada, making it likely that populations will not be limited by propagules and could expand rapidly once climate conditions become suitable.

The future presence model of *Brassica* shows high model agreement in southern California and Nevada, and throughout much of Arizona (Figure 33C). Future suitability for *Brassica* is projected by most models to occur in southern California (Figure 33D). Based on the high threshold (six or more models projecting suitability), climate conditions suitable for *Brassica* presence are projected to decrease by 34% overall, with areas in southern California, eastern Nevada, and Mexico becoming unsuitable. Using the more inclusive low threshold (one or more models projecting suitability), climatic suitability for *Brassica* could expand up to 29%.

High abundance of *Brassica* based on the high threshold could decrease by 56%, while using the more inclusive low threshold, climatic suitability for high abundance expands by 28% (Figure 33D). Expansion of high abundance with the low threshold result is substantively larger with RCP8.5 models, with ranges 71% larger primarily in western Arizona and southern Nevada. The difference between these two projections can primarily be attributed to how the BEMs interpret high temperatures for *Brassica*. Bioclim identifies a high temperature threshold, above which conditions become unsuitable, while MaxEnt considers all high temperatures suitable, including those with current no-analog conditions. While *Brassica* has a broad tolerance for warm temperatures (Suazo et al. 2012), it is not clear whether it is approaching its high temperature limit within its current range. Further experimental analyses are required to enable better interpretation of the model results.

OBJECTIVE 3: Model the impacts of recent and on-going land use disturbances on non-native plant invasion.

Task 9: Land use models of disturbance and risk

The Landsat map of *Brassica* presence/absence had an overall accuracy of 76%, determined via 566 distributed field survey locations (Table 8). This accuracy is similar to those of previously-developed landscape-scale maps of plant invasions (Bradley & Mustard 2005, Peterson 2005) and is sufficient for evaluating the relevance of geographic features to likelihood of invasive species presence.

Table 8: Contingency table for Landsat-based map of *Brassica*.

| | Map predicts present | Map predicts absent | Producer's accuracy |
|-----------------|----------------------|---------------------|---------------------|
| Field present | 118 | 85 | 58% |
| Field absent | 51 | 312 | 86% |
| User's accuracy | 69% | 79% | 76% |

Plant invasions are often strongly linked to disturbance features like roads (Gelbard & Belnap 2003, Bradley & Mustard 2006), which represent dispersal corridors for seeds transported by vehicles as well as locations of increased resource availability due to water runoff and active scraping/loss of native species along road verges. However, we found that *Brassica* invasion was not correlated with proximity to roads. Instead, *Brassica* presence was correlated to location of railroads, suggesting that these corridors facilitate invasive species establishment or spread (Figure 34). The species' presence was also correlated with physical geographic features, including shallow slopes, lower elevations, and sandy soils

(Figure 34). We used these factors to predict landscape-scale invasion risk from *Brassica* within climatically suitable areas.

Note that more recent results on disturbance and risk are detailed in section on *Phenology-based mapping of habitat suitability using Google Earth Engine* (Task 6).

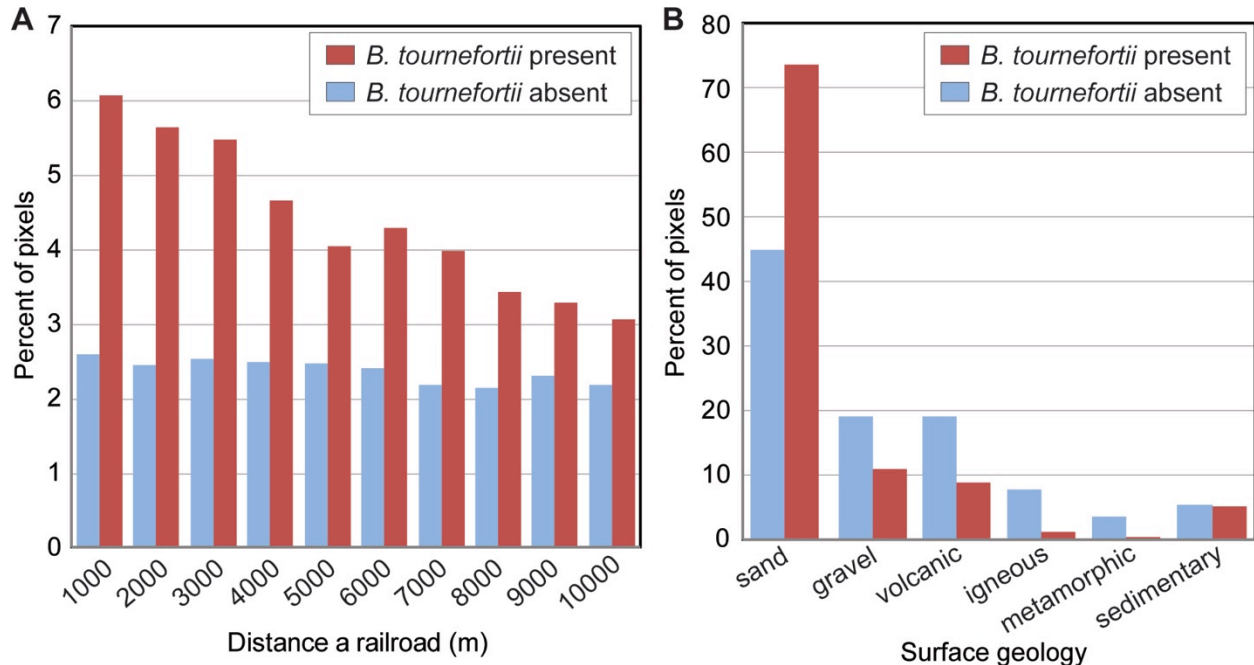


Figure 34: The relative percentage of pixels with *Brassica* present and absent relates to disturbance and geography. A) Proximity to railroads is a strong predictor of *Brassica* presence, and B) *Brassica* is highly likely to be found on sandy geologic surfaces.

OBJECTIVE 4: Model the effects of increased fuel loads caused by non-native plant invasion on regional fire risk.¹⁶

Task 10: Fire modeling outputs

Modeling and mapping large fire probability

The compiled fire occurrence dataset included 316 small and 79 large fires that burned within the study area between 1989 and 2010. Over these 22 years, large fires burned a total of 57,000 ha. The extremely high fire year of 2005 saw the greatest number of large fires ($n = 36$) and highest total area burned (51,700 ha). The median size of a large fire in 2005 was 95 ha, whereas the 22-year median size of a large fire was only 60 ha.

The AIC of our full model of large fire probability was 71 units less than (i.e. better than) a null model containing only the random effects. The Hosmer–Lemeshow test did not indicate a significant lack of fit ($P = 0.25$). The ROC value for this model was 0.85, suggesting excellent discrimination. Among explanatory variables, areas with high maximum annual NDVI ($w + j = 1.00$), low elevation (1.00) and low road density (1.00) were the most strongly associated with higher large fire probability. Low

¹⁶ For Objective 4, results have been peer-reviewed and published in Gray, M. E., B. G. Dickson, and L. J. Zachmann. 2014. Modelling and mapping dynamic variability in large fire probability in the lower Sonoran Desert of south-western Arizona. *International Journal of Wildland Fire* 23:1108-1118.

– AND –

Gray, M. E., and B. G. Dickson. 2015. A new model of landscape-scale fire connectivity applied to resource and fire management in the Sonoran Desert, USA. *Ecological Applications* 25:1099-1113.

vegetation heterogeneity was a strong predictor (0.90), as were south-facing slopes (0.80). Maximum NDVI as a lagged variable was less influential than the year-of-fire maximum NDVI, but was still a strong predictor (0.70). Topographic roughness was also a strong predictor of large fire probability (0.58), but less than the other variables we considered.

Random effects ranged from <10 to >300% of normal winter precipitation. The best linear unbiased predictors for the random effects (Faraway 2005) revealed that precipitation anomalies in the two antecedent winters had different predicted effects on large fire probability, but without discernible pattern.

Maps of the moderate (1996) and high probability (2005; Figure 35) scenarios showed very different patterns of large fire probability across the study area. In 1996 there were only a few isolated patches of very high large fire probability (e.g., >60%), whereas in 2005 there were much more widespread and spatially contiguous areas of very high probability. Over the entire study area, the mean probability of large fire was 0.13 (s.d. = 0.08) and 0.37 (0.21) in 1996 and 2005.

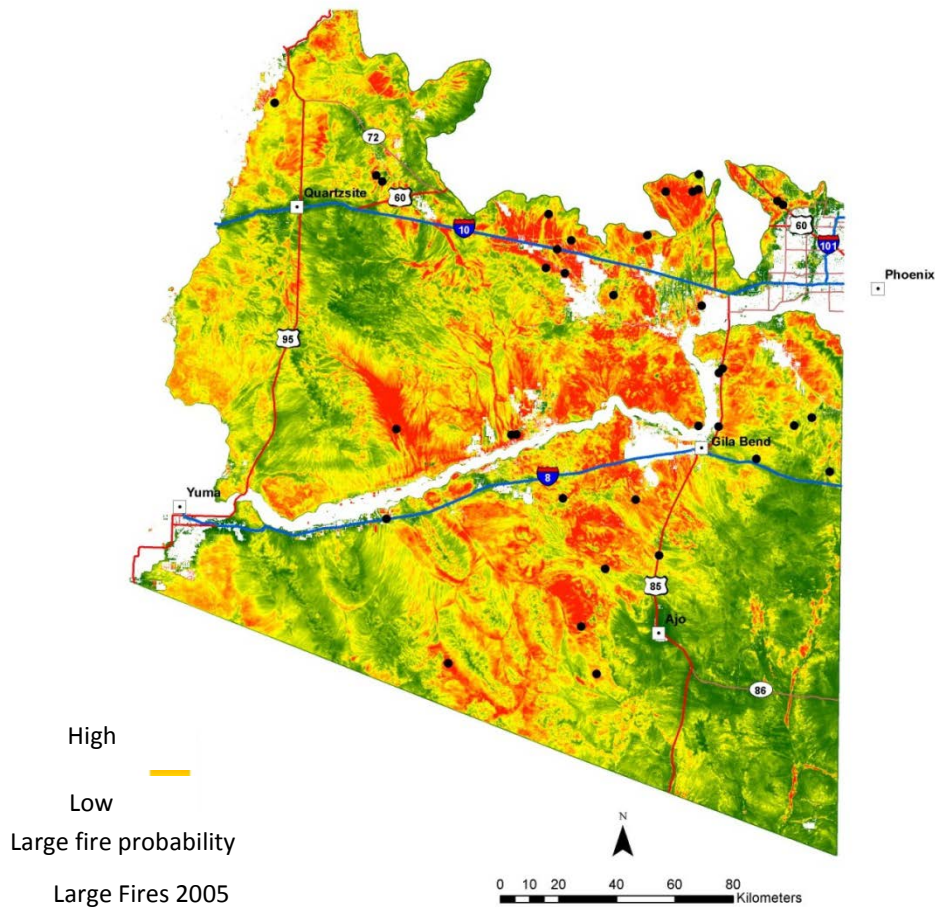


Figure 35: Map-based prediction of large fire probability in the lower Sonoran Desert of southwestern Arizona, based on 2005 conditions (i.e., high large fire probability). The ignition points of large (≥ 20 ha) fires that burned in 2005 are represented by black dots.

Models and maps of fire behavior and hazard

As expected, we observed minimal heterogeneity in fire behavior and hazard across our study extent using 'off-the-shelf' Landfire inputs under the 96th percentile weather and fuel conditions described above. Surface fire was the dominant potential fire behavior, with a few heterogeneous patches of passive and active canopy fire in the southeastern region of the study area (Figure 36). Our models predicted that surface fire was likely across most fuel models and dominant vegetation types, including those occurring on DOD installations and adjacent lands. We intentionally overestimated average wind speeds, first at 20 kph and then at 40 kph, to force potential fire behavior and hazard. Figure 36A and 36B present 20-kph wind scenarios with gridded winds, and Figure 36C shows a 40-kph wind scenario without gridded winds. With 20-kph winds, the majority of canopy fire patches were characterized by passive rather than active canopy fire, whereas active canopy fire characterized most fire patches modeled under 40-kph wind scenarios. Potential canopy fire occurred between 1000-1300 m in moderate load grass-shrub fuel types and between 700-1100 m in high load shrub types. Both current fuel models and empirical evidence suggest that canopy fire is an extremely rare fire behavior in our study area. Across the study area, the highest intensity fires burned in high load shrub fuel types and moderate load grass-shrub fuel types. In low and moderate load grass, and low load shrub and grass-shrub fuel types, fire intensity was lower. Without gridded winds, simulations predicted that topography will exert minimal influence on the rates of spread within fuel types. Fire spread was fastest in high load shrub (350+ chains/hour), very high load shrub (250-300 chains/hour), and moderate load grass (150-200 chains/hour) fuel types.

After the 2012 field season, it was possible to recalibrate fuel models using both seasons of field data and new models of vegetation composition, structure, and biomass. These efforts also integrated the utility of ArcFuels (www.fs.fed.us/wwetac/arcfuels) for developing alternative fire risk and management scenarios in a spatially explicit decision-support framework, and were further extended by an ongoing graduate student thesis project examining fuel and fire connectivity across the study area.

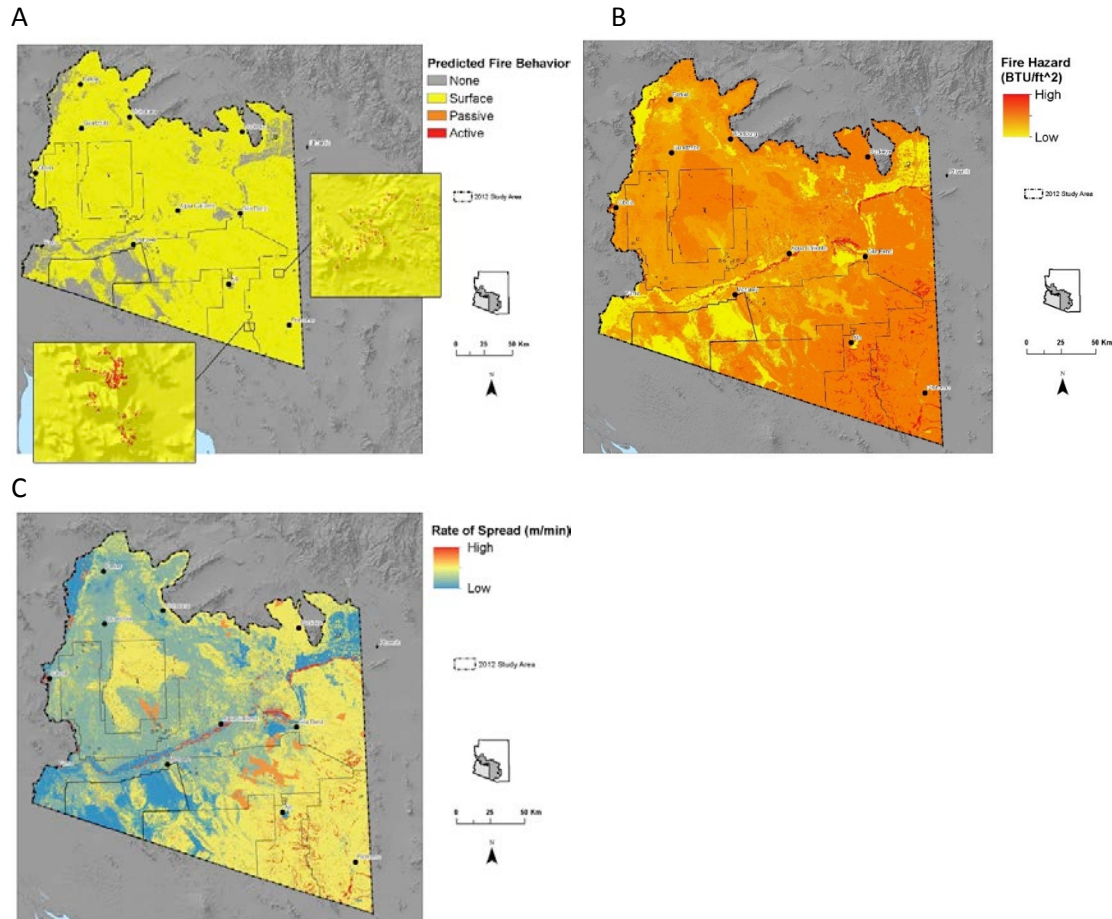


Figure 36: FlamMap simulation outputs for predicted potential (A) fire behavior, (B) hazard, and (C) rate of spread with constant winds blowing from the southwest at 40 kph and under current landscape and fuels conditions.

Modeling and mapping fire connectivity

Our historical fire evaluation dataset consisted of 4,003 burned pixels comprising approximately two percent of the study area. Our mapped predictions of fire likelihood (connectivity, Figure 37) offered exceptional empirical support ($r_s = 1.00$) when evaluated with the MODIS burned area data. The model was able to differentiate high fire likelihood (HFL) from chance expectation at the 80th percentile of predictions, offering strong support to our decision to use this percentile class to define HFL. In summary statistics, across the study area, 19% of predictions were classified as HFL. Of this HFL area, 7% was predicted to experience very high negative fire effects, 85% to experience high effects, and 8% to experience moderate effects. Patterns of wind and terrain influences on fire likelihood substantially overlapped prominent topographic features in our study area, namely the numerous mountain ranges that were oriented in a southeast-northwest direction. When winds out of the southwest were simulated, areas most conducive to burning were consistently on the immediate windward side of mountain ridgelines, contrasting with the least conducive areas, located on the leeward side. Models predicted intermediate fire likelihood for the valleys between these mountain ranges. Simulations based on winds out of the south showed similar patterns but with reduced fire likelihood for areas on the windward side of ridgelines. In general, HFL showed greater dispersal over larger areas where wind direction would most facilitate the spread of fire. This was in contrast to concentrated HFL in narrow corridors. HFL was absent in areas where dominant winds move downslope. Study region-wide, areas of

HFL had a mean elevation of 295 m (s.d. = 122), a mean slope of 6 degrees (13), and a mean topographic roughness (i.e., the standard deviation of slope) of 1.35 (2.90). In contrast, areas not characterized as HFL had a mean elevation of 396 m (186), a mean slope of 8 degrees (16), and a mean topographic roughness of 2.12 (3.89).

Fire effects in wilderness

Our HFL estimate area included 1,740 km² (14.5%) of the 16 wilderness areas within the study area, with 19%, 74%, and 7% of wilderness-area land classified as HFL predicted to experience very high, high and moderate negative fire effects, respectively. By total area characterized as HFL, the Cabeza Prieta (787 km²) and Kofa (365 km²) Wilderness Areas were most at risk, with high or very high effects likely. The area predicted to experience very high effects overlapped with two of the largest fires that occurred in 2005: the King Valley fire (130 km²) in the Kofa Wilderness and the Growler Peak fire (110 km²) in the Cabeza Prieta Wilderness. HFL was also predicted for large portions of the North Maricopa Mountains (180 km²) and Woolsey Peak (177 km²) Wilderness Areas, although a large proportion of these jurisdictions fall within the Arizona Upland Subdivision and have not experienced a large fire event since 1984. The Muggins Mountain (49%) and the East Cactus Plain (47%) Wilderness Areas had the highest percentage of HFL, and all of the HFL area was predicted to experience high effects. Only the New Water Mountains Wilderness was characterized as lacking HFL.

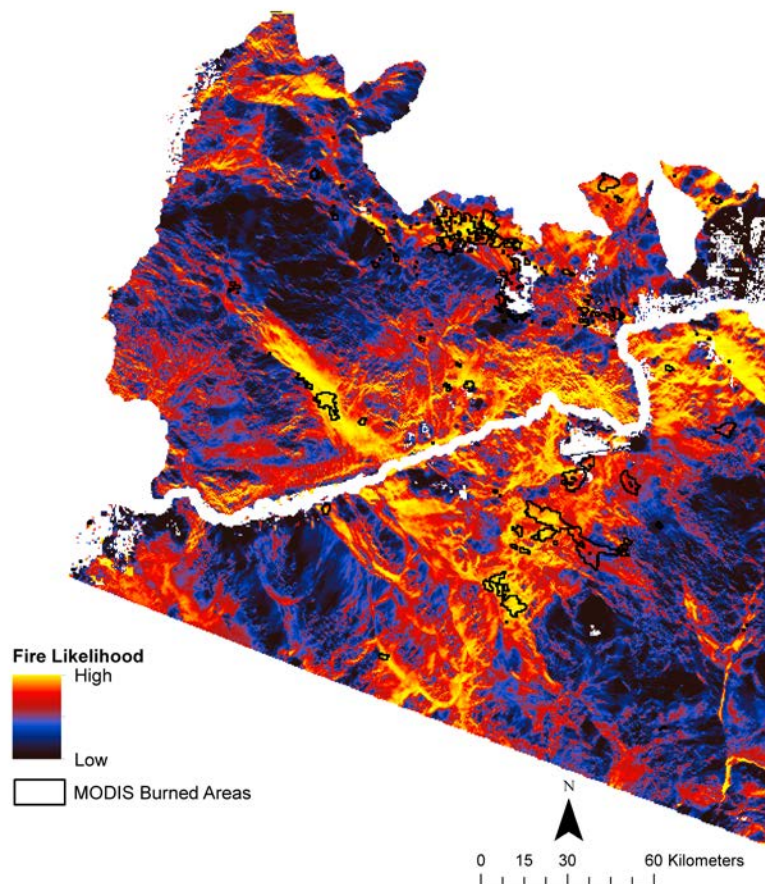


Figure 37: Map of fire likelihood across the lower Sonoran Desert of southwestern Arizona, based on a circuit theoretic model of connectivity. Warmer colors indicate relatively high current density, or higher likelihood of fire, and cooler colors indicate relatively low current density, or lower likelihood of fire. This map depicts a scenario of fire likelihood under conditions of high fire hazard, and is based on fuel conditions in 2005.

OBJECTIVE 6: Integrate the above models in a spatial decision-support package that informs sustainable resource management and recovery of native habitats and species on DOD and adjacent lands.

Task 14: Design and develop scenarios for decision support

We developed scenarios to assist collaborators with realistic decision-making guidance within the SDSS framework. These scenarios were constructed via synthesis of our results relevant to spatial relationships between invasive species, climate change and variability, land use, and disturbance. Scenario development was focused on the spatial and temporal scales befitting management and monitoring at the extent of individual installations or land management jurisdictions. We thus used scenario development as a bridge between science and management. Invasive species distribution modeling provides an avenue to support ongoing communication and facilitate new inter-jurisdictional conversations and efforts to locate and monitor invasive species populations.

Constructed scenarios presented to stakeholders at the fall 2013 focused around applications of these data towards manager's needs. Each scenario was presented as a way to use existing and developed data, at times in conjunction with data that an individual organization might already have. The group then discussed applications to management and refined the information needed to make a given scenario most useful to management. Four scenarios were presented:

Predicted change of Brassica distribution future climate 2012-2050: early detection and eradication

In this scenario, current distribution and habitat suitability under future climate were used to show stakeholders locations where *Brassica* has not been found, but is likely to be found in the future. This information can be used to focus prevention, early detection, and eradication efforts moving forward. This scenario was refined with the addition of a roads layer, due to the propensity of *Brassica* to spread through these corridors.

Cross-boundary management opportunities with extent and spatially explicit distribution of Brassica

In this scenario, distribution of *Brassica* was overlaid with management jurisdictions to identify areas for mitigation and monitoring within and across jurisdictions. Participants discussed thresholds or triggers for action based on abundance or spatial extent of greenup, as well as coordinated action across jurisdictions.

Probability of large fire occurrence, connectivity, and mitigation

In this scenario, we described how the independent layer of high fire likelihood could be overlaid with information about known ignition sites, high value areas, or important restricted areas to avoid fire ignition or protect key DOD resources. We also demonstrated that fire connectivity models could be overlaid with places where invasive plants are expected to increase, in order to identify places where fuel connectivity may be diminished across the landscape through "pinch point" management locations—places where reducing non-natives will reduce the likelihood of fire spread. The group discussed the contribution of invasive versus all herbaceous growth to fire risk, the role of NDVI in fire risk, and the potential to overlay grazing maps with fire.

Fire likelihood and wildlife

In this scenario, habitat suitability for pronghorn and fire likelihood were overlaid with current pronghorn range to explore potential impacts of fire on wildlife species of concern. Participants discussed the temporal element of the benefits and impacts of fire on pronghorn and other wildlife; in the short term, there may be no forage, but in the long term, animals may gravitate towards those areas.

Task 15: Develop collaborative process and stakeholder workshops

We identified 14 science or management collaborators representing six different jurisdictions, including our two focal DOD installations, for participation in the NAS. Thirteen (93%) of these collaborators responded. According to responses to the NAS, all participants were concerned with invasive plants and a majority were concerned about observed changes in fire behavior due to both native and non-native species within their jurisdictions. Among our target invasive plants, *Pennisetum* and *Brassica* were the species of greatest concern for 54% and 38% of respondents, respectively. There was broad support for the development of fire models and scenarios that integrated remotely sensed data with field data on invasive occurrence. Most agencies reported that they were making efforts to work across ownership boundaries in order to mitigate and manage the spread of invasive plants.

Based on our tasks and associated interactions with collaborators, spatial models of fire risk or invasion pattern, emerged as key to addressing fundamental management issues. However, collaborators also demonstrated a need for more basic information on ecosystem conditions. Collaborators expressed strong interest in obtaining our invasive species occurrence databases—both field-collected and compiled from external sources—as well as current Landsat TM satellite images encompassing installation boundaries. We made these data available upon request.

Based on the 2011 NAS synthesis and follow-up interactions with project collaborators (including the May 2012 IPR meeting in Tucson, AZ, phone interviews in March 2013, and in-person visits May 2013), we identified multiple common needs across our study area (Table 9). Generally, these needs can be organized into three thematic lines, or classes, of plant invasion, fire risk and threat, and communication (Table 9).

Collaborators identified knowledge of invasive species distribution as a ‘high priority’ in the NAS. Similarly, Villarreal et al. (2011) reported that the development of invasive species distribution maps were of high priority in the monitoring priority matrix for BMGR-W. Baseline distribution maps of invasive populations extend knowledge of both installation and landscape level locations, and also provide ready products for resource specialists and installation managers to support decisions on timing of DOD activities. Given that we were permitted to collect data within YPG, BMGR-E, and BMGR-W, our current landscape models of invasive species risk and distribution are particularly relevant to this request. The data we have compiled on invasive species locations from various databases will help fulfill this need.

Our ability to identify fuel load characteristics in the form of invasive vegetation contributions and using NDVI will help address concerns on the part of resource and installation managers regarding annual potential fire risk and threat (e.g., behavior and hazard). Base managers were particularly wary of fire and most interested in the distribution of fire risk. They also noted that the sources of fuel (i.e., invasive vs. native herbaceous fine fuels) are less important than identifying locations that are prone to burning or that need to be assessed for their burn potential.

Table 9. Informational needs identified by stakeholders

| Theme | Topic | Components |
|---------------------------------|--|---|
| Non-native plant invasion | Distributions | Knowledge of where invasive plants occur Identification of potential suitable habitat |
| | Remote sensing-based solutions to invasive species mapping | Efficient mapping of invasive plant distributions, especially when true distribution is unknown |
| | Determination of potential impacts on native species | |
| Fire risk and threat | Fire and fine fuels characterization | Determination of: thresholds for fine fuel loads and fire spread potential; the fuels types that lead to increasing severity and intensity; susceptible dominant vegetation types; and the rates of recovery among different vegetation and terrain types |
| | Establishment of remote sensing-based solutions to capture fire patterns and fire risk | Need for data and maps on annual plant productivity and herbaceous biomass, fire connectivity, and fire risk |
| | Management plan facilitation | Context-based scenarios of fire outcomes and risk characterization translated into reports, software, and maps |
| | Decision support on DOD installations | Understanding where flammable herbaceous fuels are likely to develop in order to reduce the 'search space' and help guide decisions about operational activities |
| Communications and data sharing | Information exchange | Efficient information exchange that takes firewalls and other agency-specific limiting factors into consideration |
| | GIS solutions to managers | Acknowledgement of limitations in GIS experience, skills, and functionality among collaborators through outreach to GIS 'officials' and by organizing collaborator workshops |

Finally, the overall lack of synthesized spatially explicit information on invasive species and fine fuels is just one of the information challenges currently facing DOD managers and their staff. GIS skills vary, and access to spatial data is limited. The ability to work with complex models and interact with dynamic tools for analysis is severely limited if not absent. Managers will benefit from a more comprehensive baseline database of not only invasive species distributions, but also general GIS 'base layers,' such as roads and multi-temporal satellite imagery and derived products (e.g., NDVI phenometrics). In response to this assessment of capacity on installations, we focused our GIS outreach efforts on data and scenarios, rather than specific 'tools' (e.g., software products) for conducting

dynamic analysis. Furthermore, our discussions with managers were guided by their expressed needs and priorities, but we note that many of the analyses and products from the project as a whole could be integrated and presented to managers to suit their future needs and interests; for example, the project leaves us poised to integrate the BEM projections and fire probability and connectivity modeling in future stakeholder interactions.

Task 16: Tool transfer, training, and presentations

We provided to the installation managers guidance regarding the tools and models developed under each collaborator need (i.e., plant invasions and fire risk) through our formal workshop-based information translation and transfer component toward the end of the project (Table 9, Figure 38). As noted previously, within DOD installations (and many agencies in the study area), there is wide variability in the use of spatial as well as access, analytical skills, and data interpretation. This underlies differences in the ability of resource management staff to provide meaningful recommendations to base managers. This variability can hinder the use, implementation, and interpretation of data, including the adoption of new analytical approaches. Not all spatial data support capacity exists in-house at DOD installations or in other agencies in the study region. Instead, some support is being provided by contractors, often with a high degree of turnover in staff, leaving installation resource managers and decision-makers at risk of losing the institutional memory needed to support the use of information and data provided through any process. We have encountered and overcome many of these challenges in our past collaborative landscape work, and we know that sufficient planning can make them surmountable. Molding our deliverable package to address these issues included product delivery in multiple formats (hard copy map product scenario outputs and raw foundational and derived data delivery) (Table 10), as well as expanded support or step-wise information exchange.



Figure 38: Images from the 'Managers Workshop' November 15, 2013, designed to foster tech transfer and cross-jurisdictional discussions. The meeting was hosted by NAU staff, in collaboration with staff from the Gila Bend Air Force Auxiliary Field.

Table 10: List of data products delivered to collaborators, given three general ‘needs’ classes identified during a formal NAS process.

| Data products | Completion | Needs addressed |
|---|------------|-----------------|
| Non-native species distribution assessment | | |
| Sampled presence, cover, and biomass from 2011 and 2012 | Completed | 1a |
| Habitat suitability models of <i>Pennisetum</i> , <i>Brassica</i> , and <i>Schismus</i> | Completed | 1a |
| Remote sensing time-series models of <i>Brassica</i> and <i>Schismus</i> | Completed | 1b |
| Evaluation of trajectory of fire risk | | |
| Fire risk models based on historical fire and NDVI | Completed | 2a |
| Fire behavior and hazard models | Completed | 2a |
| Prediction of impact under climate change | | |
| Models of <i>Brassica</i> and <i>Bromus</i> under current climate | Completed | 1a,2b |
| Models of <i>Brassica</i> and <i>Bromus</i> under future climate | Completed | 1a,2b |
| Landscape disturbance risk assessment | | |
| Disturbance risk based on <i>Brassica</i> models and other factors | Completed | 1a |
| Ancillary data | | |
| Compiled non-native species occurrence data | Completed | 3b |
| Time-series phenometrics based on amplitude of NDVI | Completed | 3b |
| Refined topographic data layers | Completed | 3b |

During this project, we encountered varied levels of engagement horizontally (across agencies) and vertically (within agencies). Participation and collaboration at each level of resource manager, decision maker, and technical GIS staff would lead to greater success, which we define as greater agency-level understanding of data uses and greater support to include data products in project planning.

Conclusions and Implications for Future Research/Implementation

Desert ecosystems have high climatic variation that results in complex spatial and temporal patterns in plant phenology and occurrence patterns (Van Leeuwen et al. 2010; Sponseller et al. 2012). Precise mapping of invasive plant distributions is important to land management agencies seeking to monitor and mitigate non-native plant impacts on native flora, biodiversity, and disturbance factors, such as wildland fire (Olsson & Morisette 2014). Accurate plant distribution data are also needed for predicting distributions or habitat suitability under future climate change scenarios (Bradley et al. 2009, 2012; Wang et al. 2014). Spatial models, like those we have developed, that incorporate local-scale non-stationary factors and other broad-scale, ecologically based phenological predictors can improve estimates of species distribution, cover, abundance, and biomass. Moreover, model performance can be improved by utilizing important phenological differences between native and non-native plants for prediction.

Between 2011-2012, detections of *Brassica* and *Schismus* were widespread across the study area, whereas *Pennisetum*, *Eruca*, and *Bromus* were relatively uncommon. Although our field seasons occurred during two relatively dry years, we found consistent spatial trends year after year, and were able to identify key invasive species habitat—particularly for *Brassica*, which appeared to have more specific conditions under which it becomes dominant. *Schismus* appeared to be more of a generalist and was found to be almost ubiquitous as a minor component of most ecosystems we sampled in the Lower Colorado River Desert (LRCO). *Eruca* was in the early stages of expansion and will likely cover a much more extensive range than it currently inhabits, whereas *Bromus* and *Pennisetum* seemed to be better suited for upland ecosystems with higher winter and summer precipitation than are typical of the LRCO in southwestern Arizona. As a result, we predict that these species will remain rare on DOD lands in southwestern Arizona.

Modeling approaches and performance

Our iterative and targeted sampling design and habitat suitability models provide practical use of existing invasive plant distribution data and utility for developing sampling strata and detecting focal species over large geographic areas to satisfy key management objectives. These objectives can include 1) detecting populations of non-native invasive plants across previously unsampled gradients and 2) characterizing the distribution of non-native invasive plants at landscape to regional spatial scales. Our project attempted to rigorously examine this design in a desert system where species invasions pose a threat to native plant composition and structure that are likely to undergo community shifts in the coming decades as a result of climate change. Indeed, climate change may promote invasion by increasing the transport of propagules, decreasing the resistance of native species to invasion, reducing the space suitable for native species, and creating shifts in ecosystem distributions (Bradley 2010; Diez et al. 2012). Thus, our sampling design framework can play a key role in facilitating monitoring and mitigation activities by land management agencies. Moreover, our novel approach to the nested integration of common and freely available satellite images with field data can be readily extended to other species and ecosystems. Our results highlighted where potentially suitable habitats might be vulnerable to invasion by one or more of our focal species and where monitoring efforts might be focused. Importantly, our methods and results provide a framework for establishing an ‘early warning system’ that is critical to helping installation and other land managers to recognize the possible extent of future problematic non-native invasive plants across multiple ownerships.

We found MODIS and Landsat TM to be particularly adequate for describing likelihood of finding *Brassica*, owing to the unique phenology of the species and a strong contrast in green-up with native vegetation. *Schismus* was not as distinct from a spectral or temporal perspective. Across methods, remote sensing-derived models of *Schismus* were not as accurate as similarly-derived models of *Brassica*. *Brassica* models were improved when we used a SWE approach to mapping, likely due to spatial heterogeneity of precipitation causing phenological asynchrony across the study area. Models of both species were challenged by relatively low abundances of the target species because of low precipitation in both 2011 and 2012.

Ensemble methods for predicting species distributions, such as those proposed by Thuiller et al. (2009) can benefit from the SWE approach to enhance different classes of models when making future projections of species distributions (Olsson et al. In prep.). Elith et al. (2010) also point out that ensembles including poorly specified models may also improperly confuse model uncertainty with prediction errors. While a machine learning (RandomForest) approach was applied in our efforts, the SWE method for assigning spatial model weights can be applied to any class of empirical model. SWE models incorporating seasonal and annual phenology metrics derived from time series MODIS VI showed promise for detecting non-native plant species when germination and growing cycles differ from surrounding native plants species. In future studies, we expect the SWE approach to be applied to

other classes of models and datasets so as to better characterize non-stationary ecological processes important to mapping invasive plant distributions over large areas and complex environments.

As our results have demonstrated, phenology-based models of invasive species occurrence often rely on a large contrast between the phenology of native and invasive species. Desert vegetation is often distributed in small diffuse patches during dry years and their spectral signature is largely overwhelmed by the prominent reflectance from bareground and geologic substrates (Shupe & Marsh 2004). The Sonoran Desert is characterized by minimal native vegetative cover, low levels of standing dead biomass, and large interspaces composed of bare mineral soil and invasive grasses (Olsson & Morisette 2014). When invasive species occur in low abundances (i.e., <25% vegetative cover), those contrasts are minimized and instead, multispectral reflectances are dominated by the bare earth background. For this reason, we sought approaches to leverage the rich spectral resolution of hyperspectral imagery and sought specifically to evaluate a multi-temporal approach to hyperspectral remote sensing. Unfortunately, our requests for Hyperion imagery went mostly unfulfilled, providing us with the opportunity to assess this potential with just one scene that covered a small part of our study area. Given the sparse coverage and the one available scene, we were unable to meet the Go/No-Go decision point and objective of evaluating multitemporal hyperspectral imagery for invasive species mapping on DOD lands in the Sonoran Desert. Importantly, this circumstance resulted from a lack of access to data and does not reflect on the potential of hyperspectral imagery (or our efforts) to meet this objective.

Satellite imagery and derived data: challenges and opportunities

During the course of our study, Landsat-5 TM went offline, though it was a critical data source. Meanwhile, Landsat-7 spectral data have gaps that increase the cross-track from nadir, making it difficult to work with over our large study area. Thus, prior to the launch of the Landsat-8 sensor (and availability of data in late 2013), we identified a number of alternative satellite image sources that could provide similar (if not superior) spatial and spectral features for mapping invasive species. Specifically, we acquired and tested imagery from the high spatial resolution WV2 and SPOT sensors for subsets of the study area where we had placed numerous plots that were visited in 2011 and 2012. The potential benefits of these sensors are largely unexplored, but the spatial and spectral characteristics are well-designed for vegetation analysis and will likely provide a different perspective on vegetation in dryland ecosystems where vegetative condition is largely biased towards dormancy. Our work demonstrated that WV2 imagery can perform well in detecting small populations of invasive plants in a southwestern desert ecosystem (Sankey et al. 2014). In particular, WV2 image subpixel classification using the MTFM technique performed well in mapping a winter annual invasive species of *Brassica*. Still, robust, quantitative estimates of vegetation canopy cover and biomass during extremely dry years will always be a challenge in arid ecosystems, even with high resolution data such as WV2.

Although the use of remote sensing variables (e.g., NDVI, EVI) has been widely and reasonably applied to modelling animal habitat, there is substantial potential for bias when remote sensing variables are included in models of plant habitat (Bradley et al. 2012). Nevertheless, the growing availability of remotely sensed data suggests that their application to habitat suitability models will continue to increase. We therefore encourage both plant and animal habitat modelers to interpret remote sensing predictor variables relative to the habitat they aim to model by developing hypotheses about the ecological relationships those variables might reveal. This practice, along with explicitly stating how habitat is defined relative to existing land use or land cover, will help to reduce the likelihood of developing biased models and improve overall model interpretation and application (Bradley et al. 2012).

In addition to using remote sensing tools in habitat suitability analyses, researchers are increasingly using remote sensing to directly map invasive plant distributions. However, the remote

characterization of invasive plants remains an underutilized tool, particularly at landscape and regional scale (Bradley 2014). Many local-scale studies focus on hyperspectral remote sensing to detect invasive species based on their color and/or chemistry. But, our landscape scale results for *B. tournefortii* coupled with a few other studies suggest that unique phenologies of invasive plants could enable widespread mapping with satellites such as Landsat and MODIS (Bradley 2014). Our results also underscore the need for better communication and collaboration between invasion ecologists and scientists trained in remote sensing. Field design in particular is important to consider – measurements of percent cover (including absence) within square ‘pixel’-like plots are directly transferrable to remote sensing analysis (Bradley 2014, Wang et al., 2014).

The remote characterization of invasive plants is an underutilized tool for identifying invasions and informing models of distribution and invasion risk (Bradley 2014). Beyond the present study, and considering the large number of problematic invasive plants and widespread availability of imagery, it is likely that there are a number of opportunities for remote detection of invasives that have yet to be tested. If indeed invasive species are spectrally or phenologically unique, then collaborations between invasion ecologists and scientists trained in remote sensing may prove fruitful (Bradley 2014).

Implications for future research and implementation

As deserts globally are threatened by ongoing land cover and climate changes, spatial and temporal dynamics in precipitation, fuels and subsequent large fire occurrence will become an increasingly important factor in effective fire planning and management. The fire-specific work and applications we have developed for this project are transferable to other deserts in North America, as well as globally, where annual plant production can be an important component of fuels and where precipitation is typically highly heterogeneous. Our modelling approach and associated map products can be used by DOD and partners to monitor ignitions and mitigate the occurrence or negative consequence of large fire in the lower Sonoran Desert (Gray et al. 2014) and across large portions of the Mojave Desert (e.g., Hegeman et al. 2014). Maps of large fire probability will be useful for management decisions, such as fuels reductions, prevention programs to curb human-caused ignitions and suppression planning in advance of fire occurrence that could result in more rapid response. Our scenario-based maps will allow managers to base these decisions on empirical average and ‘worst-case’ conditions reflected by the time periods we examined. For instance, management actions based on a high fire probability scenario could make the landscape more resilient to extreme events such as those that occurred in 2005. These activities, including implementation of adaptive prevention and suppression plans by installation managers, will be especially important when and where fire season weather is extreme and likely to exacerbate the probability of an ignition becoming a large fire over time. In addition, analyses of fire likelihood and effects can contribute new and important information to fire and fuels management in the Sonoran Desert and beyond (see Gray & Dickson 2015). Our novel approach to modeling fire connectivity addresses challenges in quantifying and communicating wildfire risk and is applicable to other ecosystems and management issues globally.

Our ongoing dialogue with project collaborators on DOD, USFWS, NPS, and BLM lands culminated in an interactive, multi-collaborator workshop designed to bring resource (land and ‘landless’) managers, base managers (decision makers), and technical GIS staff together to learn about the use of our products, to support decisions within their specific management needs context, and to support their monitoring and treatment planning for invasive species. This workshop focused on the integration of outcomes of the remote sensing mapping efforts, fire modeling efforts, and many of the scenarios described above. The attendees at the workshop identified assessment of factors connected to high fire risk and invasive species spread risk as important information relevant to their work. They discussed the value of our maps as easily-interpretable outputs and discussed the possibility of prioritizing invasive species control in areas with high fire risk. We discussed options for transferring the

model codes and meta-data to attendee entities, and were told by at least one attending jurisdiction that this type of direct tool transfer and information exchange was unprecedented among scientific collaborators from other projects.

Here we highlight some of the lessons learned in this study:

1. The use of remote sensing techniques for predicting invasive plant parameters should be tightly integrated with designed field sampling efforts if model building and monitoring steps are to be effective. In light of the dry periods we experienced during sampling (2011-2012), this integration was critical to our success, but also helped to illuminate shortcomings in our design;
2. Sampling in hot desert areas should be as frequent as every three years to capture high and low rainfall events or important changes in annual native and non-native plant abundances will be missed. Temperature and precipitation patterns in the Sonoran Desert can vary substantially enough that two years of field data may not capture a season of high plant productivity. Field measurements taken during high productivity periods (e.g., 2005) can be key to the effective modeling of recent or ongoing invasive plant distributions;
3. Control of non-native plant invasions is something that all agency participants in our efforts agreed was important;
4. A standardized, cross-jurisdiction sampling and monitoring design is needed, as planning for invasive plant control or vegetation recovery should also occur across neighboring jurisdictions;
5. There should be greater agency involvement in efforts to implement and monitor a system of rapid plots (if everyone contributes, it is less expensive);
6. The recent advent of tools, such as Google Earth Engine, has permitted extracting data for the purposes of building models and generating large-scale predictions easier and faster. This opens the door to near real-time monitoring and risk assessment. We see this as an invaluable tool for researchers and managers going forward, and one which could enable tight, effective iteration between modelers, the models they build, and the managers who use them. This integration would help improve the accuracy and ecological realism of models, and would enable researchers to develop data products in response to emerging needs. In particular, the ability to create scenarios of landscape risk under changing climatic conditions will be critical to invasive species monitoring, as they respond quickly to climate and land-use change;
7. Future directions for further developing analyses and results will entail evaluating the sensitivity of the results to different cost specifications. Fine-tuning of models with additional feature selection would also improve already strong models. Moreover, exploring the possible applications of our cover data generated during sampling might add another critical dimension to risk assessment in the context of plant invasions. Namely, risk might be evaluated as a function of the abundance and presence of a given invasive species under different climate scenarios;
8. Models based on plant occurrence points should be interpreted as risk of establishment only, not risk of abundance or impact. In the future, if suitability models aim to be more management relevant, invasion risk models should include abundance as well as occurrence;
9. Models and maps of large fire probability that were developed for this region are robust to the resolution of analysis. Using 1-km NDVI data derived from National Oceanic and Atmospheric Administration's (NOAA) Advanced Very High Resolution Radiometer (AVHRR) sensor, model results were similarly robust to the results obtained using 30-m Landsat data. This suggests that an NDVI forecasting tool would be appropriate at multiple resolutions and sensor sources;
10. Models of fire connectivity should account for probabilistic flow across all possible paths, and not attempt to constrain the fire spread process to only 'optimal' pathways. A deterministic connectivity algorithm that optimizes flow also was also used to model and map fire movement.

When visually compared to historic burned area data, these results were far less accurate than results obtained from a stochastic model of fire connectivity based on circuit theory.

Literature Cited

- Abatzoglou, J. T. 2013. Development of gridded surface meteorological data for ecological applications and modelling. *International Journal of Climatology* **33**:121–131.
- Abatzoglou, J. T., R. Barbero, J. W. Wolf, and Z. A. Holden. 2014. Tracking Interannual Streamflow Variability with Drought Indices in the U.S. Pacific Northwest. *Journal of Hydrometeorology* **15**:1900–1912.
- Abrams, M., S. Hook, and B. Ramachandran. 2002. ASTER user handbook, version 2. Jet propulsion laboratory **4800**:135.
- Ager, A., M. A. Finney, and N. M. Vaillant. 2012. Analyzing the spatial transmission of wildfire risk from large fires. Pages 108-113 *in* Spano, D., V. Bacchi, M. Salis, and C. Sirca, editors. *Modelling fire behaviour and risk*. Italy, University of Sassari Press.
- Allen, L. H. 1991. Effects of increasing carbon dioxide levels and climate change on plant growth, evapotranspiration, and water resources. Pages 101-147 *in* *Managing water resources in the West under conditions of climate uncertainty*. National Academy Press, Washington, DC.
- Anderson, D. R. 2007. *Model based inference in the life sciences: a primer on evidence*. Springer Science & Business Media.
- Araújo, M. B., and A. T. Peterson. 2012. Uses and misuses of bioclimatic envelope modeling. *Ecology* **93**:1527–1539.
- Araújo, M. B., and M. New. 2007. Ensemble forecasting of species distributions. *Trends in Ecology and Evolution* **22**:42–47.
- ASD, Analytical Spectral Devices, Inc. 2008. *FieldSpec 3 User Manual*. Document 600540 Rev. H.
- Asner, G. P., and R. Green. 2001. Imaging spectroscopy measures desertification in United States and Argentina. *Eos, Transactions American Geophysical Union*, 82(49), 601-606.
- Asner, G. P., D. E. Knapp, T. Kennedy-Bowdoin, M. O. Jones, R. E. Martin, J. Boardman, and R. F. Hughes. 2008. Invasive species detection in Hawaiian rainforests using airborne imaging spectroscopy and LiDAR. *Remote Sensing of Environment* **112**:1942–1955.
- Balch, J. K., B. A. Bradley, C. M. D’Antonio, and J. Gómez-Dans. 2013. Introduced annual grass increases regional fire activity across the arid western USA (1980–2009). *Global Change Biology* **19**:173–183.
- Barbieri, M. M., and J. O. Berger. 2004. Optimal predictive model selection. *Annals of Statistics* **32**:870–897.
- Bass, D. A., N. D. Crossman, S. L. Lawrie, and M. R. Lethbridge. 2006. The importance of population growth, seed dispersal and habitat suitability in determining plant invasiveness. *Euphytica* **148**:97–109.
- Beck, R. N., and P. E. Gessler. 2008. Technical note: development of a Landsat time series for application in forest status assessment in the inland northwest United States. *Western Journal of Applied Forestry* **23**:53–62.
- Beier, P., K. L. Penrod, C. Luke, W. D. Spencer, and C. Cabañero. 2006. South coast missing linkages: restoring connectivity to wildlands in the largest metropolitan area in the United States. Pages 555-586 *in* Crooks, K. R., and M. A. Sanjayan, editors. *Connectivity conservation*. Cambridge University Press, Cambridge, United Kingdom.
- Berger, J. 2004. The last mile: how to sustain long-distance migration in mammals. *Conservation Biology* **18**:320–331.
- BLM. 1996. *Sampling vegetation attributes: Interagency technical reference*. Project BLM/RS/ST-96/002+ 1730.
- Boardman, J. 1998. Leveraging the high dimensionality of AVIRIS data for improved subQpixel target unmixing and rejection of false positives: mixture tuned matched filtering. *Summaries of the Seventh Annual JPL Airborne Geoscience Workshop*. Pasadena, CA.

- Bolker, B. M., M. E. Brooks, C. J. Clark, S. W. Geange, J. R. Poulsen, M. H. H. Stevens, and J.-S. S. White. 2009. Generalized linear mixed models: a practical guide for ecology and evolution. *Trends in Ecology & Evolution* **24**:127–135.
- Botha, E. J., V. E. Brando, J. M. Anstee, A. G. Dekker, and S. Sagar. 2013. Increased spectral resolution enhances coral detection under varying water conditions. *Remote Sensing of Environment* **131**:247–261.
- Box, E. O., B. N. Holben, and V. Kalb. 1989. Accuracy of the AVHRR vegetation index as a predictor of biomass, primary productivity and net CO₂ flux. *Vegetatio* **80**:71–89.
- Boyce, M. S., P. R. Vernier, S. E. Nielsen, and F. K. Schmiegelow. 2002. Evaluating resource selection functions. *Ecological Modelling* **157**:281–300.
- Bradley, B. A. 2009. Regional analysis of impacts of climate change on cheatgrass invasion shows potential risk and opportunity. *Global Change Biology* **15**:196–208.
- Bradley, B. A. 2010. Assessing ecosystem threats from global and regional change: hierarchical modeling of risk to sagebrush ecosystems from climate change, land use and invasive species in Nevada, USA. *Ecography* **33**:198–208.
- Bradley, B. A. 2013. Distribution models of invasive plants over-estimate potential impact. *Biological Invasions* **15**:1417–1429.
- Bradley, B.A. 2014. Remote detection of invasive plants, a review of spectral, textural and phenological approaches. *Biological Invasions* **16**:1411–1425.
- Bradley, B. A., and J. F. Mustard. 2005. Identifying land cover variability distinct from land cover change: cheatgrass in the Great Basin. *Remote Sensing of Environment* **94**:204–213.
- Bradley, B. A., and J. F. Mustard. 2006. Characterizing the landscape dynamics of an invasive plant and risk of invasion using remote sensing. *Ecological Applications* **16**:1132–1147.
- Bradley, B. A., A. D. Olsson, O. Wang, B. G. Dickson, L. Pelech, S. E. Sesnie, and L. J. Zachmann. 2012. Species detection vs. habitat suitability: are we biasing habitat suitability models with remotely sensed data? *Ecological Modelling* **244**:57–64.
- Bradley, B. A., M. Oppenheimer, and D. S. Wilcove. 2009. Climate change and plant invasions: restoration opportunities ahead? *Global Change Biology* **15**:1511–1521.
- Breiman, L. 2001. Random forests. *Machine Learning* **45**:5–32.
- Breshears, D. D., N. S. Cobb, P. M. Rich, K. P. Price, C. D. Allen, R. G. Balice, W. H. Romme, et al. 2005. Regional vegetation die-off in response to global-change-type drought. *Proceedings of the National Academy of Sciences of the United States of America* **102**:15144–15148.
- Bright, J. L., and J. J. Hvert. 2005. Adult and fawn mortality of Sonoran pronghorn. *Wildlife Society Bulletin* **33**:43–50.
- Brillinger, D. R., H. K. Preisler, and J. W. Benoit. 2003. Risk assessment: a forest fire example. *Lecture Notes-Monograph Series* **40**:177–196.
- Brooks, M. L., and J. C. Chambers. 2011. Resistance to invasion and resilience to fire in desert shrublands of North America. *Rangeland Ecology & Management* **64**:431–438.
- Brooks, M. L., C. M. D’Antonio, D. M. Richardson, J. B. Grace, J. E. Keeley, J. M. DiTomaso, R. J. Hobbs, M. Pellant, and D. Pyke. 2004. Effects of invasive alien plants on fire regimes. *BioScience* **54**:677–688.
- Brooks, M. L., and J. R. Matchett. 2006. Spatial and temporal patterns of wildfires in the Mojave Desert, 1980–2004. *Journal of Arid Environments* **67**:148–164.
- Brown, D. E. 1994. *Biotic communities: southwestern United States and northwestern Mexico*. Salt Lake City, University of Utah Press.
- Brown, D. E., C. H. Lowe, and others. 1980. *Biotic communities of the Southwest*. General Technical Report, Rocky Mountain Forest and Range Experiment Station, USDA Forest Service.

- Burnham, K. P., and D. R. Anderson. 2002. Model selection and multimodel inference: a practical information-theoretic approach. New York, Springer.
- Busby, J. R. 1991. BIOCLIM—a bioclimate analysis and prediction system. *Plant Protection Quarterly* **6**:8–9 .
- Carroll, C., B. McRAE, and A. Brookes. 2012. Use of linkage mapping and centrality analysis across habitat gradients to conserve connectivity of gray wolf populations in western North America. *Conservation Biology* **26**:78–87.
- Casady, G. M., W. J. Van Leeuwen, and B. C. Reed. 2013. Estimating winter annual biomass in the Sonoran and Mojave deserts with satellite-and ground-based observations. *Remote Sensing* **5**:909–926.
- Chen, D., and D. Stow. 2002. The effect of training strategies on supervised classification at different spatial resolutions. *Photogrammetric Engineering and Remote Sensing* **68**:1155–1162.
- Cho, M. A., R. Mathieu, G. P. Asner, L. Naidoo, J. van Aardt, A. Ramoelo, et al. 2012. Mapping tree species composition in South African savannas using an integrated airborne spectral and LiDAR system. *Remote Sensing of Environment* **125**:214–226.
- Cleland, E. E., I. Chuine, A. Menzel, H. A. Mooney, and M. D. Schwartz. 2007. Shifting plant phenology in response to global change. *Trends in Ecology & Evolution* **22**:357–365.
- Comrie, A. C., and B. Broyles. 2002. Variability and spatial modeling of fine-scale precipitation data for the Sonoran Desert of south-west Arizona. *Journal of Arid Environments* **50**:573–592.
- Congalton, R. G., and K. Green. 1999. Assessing the accuracy of remotely sensed data: principles and applications. Boca Raton, Lewis Publishers.
- Cortes, C., and V. Vapnik. 1995. Support-Vector Networks. *Machine Learning* **20**:273–297.
- Crist, E. P. 1985. A TM tasseled cap equivalent transformation for reflectance factor data. *Remote Sensing of Environment* **17**:301–306.
- Crosby, J. S., and C. C. Chandler. 2004. Get the most from your windspeed observation. *Fire Management Today* **64**:53-55.
- Curtis, C.A. and B.A. Bradley. 2015. Climate change may alter both establishment and high abundance of red brome (*Bromus rubens*) and African mustard (*Brassica tournefortii*) in the semiarid Southwest United States. *Invasive Plant Science and Management* **38**:341-352.
- D’Antonio, C. M., and P. M. Vitousek. 1992. Biological invasions by exotic grasses, the grass/fire cycle, and global change. *Annual Review of Ecology and Systematics* **23**:63–87.
- Datt, B., T. R. McVicar, T. G. Van Niel, D. L. Jupp, and J. S. Pearlman. 2003. Preprocessing EO-1 Hyperion hyperspectral data to support the application of agricultural indexes. *IEEE Transactions on Geoscience and Remote Sensing* **41**:1246–1259.
- Daughtry, C. S., P. C. Doraiswamy, E. R. Hunt, A. J. Stern, J. E. McMurtrey, and J. H. Prueger. 2006. Remote sensing of crop residue cover and soil tillage intensity. *Soil and Tillage Research* **91**:101–108.
- Davis, M. B., and R. G. Shaw. 2001. Range shifts and adaptive responses to Quaternary climate change. *Science* **292**:673–679.
- Despain, D. W., and E. L. Smith. 1997. The comparative yield method for estimating range production. Some methods for monitoring rangelands. Tucson, AZ: University of Arizona Cooperative Extension Report **9043**:49–61.
- Dickson, B. G., J. S. Jenness, and P. Beier. 2005. Influence of vegetation, topography, and roads on cougar movement in southern California. *Journal of wildlife Management* **69**:264–276.
- Dickson, B. G., J. W. Prather, Y. Xu, H. M. Hampton, E. N. Aumack, and T. D. Sisk. 2006. Mapping the probability of large fire occurrence in northern Arizona, USA. *Landscape Ecology* **21**:747–761.

- Diez, J. M., C. M. D'Antonio, J. S. Dukes, E. D. Grosholz, J. D. Olden, C. J. B. Sorte, D. M. Blumenthal, B. A. Bradley, R. Early, I. Ibáñez, S. J. Jones, J. J. Lawler, and L. P. Miller 2012. Will extreme climatic events facilitate biological invasions? *Frontiers in Ecology and the Environment* **10**:249–257.
- Diffenbaugh, N. S., F. Giorgi, and J. S. Pal. 2008. Climate change hotspots in the United States. *Geophysical Research Letters* **35**:L16709.
- Diffenbaugh, N. S., J. S. Pal, R. J. Trapp, and F. Giorgi. 2005. Fine-scale processes regulate the response of extreme events to global climate change. *Proceedings of the National Academy of Sciences of the United States of America* **102**:15774–15778.
- Ehrenfeld, J. G. 2010. Ecosystem consequences of biological invasions. *Annual Review of Ecology, Evolution, and Systematics* **41**:59–80.
- Elith, J., C. H. Graham, R. P. Anderson, M. Dudik, and S. Ferrier. 2006. Novel methods improve prediction of species' distributions from occurrence data. *Ecography* **29**:129–151.
- Elith, J., M. Kearney, and S. Phillips. 2010. The art of modelling range-shifting species. *Methods in Ecology and Evolution* **1**:330–342.
- Esque, T. C., and C. R. Schwalbe. 2002. Alien annual grasses and their relationship to fire and biotic change in Sonoran desertscrub. Pages 126–146 *Invasive exotic species in the Sonoran region*. Tucson, Arizona, Arizona-Sonora Desert Museum and University of Arizona Press.
- Esque, T. C., C. R. Schwalbe, L. A. Defalco, R. B. Duncan, T. J. Hughes, and G. C. Carpenter. 2003. Effects of desert wildfires on desert tortoise (*Gopherus agassizii*) and other small vertebrates. *The Southwestern Naturalist* **48**:103–111.
- Esque, T. C., R. H. Webb, C. S. Wallace, C. van Riper III, C. McCreedy, and L. Smythe. 2013. Desert fires fueled by native annual forbs: effects of fire on communities of plants and birds in the lower Sonoran Desert of Arizona. *The Southwestern Naturalist* **58**:223–233.
- Faraway, J. J. 2005. *Extending the linear model with R: generalized linear, mixed effects and nonparametric regression models*. Boca Raton, CRC Press.
- Farr, T. G. et al. 2007. The Shuttle Radar Topography Mission. *Reviews of Geophysics* **45**:RG2004.
- Fawcett, T. 2006. An introduction to ROC analysis. *ROC Analysis in Pattern Recognition* **27**:861–874.
- Finney, M. A., I. C. Grenfell, C. W. McHugh, R. C. Seli, D. Trethewey, R. D. Stratton, and S. Brittain. 2011a. A method for ensemble wildland fire simulation. *Environmental Modeling & Assessment* **16**:153–167.
- Fielding, A. H., and J. F. Bell. 1997. A review of methods for the assessment of prediction errors in conservation presence/absence models. *Environmental Conservation* **24**:38–49.
- Finney, M. A., C. W. McHugh, I. C. Grenfell, K. L. Riley, and K. C. Short. 2011. A simulation of probabilistic wildfire risk components for the continental United States. *Stochastic Environmental Research and Risk Assessment* **25**:973–1000.
- Franklin, J. 2009. *Mapping species distributions: spatial inference and prediction*. New York: Cambridge University Press.
- Franklin, K. A., K. Lyons, P. L. Nagler, D. Lampkin, E. P. Glenn, F. Molina-Freaner, T. Markow, and A. R. Huete. 2006. Buffelgrass (*Pennisetum ciliare*) land conversion and productivity in the plains of Sonora, Mexico. *Biological Conservation* **127**:62–71.
- Garrity, S. R., C. D. Allen, S. P. Brumby, C. Gangodagamage, N. G. McDowell, and D. M. Cai. 2013. Quantifying tree mortality in a mixed species woodland using multitemporal high spatial resolution satellite imagery. *Remote Sensing of Environment* **129**:54–65.
- Gelbard, J. L., and J. Belnap. 2003. Roads as conduits for exotic plant invasions in a semiarid landscape. *Conservation Biology* **17**:420–432.
- Glenn, N. F., J. T. Mundt, K. T. Weber, T. S. Prather, L. W. Lass, and J. Pettingill. 2005. Hyperspectral data processing for repeat detection of small infestations of leafy spurge. *Remote Sensing of Environment* **95**:399–412.

- Gray, M. E., B. G. Dickson, and L. J. Zachmann. 2014. Modelling and mapping dynamic variability in large fire probability in the lower Sonoran Desert of south-western Arizona. *International Journal of Wildland Fire* **23**:1108-1118.
- Green, A. A., M. D. Craig, and C. Shi. 1988. The application of the minimum noise fraction transform to the compression and cleaning of hyper-spectral remote sensing data. Pages 1807–1807 *in* Geoscience and Remote Sensing Symposium. IGARSS'88. Remote Sensing: Moving Toward the 21st Century.
- Gruninger, J. H., A. J. Ratkowski, and M. L. Hoke. 2004. The sequential maximum angle convex cone (SMACC) endmember model. Pages 1–14 *in* Proceedings SPIE 5425, Algorithms and Technologies for Multispectral, Hyperspectral, and Ultraspectral Imagery X, 1.
- Guisan, A., and N. E. Zimmermann. 2000. Predictive habitat distribution models in ecology. *Ecological Modelling* **135**:147–186.
- Hampton, H. M., S. E. Sesnie, B. G. Dickson, J. M. Rundall, T. D. Sisk, G. B. Snider, and J. D. Bailey. 2008. Analysis of small-diameter wood supply in Northern Arizona. Forest Ecosystem Restoration Analysis Project, Center for Environmental Sciences and Education, Northern Arizona University: Flagstaff.
- Hand, D. J. 2009. Measuring classifier performance: a coherent alternative to the area under the ROC curve. *Machine Learning* **77**:103–123.
- Hansen, M. C., P. V. Potapov, R. Moore, M. Hancher, S. A. Turubanova, A. Tyukavina, D. Thau, S. V. Stehman, S. J. Goetz, T. R. Loveland, A. Kommareddy, A. Egorov, L. Chini, C. O. Justice, and J. R. G. Townshend. 2013. High-resolution global maps of 21st-century forest cover change. *Science* **342**:850–853.
- Hanson, R. B., J. Hanson, S. J. Phillips, and P. W. Comus. 1999. Sonoran desert natural events calendar. Pages 19-28 in Phillips, S. J., and P. Wentworth, editors. A natural history of the Sonoran Desert. Tucson, University of Arizona Press.
- Hegeman, E. E., B. G. Dickson, and L. J. Zachmann. 2014. Probabilistic models of fire occurrence across NPS units within the Mojave Desert Network, USA. *Landscape Ecology* **29**:1587–1600.
- Hervert, J. J., J. L. Bright, R. S. Henry, L. A. Piest, and M. T. Brown. 2005. Home-range and habitat-use patterns of Sonoran pronghorn in Arizona. *Wildlife Society Bulletin* **33**:8–15.
- Hijmans, R. J., S. E. Cameron, J. L. Parra, P. G. Jones, A. Jarvis, and others. 2005. Very high resolution interpolated climate surfaces for global land areas. *International Journal of Climatology* **25**:1965–1978.
- Hijmans, R. J., and J. van Etten. 2012. raster: Geographic analysis and modeling with raster data. R package version **1**:9–92.
- Hirzel, A. H., G. Le Lay, V. Helfer, C. Randin, and A. Guisan. 2006. Evaluating the ability of habitat suitability models to predict species presences. *Ecological Modelling* **199**:142–152.
- Hobbs, R. J., and L. F. Huenneke. 1992. Disturbance, diversity, and invasion: implications for conservation. *Conservation Biology* **6**:324–337.
- Holt, R. D. 2003. On the evolutionary ecology of species' ranges. *Evolutionary Ecology Research* **5**:159–178.
- Hosmer, D. W., and S. Lemeshow. 2000. Applied logistic regression. New York, John Wiley & Sons, Inc..
- Hosmer, D. W., S. Lemeshow, and E. D. Cook. 2000. Applied logistic regression, 2nd edition. New York, John Wiley & Sons.
- Hosmer Jr, D. W., and S. Lemeshow. 2004. Applied logistic regression. New York, John Wiley & Sons.
- Huang, C., and E. L. Geiger. 2008. Climate anomalies provide opportunities for large-scale mapping of non-native plant abundance in desert grasslands. *Diversity and Distributions* **14**:875–884.
- Hubbard, J. A., C. L. McIntyre, S. E. Studd, T. Nauman, D. Angell, K. Beaupre, B. Vance, and M. K. Connor. 2012. Terrestrial vegetation and soils monitoring protocol and standard operating procedures:

- Sonoran Desert and Chihuahuan Desert networks, version 1.1. Natural Resource Report NPS/SODN/NRR—2012/509. NPS, Fort Collins, Colorado.
- Hunt Jr, E. R., and A. E. Parker Williams. 2006. Detection of flowering leafy spurge with satellite multispectral imagery. *Rangeland Ecology & Management* **59**:494–499.
- Hutchinson, C. F. 1982. Techniques for combining Landsat and ancillary data for digital classification improvement. *Photogrammetric Engineering and Remote Sensing* **48**:123–130.
- Immitzer, M., C. Atzberger, and T. Koukal. 2012. Tree species classification with random forest using very high spatial resolution 8-band WorldView-2 satellite data. *Remote Sensing* **4**:2661–2693.
- Jensen, J.R. 2007. *Remote sensing of environment: an Earth resource perspective*. Prentice Hall, Upper Saddle River, New Jersey, USA.
- Jones, C. C., S. A. Acker, and C. B. Halpern. 2010. Combining local-and large-scale models to predict the distributions of invasive plant species. *Ecological Applications* **20**:311–326.
- Kalkhan, M. A., E. J. Stafford, and T. J. Stohlgren. 2007. Rapid plant diversity assessment using a pixel nested plot design: a case study in Beaver Meadows, Rocky Mountain National Park, Colorado, USA. *Diversity and Distributions* **13**:379–388.
- Kearney, M. 2006. Habitat, environment and niche: what are we modelling? *Oikos* **115**:186–191.
- Knutti, R., R. Furrer, C. Tebaldi, J. Cermak, and G. A. Meehl. 2010. Challenges in combining projections from multiple climate models. *Journal of Climate* **23**: 2739–2758.
- Kramer-Schadt S., J. Niedballa, J. D. Pilgrim, B. Schröder, J. Lindenborn, V. Reinfelder, M. Stillfried, I. Heckmann, A. K. Scharf, D. M. Augeri, S. M. Cheyne, A. J. Hearn, J. Ross, D. W. Macdonald, J. Mathai, J. Eaton, A. J. Marshall, G. Semiadi, R. Rustam, H. Bernard, R. Alfred, H. Samejima, J. W. Duckworth, C. Breitenmoser-Wuersten, J. L. Belant, H. Hofer, A. Wilting. 2013. The importance of correcting for sampling bias in MaxEnt species distribution models. *Diversity and Distributions* **19**:1366–1379.
- Krausman, P. R., L. K. Harris, S. K. Haas, K. K. G. Koenen, P. Devers, D. Bunting, and M. Barb. 2005. Sonoran pronghorn habitat use on landscapes disturbed by military activities. *Wildlife Society Bulletin* **33**:16–23.
- Kruse, F. A., and S. L. Perry. 2013. Mineral mapping using simulated WorldView-3 short-wave-infrared imagery. *Remote Sensing* **5**:2688–2703.
- Kuhn, M. 2008. Building predictive models in R using the caret package. *Journal of Statistical Software* **28**:1–26.
- Lantz N.J. and J. Wang. 2013. Object-based classification of WorldView-2 imagery for mapping invasive common reed, *Phragmites australis*. *Canadian Journal of Remote Sensing*. **39**:328–340.
- Larson, D. L. 2002. Native weeds and exotic plants: relationships to disturbance in mixed-grass prairie. *Plant Ecology* **169**:317–333.
- Lass, L. W., T. S. Prather, N. F. Glenn, K. T. Weber, J. T. Mundt, and J. Pettingill. 2009. A review of remote sensing of invasive weeds and example of the early detection of spotted knapweed (*Centaurea maculosa*) and babysbreath (*Gypsophila paniculata*) with a hyperspectral sensor. *Weed Science* **53**:242-251.
- Latif, Z. A., I. Zamri, and H. Omar. 2012. Determination of tree species using WorldView-2 data. Pages 383–387 in *Signal processing and its applications (CSPA), 2012 IEEE 8th International Colloquium on. IEEE*.
- Lawrence, R. L., S. D. Wood, and R. L. Sheley. 2006. Mapping invasive plants using hyperspectral imagery and Breiman Cutler classifications (RandomForest). *Remote Sensing of Environment* **100**:356–362.
- Lehan, N. E., J. R. Murphy, L. P. Thorburn, and B. A. Bradley. 2013. Accidental introductions are an important source of invasive plants in the continental United States. *American Journal of Botany* **100**:1287–1293.

- Le Lay, G., R. Engler, E. Franc, and A. Guisan. 2010. Prospective sampling based on model ensembles improves the detection of rare species. *Ecography* **33**:1015–1027.
- Longbotham, N., C. Chaapel, L. Bleiler, C. Padwick, W. J. Emery, and F. Pacifici. 2012. Very high resolution multiangle urban classification analysis. *Geoscience and Remote Sensing, IEEE Transactions on* **50**:1155–1170.
- Mack, R. N. 2000. Assessing the extent, status, and dynamism of plant invasions: current and emerging approaches. Pages 141-169 *in* Mooney, H. A., and R. J. Hobbs, editors. *Invasive species in a changing world*. Washington, DC, Island Press.
- Manakos, I., Manevski, K., Kalaitzidis, C., & Edler, D. 2011. Comparison between atmospheric correction modules on the basis of WorldView-2 imagery and in situ spectroradiometric measurements. In 7th EARSeL SIG Imaging Spectroscopy workshop, April, Edinburgh (pp. 11-13).
- Marushia, R. G., M. W. Cadotte, and J. S. Holt. 2010. Phenology as a basis for management of exotic annual plants in desert invasions. *Journal of Applied Ecology* **47**:1290-1299.
- Maselli, F., S. Romanelli, L. Bottai, and G. Zipoli. 2003. Use of NOAA-AVHRR NDVI images for the estimation of dynamic fire risk in Mediterranean areas. *Remote Sensing of Environment* **86**:187–197.
- Matthew M.W., Alder-Golden, S.M., Berk, A. Felde, G., Anderson, G.P. Gorodetzky, D., P)aswaters, S. Shippert, M., 2003. Atmospheric correction of spectral imagery: evaluation of the FLAASH algorithm with AVIRIS data. In: *SPIE Algorithms and Technologies for Multispectral, Hyperspectral, and Ultraspectral Imagery, IX*, pp. 474-482.
- Maxwell, B. D., V. Backus, M. G. Hohmann, K. M. Irvine, P. Lawrence, E. A. Lehnhoff, and L. J. Rew. 2012. Comparison of transect-based standard and adaptive sampling methods for invasive plant species. *Invasive Plant Science and Management* **5**:178–193.
- McCarty, J. P. 2001. Ecological consequences of recent climate change. *Conservation Biology* **15**:320–331.
- McRae, B. H., B. G. Dickson, T. H. Keitt, and V. B. Shah. 2008. Using circuit theory to model connectivity in ecology, evolution, and conservation. *Ecology* **89**:2712–2724.
- McRae, B. H., and V. B. Shah. 2009. *Circuitscape user guide*. University of California, Santa Barbara <http://circuitscape.org>.
- Merow, C., M. J. Smith, and J. A. Silander. 2013. A practical guide to MaxEnt for modeling species' distributions: what it does, and why inputs and settings matter. *Ecography* **36**:1058–1069.
- Mika, A. M. 1997. Three decades of Landsat instruments. *Photogrammetric Engineering and Remote Sensing* **63**:839–852.
- Mildrexler, D. J., M. Zhao, and S. W. Running. 2009. Testing a MODIS global disturbance index across North America. *Remote Sensing of Environment* **113**:2103–2117.
- Mitchell, J. J., and N. F. Glenn. 2009. Subpixel abundance estimates in mixture-tuned matched filtering classifications of leafy spurge (*Euphorbia esula* L.). *International Journal of Remote Sensing* **30**:6099–6119.
- Mladinich, C. S., M. R. Bustos, S. Stitt, R. Root, K. Brown, G. L. Anderson, and S. Hager. 2006. The use of Landsat 7 Enhanced Thematic Mapper Plus for mapping leafy spurge. *Rangeland Ecology & Management* **59**:500–506.
- Mundt, J. T., N. F. Glenn, K. T. Weber, and J. A. Pettingill. 2006. Determining target detection limits and accuracy delineation using an incremental technique. *Remote Sensing of Environment* **105**:34–40.
- Mundt, J. T., D. R. Streutker, and N. F. Glenn. 2007. Partial unmixing of hyperspectral imagery: theory and methods. *Proceedings of the American Society of Photogrammetry and Remote Sensing, ASPRS 2007 Annual Conference, Tampa*.

- Nakicenovic, N., and R. Swart. 2000. Special report on emissions scenarios. Page 612 in Nakicenovic, N., and R. Swart, editors. Special report on emissions scenarios. Cambridge, UK: Cambridge University Press.
- Noujdina, N. V., and S. L. Ustin. 2009. Mapping downy brome (*Bromus tectorum*) using multirate AVIRIS data. *Weed Science* **56**:173-179.
- Okin, G. S., K. D. Clarke, and M. M. Lewis. 2013. Comparison of methods for estimation of absolute vegetation and soil fractional cover using MODIS normalized BRDF-adjusted reflectance data. *Remote Sensing of Environment* **130**:266–279.
- Olsson, A. D., J. L. Betancourt, M. A. Crimmins, and S. E. Marsh. 2012a. Constancy of local spread rates for buffelgrass (*Pennisetum ciliare* L.) in the Arizona Upland of the Sonoran Desert. *Journal of Arid Environments* **87**:136–143.
- Olsson, A. D., J. Betancourt, M. P. McClaran, and S. E. Marsh. 2012b. Sonoran Desert Ecosystem transformation by a C4 grass without the grass/fire cycle. *Diversity and Distributions* **18**:10–21.
- Olsson, A. D., and J. T. Morisette. 2014. Comparison of simulated HypSIRI with two multispectral sensors for invasive species mapping. *Photogrammetric Engineering & Remote Sensing* **80**:217–227.
- Olsson, A. D., W. J. van Leeuwen, and S. E. Marsh. 2011. Feasibility of invasive grass detection in a desertscrub community using hyperspectral field measurements and Landsat TM imagery. *Remote Sensing* **3**:2283–2304.
- Olsson, A., O. Wang, L. Zachmann, S. Sesnie, and B. Dickson. In prep. A spatially weighted ensemble and MODIS phenology-based approach for mapping a Sonoran Desert invasive annual plant *Brassica tournefortii*.
- Ozdemir, I., and A. Karnieli. 2011. Predicting forest structural parameters using the image texture derived from WorldView-2 multispectral imagery in a dryland forest, Israel. *International Journal of Applied Earth Observation and Geoinformation* **13**:701–710.
- Pearson, R. G., and T. P. Dawson. 2003. Predicting the impacts of climate change on the distribution of species: are bioclimate envelope models useful? *Global Ecology and Biogeography* **12**:361–371.
- Pearson, R. G., W. Thuiller, M. B. Araújo, E. Martinez-Meyer, L. Brotons, C. McClean, L. Miles, P. Segurado, T. P. Dawson, and D. C. Lees. 2006. Model-based uncertainty in species range prediction. *Journal of Biogeography* **33**:1704–1711.
- Pelletier, D., M. Clark, M. G. Anderson, B. Rayfield, M. A. Wulder, and J. A. Cardille. 2014. Applying circuit theory for corridor expansion and management at regional scales: tiling, pinch points, and omnidirectional connectivity. *PLoS ONE* **9**:e84135.
- Pengra, B. W., C. A. Johnston, and T. R. Loveland. 2007. Mapping an invasive plant, *Phragmites australis*, in coastal wetlands using the EO-1 Hyperion hyperspectral sensor. *Remote Sensing of Environment* **108**:74–81.
- Pennington, D. D., and S. L. Collins. 2007. Response of an aridland ecosystem to interannual climate variability and prolonged drought. *Landscape Ecology* **22**:897–910.
- Peterson, E. B. 2005. Estimating cover of an invasive grass (*Bromus tectorum*) using tobit regression and phenology derived from two dates of Landsat ETM+ data. *International Journal of Remote Sensing* **26**:2491–2507.
- Philippi, T. 2005. Adaptive cluster sampling for estimation of abundances within local populations of low-abundance plants. *Ecology* **86**:1091–1100.
- Phillips, S. 2005. A brief tutorial on MaxEnt. AT&T Research.
- Phillips, S. J., R. P. Anderson, and R. E. Schapire. 2006. Maximum entropy modeling of species geographic distributions. *Ecological Modelling* **190**:231–259.
- Phillips, S. J., and M. Dudík. 2008. Modeling of species distributions with MaxEnt: new extensions and a comprehensive evaluation. *Ecography* **31**:161–175.

- Phillips, S. J., M. Dudík, J. Elith, C. H. Graham, A. Lehmann, J. Leathwick, and S. Ferrier. 2009. Sample selection bias and presence-only distribution models: implications for background and pseudo-absence data. *Ecological Applications* **19**:181–197.
- Preisler, H. K., A. L. Westerling, K. M. Gebert, F. Munoz-Arriola, and T. P. Holmes. 2011. Spatially explicit forecasts of large wildland fire probability and suppression costs for California. *International Journal of Wildland Fire* **20**:508–517.
- Pulliam, H. R. 2000. On the relationship between niche and distribution. *Ecology Letters* **3**:349–361.
- Pu, R., and S. Landry. 2012. A comparative analysis of high spatial resolution IKONOS and WorldView-2 imagery for mapping urban tree species. *Remote Sensing of Environment* **124**:516–533.
- Raes, N., and H. ter Steege. 2007. A null-model for significance testing of presence-only species distribution models. *Ecography* **30**:727–736.
- Ramirez, J., and A. Jarvis. 2010. Downscaling global circulation model outputs: the delta method. *Decision and Policy Analysis Working Paper* 1:1–18.
- Rayfield, B., M.-J. Fortin, and A. Fall. 2011. Connectivity for conservation: a framework to classify network measures. *Ecology* **92**:847–858.
- Rencz, A. N. 1999. *Remote sensing for the earth sciences: manual of remote sensing*, Volume 3. New York, John Wiley & Sons.
- Rollins, M. G., P. Morgan, and T. Swetnam. 2002. Landscape-scale controls over 20th century fire occurrence in two large Rocky Mountain (USA) wilderness areas. *Landscape Ecology* **17**:539–557.
- Root, R. R., G. L. Anderson, S. N. Hager, K. E. Brown, K. B. Dudek, R. F. Kokaly, et al. 2004. Application of advanced remote sensing and modeling techniques for the detection and management of leafy spurge: challenges and opportunities. Page 30 *in* Proceedings of the Society for Range Management 57th Annual Meeting.
- Rorabaugh, J. C. 2010. Conservation of amphibians and reptiles in northwestern Sonora and southwestern Arizona. Pages 181-204 *in* Halvorson, W. L., C. R. Schwalbe, and C. van Riper, editors. *Southwestern Desert Resources*.
- Roy, D.P., W.A. Wulder, T.R. Loveland, C.E. Woodcock, R.G. Allen, M.C. Anderson, D. Helder, J.R. Irons, D.M. Johnson, R. Kennedy, T.A. Scambos, C.B. Schaff, J.R. Schott, Y. Sheng, E.F. Vermont, A.S. Belward, R. Bindschadler, W.B. Cohen, F. Gao, J.D. Hipple, P. Hostert, J. Huntington, C.O. Justice, A. Kilic, V. Kovalskyy, Z.P. Lee, L. Lyburner, J.G. Masek, J. McCorkel, Y. Shuai, R. Terzza, J. Vogelmann, R.H. Wynne, and Z. Zhu. 2014. Landsat-8: Science and product vision for terrestrial global change research. *Remote Sensing of Environment* **145**: 154-172.
- Sánchez-Flores, E. 2007. GARP modeling of natural and human factors affecting the potential distribution of the invasives *Schismus arabicus* and *Brassica tournefortii* in “El Pinacate y Gran Desierto de Altar” Biosphere Reserve. *Ecological Modelling* **204**:457–474.
- Sankey, T., B. Dickson, S. Sesnie, O. Wang, A. Olsson, and L. Zachmann. 2014. WorldView-2 high spatial resolution improves desert invasive plant detection. *ASPRS – Photogrammetric Engineering and Remote Sensing*. **80**: 885-893.
- Sankey, T., and N. Glenn. 2011. Landsat-5 TM and lidar fusion for sub-pixel juniper tree cover estimates in a western rangeland. *Photogrammetric Engineering & Remote Sensing* **77**:1241–1248.
- Sankey, T. T., N. Glenn, S. Ehinger, A. Boehm, and S. Hardegree. 2010. Characterizing western juniper expansion via a fusion of Landsat 5 Thematic Mapper and lidar data. *Rangeland Ecology & Management* **63**:514–523.
- Sawyer, H., F. Lindzey, and D. McWhirter. 2005. Mule deer and pronghorn migration in western Wyoming. *Wildlife Society Bulletin* **33**:1266–1273.

- Scharlemann, J. P., D. Benz, S. I. Hay, B. V. Purse, A. J. Tatem, G. R. Wint, and D. J. Rogers. 2008. Global data for ecology and epidemiology: a novel algorithm for temporal Fourier processing MODIS data. *PLoS ONE* **3**:e1408.
- Scott, J. H., and R. E. Burgan. 2005. Standard fire behavior fuel models: a comprehensive set for use with Rothermel's surface fire spread model. Rocky Mountain Research Station General Technical Report RMRS-GTR-153.
- Scott, J. H., E. D. Reinhardt, and others. 2001. Assessing crown fire potential by linking models of surface and crown fire behavior. Rocky Mountain Research Station General Technical Report RMRS-RP-29.
- Seager, R., M. Ting, I. Held, Y. Kushnir, J. Lu, G. Vecchi, H.-P. Huang, et al. 2007. Model projections of an imminent transition to a more arid climate in Southwestern North America. *Science* **316**:1181–1184.
- Sesnie, S. E., B. G. Dickson, S. S. Rosenstock, and J. M. Rundall. 2012. A comparison of Landsat TM and MODIS vegetation indices for estimating forage phenology in desert bighorn sheep (*Ovis canadensis nelsoni*) habitat in the Sonoran Desert, USA. *International Journal of Remote Sensing* **33**:276–286.
- Short, K. 2013. Spatial wildfire occurrence data for the United States, 1992-2011 [FPA FOD 20130422]. Fort Collins, CO: USDA Forest Service, Rocky Mountain Research Station.
- Shupe, S. M., and S. E. Marsh. 2004. Cover-and density-based vegetation classifications of the Sonoran Desert using Landsat TM and ERS-1 SAR imagery. *Remote Sensing of Environment* **93**:131–149.
- Sillero, N. 2011. What does ecological modelling model? A proposed classification of ecological niche models based on their underlying methods. *Ecological Modelling* **222**:1343–1346.
- Sisk, T. D., J. W. Prather, H. M. Hampton, E. N. Aumack, Y. Xu, and B. G. Dickson. 2006. Participatory landscape analysis to guide restoration of ponderosa pine ecosystems in the American Southwest. *Landscape and Urban Planning* **78**:300–310.
- Smith, C. S., W. M. Lonsdale, and J. Fortune. 1999. When to Ignore Advice: Invasion Predictions and Decision Theory. *Biological Invasions* **1**:89–96.
- Song, C., C.E. Woodcock, K.C., Seto, M.P. Lenny, S.A. Macomber. 2001. Classification and Change Detection Using Landsat TM Data: When and How to Correct Atmospheric Effects? *Remote Sensing of the Environment*, 75, pp 230-244.
- Sponseller, R. A., S. J. Hall, D. P. Huber, N. B. Grimm, J. P. Kaye, C. M. Clark, and S. L. Collins. 2012. Variation in monsoon precipitation drives spatial and temporal patterns of *Larrea tridentata* growth in the Sonoran Desert. *Functional Ecology* **26**:750–758.
- Steers, R. J., and E. B. Allen. 2010. Post-fire control of invasive plants promotes native recovery in a burned desert shrubland. *Restoration Ecology* **18**:334–343.
- Steltzer, H., and J. M. Welker. 2006. Modeling the effect of photosynthetic vegetation properties on the NDVI-LAI relationship. *Ecology* **87**:2765–2772.
- Stevens, Jr., D. L., and A. R. Olsen. 2004. Spatially balanced sampling of natural resources. *Journal of the American Statistical Association* **99**:262–278.
- Stocker T. F., D. Qin, G. K. Plattner, M. Tignor, S. K. Allen, J. Boschung, A. Nauels, Y. Xia, V. Bex, and P. M. Midgley. 2013. Climate change 2013: the physical basis. Intergovernmental Panel on Climate Change, Working Group I Contribution to the IPCC Fifth Assessment Report (AR5). New York: Cambridge University Press.
- Story, M., and R. G. Congalton. 1986. Accuracy assessment-A user's perspective. *Photogrammetric Engineering and Remote Sensing* **52**:397–399.
- Stratton, R. D. 2004. Assessing the effectiveness of landscape fuel treatments on fire growth and behavior. *Journal of Forestry* **102**:32–40.

- Sullivan, W. P., B. J. Morrison, and F. W. H. Beamish. 2008. Adaptive cluster sampling: estimating density of spatially autocorrelated larvae of the sea lamprey with improved precision. *Journal of Great Lakes Research* **34**:86–97.
- Swetnam, T. W. 1990. Fire history and climate in the southwestern United States. Pages 6–17 *in* Proceedings of Symposium on Effects on Fire in Management of Southwestern Natural Resources. General Technical Report RM-191.
- Swetnam, T. W., and J. L. Betancourt. 2010. Mesoscale disturbance and ecological response to decadal climatic variability in the American Southwest. Pages 329–359 *in* Stoffel, M., M. Bollschweiler, D. R. Butler, and B. H. Luckman, editors. *Tree rings and natural hazards*. New York, Springer.
- Swets, J. A. 1988. Measuring the accuracy of diagnostic systems. *Science* **240**:1285–1293.
- Syfert, M. M., M. J. Smith, and D. A. Coomes. 2013. The effects of sampling bias and model complexity on the predictive performance of MaxEnt species distribution models. *PLoS ONE* **8**:e55158.
- Syphard, A. D., V. C. Radeloff, N. S. Keuler, R. S. Taylor, T. J. Hawbaker, S. I. Stewart, and M. K. Clayton. 2008. Predicting spatial patterns of fire on a southern California landscape. *International Journal of Wildland Fire* **17**:602–613.
- Tellman, B. 2002. *Invasive exotic species in the Sonoran region*. Tucson, University of Arizona Press.
- Theobald, D. M., D. Harrison-Atlas., W. B. Monahan, and C. M. Albano. *In review*. Ecologically-relevant maps of landforms and physiographic diversity for climate adaptation planning. *PLOS ONE*.
- Theobald, D. M., D. L. Stevens Jr, D. White, N. S. Urquhart, A. R. Olsen, and J. B. Norman. 2007. Using GIS to generate spatially balanced random survey designs for natural resource applications. *Environmental Management* **40**:134–146.
- Thompson, M. P., and D. E. Calkin. 2011. Uncertainty and risk in wildland fire management: a review. *Journal of Environmental Management* **92**:1895–1909.
- Thuiller, W. 2003. BIOMOD—optimizing predictions of species distributions and projecting potential future shifts under global change. *Global Change Biology* **9**:1353–1362.
- Thuiller, W., B. Lafourcade, R. Engler, and M. B. Araújo. 2009. BIOMOD—a platform for ensemble forecasting of species distributions. *Ecography* **32**:369–373.
- Tsoar, A., O. Allouche, O. Steinitz, D. Rotem, and R. Kadmon. 2007. A comparative evaluation of presence-only methods for modelling species distribution. *Diversity and Distributions* **13**:397–405.
- Tucker, C. J. 1978. Are two photographic infrared sensors required. *Photogrammetric Engineering and Remote Sensing* **44**:289–295.
- Van Devender, T. R., R. S. Felger, and A. Búrquez. 1997. Exotic plants in the Sonoran Desert region, Arizona and Sonora. Pages 1–6 *in* Proceedings of the California Exotic Pest Plant Council Symposium.
- Van Leeuwen, W. J., J. E. Davison, G. M. Casady, and S. E. Marsh. 2010. Phenological characterization of desert sky island vegetation communities with remotely sensed and climate time series data. *Remote Sensing* **2**:388–415.
- VanDerWal, J., L. P. Shoo, C. Graham, and S. E. Williams. 2009. Selecting pseudo-absence data for presence-only distribution modeling: How far should you stray from what you know? *Ecological Modelling* **220**:589–594.
- Vega-García, C., and E. Chuvieco. 2006. Applying local measures of spatial heterogeneity to Landsat-TM images for predicting wildfire occurrence in Mediterranean landscapes. *Landscape Ecology* **21**:595–605.
- Villarreal, M. L., R. E. Lovich, R. L. Palmer, T. Nauman, S. E. Studd, S. Drake, A. S. Rosenberg, J. Malusa, R. L. Pearce, and others. 2011. An inventory and monitoring plan for a Sonoran Desert ecosystem; Barry M. Goldwater Range-West. US Geological Survey.

- Wallace, C. S., and K. A. Thomas. 2008. An annual plant growth proxy in the Mojave Desert using MODIS-EVI data. *Sensors* **8**:7792–7808.
- Wang, O., L. J. Zachmann, S. E. Sesnie, A. D. Olsson, and B. G. Dickson. 2014. An iterative and targeted sampling design informed by habitat suitability models for detecting focal plant species over extensive areas. *PLoS ONE* **9**:e101196.
- Weiss, J. L., and J. T. Overpeck. 2005. Is the Sonoran Desert losing its cool? *Global Change Biology* **11**:2065–2077.
- Westbrook, C., K. Ramos, and M. La. 2005. Under siege: invasive species on military bases. National Wildlife Federation.
- Westerling, A. L., H. G. Hidalgo, D. R. Cayan, and T. W. Swetnam. 2006. Warming and earlier spring increase western US forest wildfire activity. *Science* **313**:940–943.
- Whelan, R. J. 1995. *The ecology of fire*. Cambridge, Cambridge University Press.
- Williams, A. P., and E. R. Hunt. 2002. Estimation of leafy spurge cover from hyperspectral imagery using mixture-tuned matched filtering. *Remote Sensing of Environment* **82**:446–456.
- Williams, J. W., and S. T. Jackson. 2007. Novel climates, no-analog communities, and ecological surprises. *Frontiers in Ecology and the Environment* **5**:475–482.
- Wisdom, M. J., and J. C. Chambers. 2009. A landscape approach for ecologically based management of Great Basin shrublands. *Restoration Ecology* **17**:740–749.
- Wolkovich, E. M., and E. E. Cleland. 2010. The phenology of plant invasions: a community ecology perspective. *Frontiers in Ecology and the Environment* **9**:287–294.
- Xu, Y., B. G. Dickson, H. M. Hampton, T. D. Sisk, J. A. Palumbo, and J. W. Prather. 2009. Effects of mismatches of scale and location between predictor and response variables on forest structure mapping. *Photogrammetric Engineering & Remote Sensing* **75**:313–322.
- Xu, J-F., Huang, J-F., 2008. Empirical Line Method Using Spectrally Stable Targets to Calibrate IKONOS Imagery. *Pedosphere*, **18**(1), pp. 124-130.
- Zhang, J., and J. Kerekes. 2011. Unsupervised urban land-cover classification using WorldView-2 data and self-organizing maps. Pages 150–153 *in* Geoscience and Remote Sensing Symposium (IGARSS), 2011 IEEE International.

Appendix A

Peer-reviewed Publications from RC-1722

1. Bradley, B.A. 2014. Remote detection of invasive plants, a review of spectral, textural and phenological approaches. *Biological Invasions* **16**:1411-1425.
2. Bradley, B.A. 2013. Distribution models of plant invasion over-estimate potential impact. *Biological Invasions* **15**:1417-1429.
3. Bradley, B.A., A.D. Olsson, O. Wang, B.G. Dickson, L. Pelech, S.E. Sesnie, and L. Zachmann. 2012. Species detection vs. habitat suitability: Are we biasing habitat suitability models with remotely sensed data. *Ecological Modelling* **244**: 57-64.
4. Bradley, B.A., R. Early, and C.J.B. Sorte. 2015. Space to invade? Comparative range infilling and potential range of invasive and native plants. *Global Ecology and Biogeography* **24**:348-359.
5. Curtis, C.A. and B.A. Bradley. 2015. Climate change may alter both establishment and high abundance of red brome (*Bromus rubens*) and African mustard (*Brassica tournefortii*) in the semiarid Southwest United States. *Invasive Plant Science and Management* **38**:341-352.
6. Gray, M.E. 2013. Landscape-scale models and maps of large fire risk and connectivity in the Sonoran Desert. MS thesis, Northern Arizona University.
7. Gray, M.E., B.G. Dickson, L. Zachmann. 2014. Modeling and mapping dynamic variability of large fire probability in the lower Sonoran Desert of Arizona. *International Journal of Wildland Fire* **23**:1108-1118.
8. Gray, M.E., and B.G. Dickson. 2015. A new model of landscape-scale fire connectivity applied to resource and fire management in the Sonoran Desert, USA. *Ecological Applications* **25**:1099-1113.
9. Hegeman, E.E., B.G. Dickson, and L.J. Zachmann. 2014. Probabilistic models of fire occurrence across public lands in the Mojave Desert, U.S.A. *Landscape Ecology* **29**:1587-1600.
10. Hoglander, C. 2012. Developed waters for wildlife conservation: collaborative approaches and landscape models for desert bighorn sheep conservation. MS thesis, Northern Arizona University.
11. Hoglander, C., B.G. Dickson, S.S. Rosenstock, and J.J. Anderson. 2015. Landscape models of space use by desert bighorn sheep in the Sonoran Desert of southwestern Arizona. *Journal of Wildlife Management* **79**:77-91.
12. Horncastle, V, B.G. Dickson, S. Rosenstock, and J.J. Anderson. In revision. Differential use of natural and human modified features by coyotes in the Sonoran desert. *Journal of Mammalogy*.
13. Jarvis, K. 2015 (anticip.). Mortality and barrier effects of habitat and roads on landscape genetics of two Sonoran Desert rodents. PhD Dissertation, Northern Arizona University.
14. Lehan, N.E., J.R. Murphy, L.P. Thorburn and B.A. Bradley. 2013. Accidental introductions are an important source of invasive plants in the continental U.S. *American Journal of Botany* **10**:1287-1293.
15. Olsson, A. and J. Morrisette. 2014. Comparison of HypSIPI with two multispectral sensors for invasive species mapping. *Photogrammetric Engineering and Remote Sensing* **80**:217-227.
16. Sankey, T., B.G. Dickson, S.E. Sesnie, O. Wang, L.J. Zachmann, and A. Olsson. 2014. WorldView-2 high spatial resolution imagery improves desert invasive plant detection. *Photogrammetric Engineering and Remote Sensing* **80**:885-893.
17. Sesnie, S.E., B.G. Dickson, S.S. Rosenstock, and J.M. Rundall. 2012. A comparison of Landsat TM and MODIS vegetation indices for estimating forage phenology in desert bighorn sheep (*Ovis canadensis nelsoni*) habitat in the Sonoran Desert, USA. *International Journal of Remote Sensing* **33**:276-286.

18. Sesnie, S.E., A.D. Olsson, O. Wang, L. Zachmann, and B. Dickson. In revision. Phenology as a predictor of non-native species invasion in the Sonoran Desert. *Remote Sensing of Environment*.
19. Wang, O., L.J. Zachmann, B.G. Dickson, A.D. Olsson, S.E. Sesnie, and B. Bradley. 2014. A targeted sampling design informed by habitat suitability models for detecting focal plant species over extensive areas. *PLoS ONE* **9**:e101196.